Zentrum
für Biodiversität und nachhaltige Landnutzung
Sektion
Biodiversität, Ökologie und Naturschutz

− CENTRE OF BIODIVERSITY AND SUSTAINABLE LAND USE −
SECTION: BIODIVERSITY, ECOLOGY AND NATURE CONSERVATION

Effects of Land Use, Habitat Fragmentation and Climate Warming on Stem Increment, Regeneration, and Hydraulic Architecture of *Larix sibirica* in the Mongolian Forest-Steppe

Dissertation
zur Erlangung des Doktorgrades
der Mathematisch-Naturwissenschaftlichen Fakultäten
der Georg-August-Universität Göttingen

im Promotionsprogramm Biologische Dibersität und Ökologie
der Georg-August University School of Science (GAUSS)

vorgelegt von

Elmira Khansaritoreh
aus Tehran (Iran)

Göttingen, August, 2017

Thesis Committee

Prof. Dr. Markus Hauck
Plant Ecology and Ecosystem Research, Albrecht von Haller Institute of Plant Sciences, University of Göttingen

Prof. Dr. Christoph Leuschner
Plant Ecology and Ecosystem Research, Albrecht von Haller Institute of Plant Sciences, University of Göttingen

Dr. Choimaa Dulamsuren
Plant Ecology and Ecosystem Research, Albrecht von Haller Institute of Plant Sciences, University of Göttingen

Members of the Examination Board

Reviewer: Prof. Dr. Markus Hauck
Plant Ecology and Ecosystem Research, Albrecht von Haller Institute of Plant Sciences, University of Göttingen

Second Reviewer: Prof. Dr. Christoph Leuschner
Plant Ecology and Ecosystem Research, Albrecht von Haller Institute of Plant Sciences, University of Göttingen

Further members of the Examination Board

Prof. Dr. Erwin Bergmeier
Department Vegetation & Phytodiversity Analysis, Albrecht-von-Haller-Institute for Plant Sciences, Faculty of Biology and Psychology, University of Göttingen

Prof. Dr. Dirk Hölscher
Tropical Silviculture and Forest Ecology, Faculty of Forest Sciences and Forest Ecology, University of Göttingen

Prof. Dr. Hermann Behling
Department of Palynology and Climate Dynamics, Albrecht-von-Haller Institute for Plant Sciences, University of Göttingen

Prof. Dr. Holger Kreft
Biodiversity, Macroecology and Conservation Biogeography Group,
University of Göttingen

Date of the oral examination: **31st August, 2017**

List of abbreviations

a.s.l.	Above sea level
ANOVA	Analysis of variances
BAI	Basal area increment
ca.	Circa
d	Tracheid diameters
d_h	Hydraulic mean diameter
DBH	Diameter at breast height
e.g.	For example
EPS	Expressed population signal
FE	Forest edge
FI	Forest interior
GL	Gleichläufigkeit
IPCC	Intergovernmental panel on climate change
KDE	Kernel density estimation
K_p	Theoretical sapwood area-specific Hydraulic conductivity
MAP	Mean annual precipitation
MAT	Mean annual temperature
MGSP	Mean growing season precipitation
MGST	Mean growing season temperature
P	Precipitation
PET	Potential evapotranspiration
SPEI	Standardized precipitation-evapotranspiration index
T	Temperature
TD	Tracheid density
TRW	Tree ring width
TSAP	Time Series Analysis and Presentation
Vs.	Versus
η	Viscosity
ρ	Density

Table of Contents

List of figures

List of tables

Chapter 1

General introduction

1.1 Boreal forests of Mongolia, importance and threats

Coniferous forests of northern Mongolia (Mühlenberg et al. 2006) belong to the Siberian boreal forests as the largest continuous forest on earth (Shuman et al. 2011). The numerous Mongolian forest-steppe ecotones extend over roughly 6000 km in Eurasia along the borders of the southern-most fringe of the Siberian taiga and grassland biomes (Dulamsuren et al. 2016). Siberian larch (*Larix sibirica* Ledeb.) that constitutes ca. 80 % of the tree population (Tsogtbaatar 2004) forms mosaics of monospecific forests on the north-facing slopes (moister sites) in montane forest-steppe ecotones. The dominant vegetation type in this region is mostly determined by water availability and grazing pressure (Ishii and Fujita 2013).

Since this boreal forest biome is one of the most important terrestrial carbon reservoirs around the globe (Dulamsuren et al. 2016), the *L. sibirica* forests of Mongolia as a large subset of boreal forests construct a huge carbon pool and thus they play a fundamental role to offset the carbon concentration in the atmosphere (Fu et al. 2017).

Besides, coniferous forests have a key contribution to keep the soil and water quality and regulate water flow (Tsogtbaatar 2004). These forests particularly act as natural insulators which protect the permafrost layer against degradation. The permafrost layer plays a critical role in the preservation of ecosystems in semi-arid regions like Mongolia by providing soil moisture for vegetation (Sharkhuu and Sharkhuu 2012).

Furthermore, life of most Mongolians depends on the forests since nomadic pastoralism including forest grazing, fuel-wood collection and logging has remained the main type of life style throughout the country (Lkhagvadorj et al. 2013b).

Larch forests in Mongolia, however, are threatened by climate change and anthropogenic activities. Increase in annual air temperature is far beyond the global average (Batima et al. 2005; Bohannon 2008) and an even greater increase in air temperature of northern latitudes is predicted by IPCC models (IPCC 2013). Shuman et al. (2011) suggested that species composition of most Siberian larch forests will completely change likely due to climate warming. Moreover, elevated temperature will induce the northern and upslope migration of the treeline in the boreal forests based on ecological models (Soja et al. 2007). Together with climate warming, drought stress limits tree growth in forest-steppe ecotones in Mongolia (e.g., Gunin et al. 1999; Dulamsuren et al. 2013; Liu et al. 2013) and increases risk of wildfire (Girardin et al. 2009; Terrier et al. 2013).

In addition to these direct influences of climate, shrinking permafrost (Sugimoto et al. 2002; Ishikawa et al. 2005; Zhao et al. 2010; Sharkhuu and Sharkhuu 2012) and insect outbreaks and small mammal herbivores (Dulamsuren et al. 2008, 2010c; Hauck et al. 2008) can disturb forest-steppes severely.

Alongside the natural threats, Mongolia's fast-growing population is increasingly consuming timber harvested at the forest-steppe borders, thereby eliminating 60,000 ha of the total 16 million ha forested areas each year (Tsogtbaatar 2004; Mühlenberg et al. 2006; Hansen et al. 2013). Additionally, overgrazing is another factor which restricts tree growth, forest productivity and affects natural regeneration of larch forests (Tsogtbaatar 2004; Erdenechuluun 2006; Sankey et al. 2006; Dulamsuren et al. 2009, 2013).

Moreover, human activities, including livestock breeding, logging and arson alter the position of the forest-steppe borders (Dulamsuren et al. 2010a) and aggravate forest fragmentation to patches varying in size. This fragmentation generally causes bushing and steppification of forest ecotopes (Bazha et al. 2016), contrary to traditional regeneration succession which is supposed to establish birch and aspen dominated secondary forests.

Since trees record ecological and climatic relevant data in their rings during their entire life, dendrochronology and wood anatomy as closely related proxies are recommended to investigate the impact of climate change in the past and they are useful to evaluate possible scenarios for forest conservation in the future (Fonti et al. 2010).

1.2 Mutual feedback between land use and forest fragmentation

The Mongolian forest-steppe is composed of naturally fragmented woodlands of larch trees surrounded by grasslands. These forest patches are exceedingly affected by increasing anthropogenic forest destruction together with warming and drought during the last decades.

Anthropogenic activities including industrial logging, forest fires, livestock grazing and fuel wood collection by mobile pastoralists (Erdenechuluun 2006; Lkhagvadorj et al. 2013a) accelerate fragmentation processes, change the stand structures (e.g. age structure, regeneration rate, etc.) and annual stem increment (Khishigjargal et al. 2013; Dulamsuren et al. 2014) and degrade the permafrost layer (Sharkhuu and Sharkhuu 2012) inside the patches.

Indeed there is a mutual feedback between forest fragmentation and land use; while human activities exacerbate fragmentation of forests, fragmented stands with raised proportion of forest edges provide more opportunities for pastoralists to benefit from smaller patch sizes for

selective logging and intense grazing (Khishigjargal et al. 2013; Lkhagvadorj et al. 2013a, b; Dulamsuren et al. 2014). Pastoral nomads settle in the grasslands and their herds including mostly goat and sheep with some cattle, yak and horses, and rarely camels (Lkhagvadorj et al. 2013a) preferentially graze on the steppe, but also enter the forests edges and, go further into the interior of small forest stands. Therefore small forests are likely to be more severely affected by forest grazing which leads to the destruction of forest regeneration (Khishigjargal et al. 2013).

In context of socio-political events, changes in tenure and organization of pastoral livestock husbandry from state-owned and organized in collectives to decollectivized after 1992 (Sneath 2004; Fernández-Giménez 2006), have increased the land-use pressure at many places, leading to overgrazing and increased logging activities (Erdenechuluun 2006; Onda et al. 2007; Galvin et al. 2008). Industrial timber harvest has been conducted between the second half of the twentieth century until 1990 (collapse of the communist regime), whereas considerable number of trees have been logged (Erdenechuluun 2006) by the countryside population since 1991. This increased logging resulted in the increased fragmentation of forests in the forest-steppe zone.

In addition to grazing and logging, fire is one of the main reasons of deforestation in Mongolia which is caused owing to the very dry climate and/or a severe increase in the number of people who use forest and steppe areas for several purposes (Tsogtbaatar 2004; Girardin et al. 2009; Hessl et al. 2012). Irrespective of its drivers, fire is shown to cause tree mortality (Ducrey et al. 1996; Balfour and Midgley 2006; Michaletz and Johnson 2008), the replacement of conifers by broadleaved pioneer stands (to lessen the likelihood and the effect of forest fires, Terrier et al. 2013), reduced size of the tree ring width (TRW) and tracheid diameters in survived trees after fire (Arbellay et al. 2014). Recent Landsat observations by Chen et al. (2016) revealed that during the last 24 years more than 10 % of the forested areas in the Siberian larch forests has practiced stand-replacing fires.

1.3 Mongolian forests in the course of climate warming

Since the Mongol’s life mainly depends on livestock and other climate-dependent sectors, attention to climate change is a substantial issue in Mongolia. Climate change threatens forest productivity and ecology, livestock and the socio-national economic sectors, not only by warmer and drier condition, but also with severe winter (called “dzud”) (Batima et al. 2005; Lkhagvadorj et al. 2013a).

In some boreal forests where the low summer temperature is the limiting factor, increase in temperature reinforces forest productivity and expansion. However, investigations on the correlation between Normalized Difference Vegetation Index (NDVI) and summer temperature reveals a recent switch from temperature limitation to moisture limitation in extended parts of the boreal forest since the mid-1990s (Buermann et al. 2014). Such situation occurs in most forest-steppe ecotones of Mongolia (Gunin et al. 1999; Dulamsuren et al. 2013; Liu et al. 2013) but some areas did not experience moisture limitation (D'Arrigo et al. 2000; Dulamsuren et al. 2010a).

During the past century Siberian summers became warmer than any century in the past millennium, and it has been predicted that this trend will continue in the future by some accounts between 2 and 10 °C by 2100 (IPCC 2007; Soja et al. 2007). In addition to the significant elevated temperature, it is widely approved that a descending precipitation trend has been detected in the northern hemisphere, in particular over northern Eurasia including Mongolia since the mid-1950s (Dai et al. 2004).

Several researches have been conducted by analyses of tree-ring width (Barber et al. 2000; Lloyd and Bunn 2007), stable isotopes (Tei et al. 2014), frequency of drought-induced missing ring (Khishigjargal et al. 2014), tree mortality (Allen et al. 2010; Peng et al. 2011), forest regeneration (Dulamsuren et al. 2010b; Bond-Lamberty et al. 2014), tree line position (Kullman and Öberg 2009) and NDVI (Angert et al. 2005; Verbyla 2011) to show how boreal forest trees react to different climatic trends. Based on the TRW series, in Mongolia unusual warming during the twentieth century has limited forests mainly to the northern third of the country, primarily on north-facing slopes (D'Arrigo et al. 2000).

Climate warming can not only affect TRW but also influences the stand structure of forests in context of competition between trees for water. Generally there is an inverse correlation between stand density and water availability (McDowell and Allen 2015). Higher TRW in the forest edges compared to the forest interiors in Mongolia is also attributed to reduced stand density and less tense competition for water at the forest edges (Dulamsuren et al. 2010a, b; Chenlemuge et al. 2015).

In the forest-steppe region of Mongolia, small forest patches in comparison with larger continuous forests face different microclimatic conditions including more extreme maxima and minima in temperature together with lower and more variable air humidity and soil

moisture (Chen et al. 1995, 1999). These differences can influence trees' strength and productivity in fragmented forests especially at their edges (Debinski and Holt 2000).

Although there are not many published studies on hydraulic conductivity and wood anatomy of larch trees in Mongolia in relation to tree productivity, general findings in wood anatomy provide possibility to predict how climate warming and drought can influence tree growth and productivity in this area. Effect of climate change on the anatomical structure of wood is very remarkable due to the importance of these structures in the water transport system. Productivity and vitality of trees rely on a well-functioning water transport system. This system should be efficient under proper conditions of water availability and provide high photosynthetic rates, and it has to be resilient during drought periods (Hacke and Sperry 2001). Under drought stress, formation of tracheids with narrow lumens and thick walls reduce efficiency of sap flow in xylem (Tyree and Zimmermann 2002); this mechanism can support trees against cavitation, embolism, cells breakdown and hydraulic failure (Hacke et al. 2001; Cochard et al. 2004). Furthermore, leaf stomata can be closed which cause lower stomatal conductance and photosynthesis to prevent cavitation during water shortage. Consequently these mechanisms constrain tree growth and productivity by stomatal regulation (Ryan and Yoder 1997; Jones 1998; Tyree 2003; De Grandpré et al. 2011; Dulamsuren et al. 2013).

Although the main reason of tree mortality is not yet found, many studies showed that hydraulic failure and low carbon allocation to xylogenesis together with loss of conductivity and carbohydrates reserves as well as high fine root death lead to drought-induced tree mortality (Mcdowell et al. 2008; McDowell and Sevanto 2010; Sala et al. 2010, 2012; McDowell et al. 2011; Chenlemuge et al. 2013; Heres et al. 2014; Sevanto et al. 2014).

It is suggested that climate change probably will cause more limitations for forest establishment at many places in Mongolia in the future by bringing a dry and hot soil condition (Dulamsuren and Hauck 2008). In addition, since Mongolia has a severe climate if clear-cutting -which is the standard practice in the northern forests for commercial purpose- occur, it can lead to significantly reduced regrowth and productivity. Therefore replanting would be the only solution to restore the wood resource while the ecosystems still preserved their forest-regenerative potential (Tsogtbaatar 2004; Bazha et al. 2016).

1.4 Study objectives and hypotheses

This study was carried out using dendrochronology and wood anatomy as two powerful climatic proxies to answer the following research questions:

1) How severely does spatial heterogeneity in land use practices in two sites A and B (20 km far from each other) with the same tree species (*L. sibirica*) stands interfere with the climate response of forest productivity and forest health (Chapter 2)?

2 Is the climate warming sensitivity of tree growth, regeneration, missing ring frequency, microclimate etc. within forest islands with varying sizes influenced by forest size and isolation in fragmented forests (Chapter 3)?

3) How do climate change and forest size-dependent variations affect early wood (EW) anatomical traits and hydraulic conductivity in stems of dominant larch trees from four different sizes of forest patches? How is the correlation between tree-ring width and anatomical parameters (Chapter 4)?

In Chapter 2, four hypotheses were tested: (i) trees at the more heavily logged site A are less evenly distributed across age classes than trees at site B, (ii) mean sensitivity of tree-ring series to climate is higher at the less severely logged and thus less disturbed site B, (iii) stem increment at both sites is significantly limited by summer drought, and (iv) trees at both sites exhibit increasing missing ring frequency and increasing mortality rates since the late twentieth century.

In Chapter 3, four hypotheses among four different size classes of forests located in a woodland-dominated forest-steppe area and small forest patches in a grassland-dominated area, were tested: (i) decreasing stand size increases climate sensitivity and thus the susceptibility of radial stem increment to summer drought, (ii) the frequency of drought-induced missing rings increases with decreasing stand size, and (iii) success in forest regeneration increases with increase in stand size. In addition to stands of varying sizes, we compared forest islands of the same size in a forest-dominated subregion with isolated stands in a grassland-dominated subregion to test the hypothesis (iv) that forests in the grassland-dominated landscape are more sensitive to variation in climate, since climatic parameters can be expected to be more variable here than in forest-dominated areas of the forest-steppe ecotone.

In Chapter 4, the objective of our study was to test the hypotheses that (i) drought years cause signals in the trees' hydraulic architecture in addition to their effect on tree-ring width, (ii) tracheid diameters that are crucial for shaping hydraulic conductivity are correlated with tree-ring width, and (iii) tracheid diameter, tracheid density, and hydraulic conductivity vary in dependence of stand size.

1.5 Study design and methodology

1.5.1 Study areas

The study was conducted at the southern fringe of the Eurosiberian boreal forest belt. Studied larch forests are located in the forest-steppe of north-western Mongolia (in the northern Khangai Mountains), in the Zavkhan province, approx. 630 km W of Ulan Bator and 550 km SW of Lake Baikal (Fig. 1.1).

Field work for chapter 3 and 4 was carried out in highly fragmented larch forests near Tosontsengel (48°45' N, 98°16' E, 1700 m a.s.l.), whereas the study sites (A and B) for chapter 2 were located approx. 70−90 km SW of Tosontsengel, at the border between Tosontsengel and Ider administrative subunits of the Zavkhan province. Site A (exposed to high logging intensity until 1990 and low livestock grazing pressure) was located at 48°29−31' N, 97°52−54' E, and site B was located at 48°20−22' N, 97°41−47' E. Site B experienced unplanned occasional selective logging and moderate (but higher than site A) livestock grazing pressure.

In general, Mongolia has an extreme continental climate which is characterized by short warm summers and long cold winters coined by the stable Siberian High Pressure Cell. In most forest-steppe regions, annual mean temperature is around subzero or near zero and minima are between -40 and -50 °C. The maximum annual precipitation of roughly 200−300 mm is received mainly during summer, with most rainfall in July (Table 1.1).

Siberian larch (*Larix sibirica* Ledeb.) is the dominant species in the monospecific larch woodlands in the forest-steppe regions. Typical landscape consists of forest islands of variable sizes which occur on north-facing slopes, whereas grasslands cover south-facing slopes and the bottoms of dry valleys.

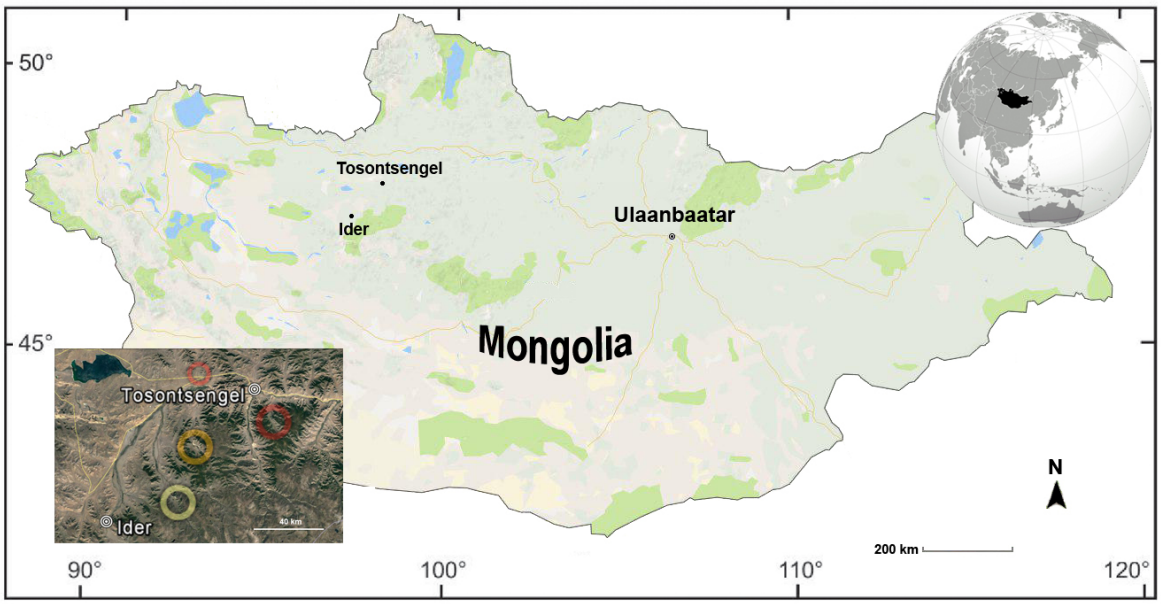

Fig. 1.1 Location of study sites in north-western Mongolia (Zavkhan province, near Tosontsengel). 2012: orange (site A) and yellow (site B) circles. 2014: large red (F type plots, chapters 3 and 4) and small red (G type plots) circles.
(Map sources: http://maps.google.de; https://www.google.com/earth/)

Table 1.1 Temperature (1964-2014) and precipitation (1968-2014) according to records from Tosontsengel meteorological station located 48°73' N, 98°28' E.

	Temperatue (°C)			Precipitation (mm)		
	minimum	mean	maximum	minimum	mean	maximum
annual	-8.4	**-6.1**	-3.4	135	221	430
growing season	9.1	**10.7**	13.4	88	181	360

Growing season starts from May and ends in September. Bold values indicate a significant ascending trend; increase in mean annual temperature (y=0.05x-108.38, $p < 0.001$, r = 0.6) and increase in mean growing season temperature (y=0.04x-71.93, $p < 0.001$, r = 0.6).

1.5.2 Sample plots

Field work and sampling was carried out in August 2012 and 2014 in 20 m × 20 m plots. Sampling for the first study (chapter 2, 2012) was conducted in 6 randomly selected locations per study site with 2 replicates for each; one in the forest interior (50–100 m from the forest line) and one in the forest edges. The lower boundary of the forest edge plots was identical with the forest line. In addition, 5 extra replicates in the forest interior of each site were selected but their data were not included in age and stand structure studies. Thus, a total of 34 plots for the entire study were investigated. Plots of site A and site B were distributed over an area of approx. 5 km^2 and approx. 10 km^2 respectively.

Sampling for the second study (chapter 3, 2014) was conducted in one forest-dominated (class F) and one grassland-dominated (class G) subregion, based on the remote sensing analysis. We selected forests of four different size classes (classes F1 to F4) to analyze the influence of patch size. For analyzing the impact of isolation degree, 3 replicates from G1 forests were compared with F1 replicates. Three replicates in the interior of each forest stand (at least 30 m away from the forest edge) were studied for each plot type (F1 to F4 and G1) yielding a total of 15 sampled forests. To limit the effect of spatial heterogeneity in the forest islands, 2 plots were selected in each F type sampled forests. In addition, micro climatic data including air temperature and relative air humidity were recorded in every sample plot and soil temperature was measured in one randomly selected plot cluster within the smallest (F1) and the largest (F4) forest stands.

Sampling in the third study for anatomical investigation (chapter 4, 2014) was conducted in the same plots from the prior study (chapter 3). For this part we took cores randomly from 5 trees grown in each patch size (class F).

1.5.3 Wood cores sampling and tree-ring measurements

In August 2012 and 2014, wood cores from all trees with a stem diameter of ≥3 cm at breast height (DBH; approx. 1.3 m above the ground) were collected for tree-ring analysis. All live trees as well as dead trees with largely intact wood that permitted proper wood core sampling were included. In addition to these samples, living old trees located outside the plots were sampled as reference samples to establish long-term tree-ring chronologies but their data were not included in the analysis of age and stand structure. Wood cores were taken with an increment borer with an inner diameter of 5 mm (Haglöf, Långsele, Sweden) at breast height parallel to the contour lines of the mountain slopes to avoid compression of the wood. In

addition, we recorded other available information e.g. trunk circumference, tree height, dominance (dominant, subdominant and suppressed), fire traces, neighboring stumps data, etc.

The wood cores were mounted on the wooden strips and cut lengthwise with a microtome; the contrast between annual tree rings was enhanced with chalk. The TRW was measured with a precision of 10 µm on a movable object table (Lintab 6, Rinntech, Heidelberg, Germany). Movements were electronically transmitted to a computer system equipped with Time Series Analysis and Presentation (TSAP)-Win software (Rinntech).

In 2012 (chapter 2) approx. 1000 *L. sibirica* trees were sampled; 729 trees from the main 24 plots, 140 trees from outside of the plots and the rest from additional interior plots.

In 2014 (chapter 3) wood cores from 1755 *L. sibirica* trees were collected of which 135 grew outside of our plots and attended only in building tree-ring chronologies.

1.5.4 Evaluation of tree-ring data

All chronologies were cross-dated visually and via TSAP-Win software (Rinntech) to check the quality of the tree-ring counts and recognize missing rings. Cross-dating based on the calculation of agreement coefficients ('Gleichläufigkeit' [GL]) >65% and a (standard) *t*-value >3 (Eckstein and Bauch 1969) before mean TRW was computed. Trees were classified into four age classes including 'very old trees' (>160 years), 'old trees' (101–160 years), 'middle-aged trees' (61–100 years) and 'young trees' (≤60 years), based on their cambial age at 1.3 m above the ground. Most of the tree ring studies were done separately in these age groups. The expressed population signal (EPS) (Wigley et al. 1984) was calculated to quantify how well our tree-ring series represented the stem increment dynamics of the studied stands. Good representation by a given tree-ring series is accepted at EPS > 0.85.

To extract the climate information and to remove the age-related trend in the data, which resulted from increasing stem diameter, raw tree-ring series were standardized. The relationships between the annual tree-ring index and monthly temperature and precipitation for current and prior year of tree ring formation (over the period which climatic data are available by the climate station in Tosontsengel), were examined as climate response analysis. In addition to climate-response analysis, principal component analysis (PCA) was carried out for the tree-ring index depending on monthly temperature and precipitation values for sampled trees in 2014 (chapter 3).

For 20 selected trees, we conducted anatomical studies (chapter 4): climate response analysis was done for tree-ring index, mean tracheid diameter (d), hydraulic mean diameter (d_h), tracheid density (TD) and potential sapwood area-specific hydraulic conductivity (K_p) with temperature and precipitation of current and prior years between 1985 and 2014. Moreover, based on the monthly temperature and precipitation data and latitude of our study site in 2014, we calculated potential evapotranspiration (PET) by the Thornthwaite approach (Thornthwaite 1948). PET is a prerequisite to quantify the standardized precipitation-evapotranspiration index (SPEI) (Vicente-Serrano et al. 2010) by the R package "SPEI" (v 1.6).

Regional growth curves (RGC) were used to remove age-related long-term (low-frequency) trends, but to preserve all other long-term trends in annual stem increment (Sarris et al. 2007; Dulamsuren et al. 2010a). In RGC, the cumulative annual stem increment is plotted versus tree age, not the calendar year. This test was conducted only between old and middle-aged trees, since the productivity of such trees is more strongly influenced by climate.

Based on the raw increment data over the whole lifespan of each sampled tree, mean sensitivity and autocorrelation coefficients (Fritts 1976) were calculated with TSAP-Win. The sensitivity is a measure for the strength of the climate signals in the tree-ring series. The autocorrelation coefficient delivers information about the physiological buffering ability of trees. Mean sensitivity is calculated as the difference in the tree-ring width of two consecutive years divided by the mean tree-ring width of the two years. Autocorrelation which analyzes the linear correlation of the tree-ring width in a given year with the tree-ring width in the previous year was calculated for all consecutive years of a tree-ring series. High mean sensitivity together with low first-order autocorrelation coefficients is an indication of vulnerability of trees against unfavorable climatic conditions, probably due to the low stored carbohydrates.

1.5.5 Age and stand structure

For both studies (chapter 2 and 3, 2012 and 2014) age and stand structure including mean and maximum age, basal area and stand density were presented for main plots. The recent regeneration of *L. sibirica* was found by counting seedlings and saplings (stem diameter <3 cm at 1.3 m height, or trees not reaching 1.3 m height) and categorizing them in 5 different height classes (<50 cm, 50-100 cm, 100-150 cm, 150-200 cm, >200 cm) in the field. Saplings age was estimated by counting their annual rings in stem cross-sections which were collected

randomly. Effect of selective logging has been estimated by counting tree stumps and differentiating them from those which originated from natural mortality in each plot.

1.5.6 Microclimate measurements

Air temperature and relative air humidity were recorded in every sample plot (chapter 3) using HOBO U23 ProV2 sensors (Onset Computer Cooperation, Bourne, Massachusetts, U.S.A.). The sensors were placed on the northern side of three randomly selected trees at approx. 150 cm above the ground. Temperature and relative air humidity were logged hourly for one year from August 2014 to July 2015.

Soil temperature was recorded with tempmate B4 Miniature Hygrologgers (imec Messtechnik, Heilbronn, Germany) in one randomly selected plot cluster within the smallest (F1) and the largest (F4) forest stands for the same period. Soil temperature was recorded twice a day at 3:00 AM and 3:00 PM.

1.5.7 Remote sensing analysis of forest distribution

To determine stand sizes (chapter 3 and 4) and control temporal dynamics of forest stand sizes, remote sensing analysis of forest distribution was performed within ArcGIS 3.2 by supervised classification of a Spot 6 multispectral satellite image of September 14, 2014. The spatial resolution of 1.6 m × 1.6 m in Spot images enabled a detailed delineation of forest stands and isolated trees. The classification result was visually corrected and transformed into vectored data. The size of the single polygons bordering the closed forests was used to calculate the forest areas. To proof the spatial permanence of the investigated forests during the last 30 years, a change detection analysis was performed using three different Landsat satellite images: Landsat 5 TM of July 23, 1986; Landsat 7 ETM+ from June 9, 2002; Landsat 8 OLT/TIRS of September 19, 2013. Initially the forest distribution of every satellite image was delineated by supervised classification. The computed forest areas of every time slice were subtracted from each other to analyze potential area changes.

1.5.8 Hydraulic conductivity measurement and xylem anatomy analysis

A total of 40 stem wood cores from 20 intact, stout and dominant trees (5 trees per patch size of F type) were collected with the same method as mentioned in the section 1.5.3, in the northern part of Khangai Mountains in August 2014 (chapter 4). One core from each tree which was used for anatomical studies was stored in 70 % ethanol prior to laboratory preparation and another core was prepared for tree ring analyses (e.g. climate response analysis, EPS, mean sensitivity, autocorrelation) with the same methods given in 1.5.4.

Wood anatomical laboratory preparation, Image analysis and calculation were carried out for EW of the last 30 rings. Wood anatomical parameters including idealized tracheid diameters (D), hydraulic mean diameter (D_h), tracheid density (TD) and potential sapwood area-specific hydraulic conductivity (Kp) were analysed (the methods are explained in detail in 4.3.4.).

References

Allen CD, Macalady AK, Chenchouni H, et al (2010) A global overview of drought and heat-induced tree mortality reveals emerging climate change risks for forests. For Ecol Manage 259:660–684. doi: 10.1016/j.foreco.2009.09.001

Angert A, Biraud S, Bonfils C, et al (2005) Drier summers cancel out the CO2 uptake enhancement induced by warmer springs. Proc Natl Acad Sci U S A 102:10823–7. doi: 10.1073/pnas.0501647102

Arbellay E, Stoffel M, Sutherland EK, et al (2014) Changes in tracheid and ray traits in fire scars of North American conifers and their ecophysiological implications. Ann Bot 114:223–32. doi: 10.1093/aob/mcu112

Balfour DA, Midgley JJ (2006) Fire induced stem death in an African acacia is not caused by canopy scorching. Austral Ecol 31:892–896. doi: 10.1111/j.1442-9993.2006.01656.x

Barber VA, Juday GP, Finney BP (2000) Reduced growth of Alaskan white spruce in the twentieth century from temperature-induced drought stress. Nature 405:668–673. doi: 10.1038/35015049

Batima P, Natsagdorj L, Gombluudev P, Erdenetsetseg B (2005) Observed Climate Change in Mongolia. AIACC Work Pap 25.

Bazha SN, Baldanov BT, Baskhaeva TG, et al (2016) Diagnostic features of reforestation potential of Larix sibirica Ledeb. in ecosystems at the southern boundary of the boreal belt in Asia. Arid Ecosyst 6:169–176. doi: 10.1134/S2079096116030033

Bohannon J (2008) The Big Thaw Reaches Mongolia ' s Pristine North. Science (80-) 1–2.

Bond-Lamberty B, Rocha A V., Calvin K, et al (2014) Disturbance legacies and climate jointly drive tree growth and mortality in an intensively studied boreal forest. Glob Chang Biol 20:216–227. doi: 10.1111/gcb.12404

Buermann W, Parida B, Jung M, et al (2014) Recent shift in Eurasian boreal forest greening response may be associated with warmer and drier summers. Geophys Res Lett 41:1995–2002. doi: 10.1002/2014GL059450

Chen D, Loboda T V., Krylov A, Potapov P V. (2016) Mapping stand age dynamics of the Siberian larch forests from recent Landsat observations. Remote Sens Environ 187:320–331. doi: 10.1016/j.rse.2016.10.033

Chen J, Franklin JF, Spies TA (1995) Growing-Season Microclimatic Gradients from Clearcut Edges into Old-Growth Douglas-Fir Forests. Ecol Appl 5:74–86. doi: 10.2307/1942053

Chen J, Saunders SC, Crow TR, et al (1999) Microclimate in Forest Ecosystem and Landscape Ecology. Bioscience 49:288–297.

Chenlemuge T, Dulamsuren C, Hertel D, et al (2015) Hydraulic properties and fine root mass of Larix sibirica along forest edge-interior gradients. Acta Oecologica 63:28–35. doi: 10.1016/j.actao.2014.11.008

Chenlemuge T, Hertel D, Dulamsuren C, et al (2013) Extremely low fine root biomass in Larix sibirica forests at the southern drought limit of the boreal forest. Flora Morphol Distrib Funct Ecol Plants 208:488–496. doi: 10.1016/j.flora.2013.08.002

Cochard H, Froux F, Mayr S, Coutand C (2004) Xylem wall collapse in water-stressed pine needles. Plant Physiol 134:401–8. doi: 10.1104/pp.103.028357

D'Arrigo R, Jacoby G, Pederson N, et al (2000) Monogolian tree-rings, temperature sensitivity and reconstructions of Northern Hemisphere temperature. The Holocene 10:669–672. doi: 10.1191/09596830094926

Dai A, Trenberth KE, Qian T (2004) A Global Dataset of Palmer Drought Severity Index for 1870–2002: Relationship with Soil Moisture and Effects of Surface Warming. J Hydrometeorol 5:1117–1130. doi: 10.1175/JHM-386.1

De Grandpré L, Tardif JC, Hessl A, et al (2011) Seasonal shift in the climate responses of Pinus sibirica , Pinus sylvestris , and Larix sibirica trees from semi-arid, north-central Mongolia. Can J For Res 41:1242–1255. doi: 10.1139/x11-051

Debinski DM, Holt RD (2000) Survey and review of habitat fragmentation experiments. Conserv. Biol. 14:342–355.

Ducrey M, Duhoux F, Huc R, Rigolot E (1996) The ecophysiological and growth responses of Aleppo pine (Pinushalepensis) to controlled heating applied to the base of the trunk. Can J For Res 26:1366–1374. doi: 10.1139/x26-152

Dulamsuren C, Hauck M (2008) Spatial and seasonal variation of climate on steppe slopes of the northern Mongolian mountain taiga. Grassl Sci 54:217–230. doi: 10.1111/j.1744-697X.2008.00128.x

Dulamsuren C, Hauck M, Bader M, et al (2009) Water relations and photosynthetic performance in Larix sibirica growing in the forest-steppe ecotone of northern Mongolia. Tree Physiol 29:99–110. doi: 10.1093/treephys/tpn008

Dulamsuren C, Hauck M, Khishigjargal M, et al (2010a) Diverging climate trends in Mongolian taiga forests influence growth and regeneration of Larix sibirica. Oecologia 163:1091–1102. doi: 10.1007/s00442-010-1689-y

Dulamsuren C, Hauck M, Leuschner C (2010b) Recent drought stress leads to growth reductions in Larix sibirica in the western Khentey, Mongolia. Glob Chang Biol 16:3024–3035. doi: 10.1111/j.1365-2486.2009.02147.x

Dulamsuren C, Hauck M, Leuschner HH, Leuschner C (2010c) Gypsy moth-induced growth decline of Larix sibirica in a forest-steppe ecotone. Dendrochronologia 28:207–213. doi: 10.1016/j.dendro.2009.05.007

Dulamsuren C, Hauck M, Mühlenberg M (2008) Insect and small mammal herbivores limit tree establishment in northern Mongolian steppe. Plant Ecol 195:143–156. doi: 10.1007/s11258-007-9311-z

Dulamsuren C, Khishigjargal M, Leuschner C, Hauck M (2014) Response of tree-ring width to climate warming and selective logging in larch forests of the Mongolian Altai. J Plant Ecol 7:24–38. doi: 10.1093/jpe/rtt019

Dulamsuren C, Klinge M, Degener J, et al (2016) Carbon pool densities and a first estimate of the total carbon pool in the Mongolian forest-steppe. Glob Chang Biol 22:830–844. doi: 10.1111/gcb.13127

Dulamsuren C, Wommelsdorf T, Zhao F, et al (2013) Increased Summer Temperatures Reduce the Growth and Regeneration of Larix sibirica in Southern Boreal Forests of Eastern Kazakhstan. Ecosystems 16:1536–1549. doi: 10.1007/s10021-013-9700-1

Eckstein D, Bauch J (1969) Beitrag zur Rationalisierung eines dendrochronologischen Verfahrens und zur Analyse seiner Aussagesicherheit. Forstwissenschaftliches Cent 88:230–250. doi: 10.1007/BF02741777

Erdenechuluun T (2006) Wood Supply in Mongolia: the Legal and Illegal Economies.

Fernández-Giménez ME (2006) Land Use and Land Tenure in Mongolia : A Brief History and Current Issues. In: Rangelands of Central Asia: Proceedings of the Conference on Transformations, Issues, and Future Challenges. USDA Forest Service Proceedings. pp 30–36

Fonti P, Von Arx G, García-González I, et al (2010) Studying global change through investigation of the plastic responses of xylem anatomy in tree rings. New Phytol 185:42–53. doi: 10.1111/j.1469-8137.2009.03030.x

Fritts HC (1976) Tree rings and climate. Academic Press

Fu L, Sun W, Wang G (2017) A climate-sensitive aboveground biomass model for three larch species in northeastern and northern China. Trees 31:557–573. doi: 10.1007/s00468-016-1490-6

Galvin KA, Reid RS, Behnke RH, Hobbs NT (2008) Fragmentation in Semi-Arid and Arid Landscapes: Consequences for Human and Natural Systems. Dordrecht, the Netherlands: Springer.

Girardin MP, ALI AA, CARCAILLET C, et al (2009) Heterogeneous response of circumboreal wildfire risk to climate change since the early 1900s. Glob Chang Biol 15:2751–2769. doi: 10.1111/j.1365-2486.2009.01869.x

Gunin PD, Vostokova EA, Dorofeyuk NI, et al (eds) (1999) Vegetation Dynamics of Mongolia. Springer Netherlands, Dordrecht

Hacke UG, Sperry JS (2001) Functional and ecologycal xylem anatomy. Perspect Plant Ecol Evol Syst 4:97–115. doi: 10.1007/978-3-319-15783-2

Hacke UG, Sperry JS, Pockman WT, et al (2001) Trends in wood density and structure are linked to prevention of xylem implosion by negative pressure. Oecologia 126:457–461. doi: 10.1007/s004420100628

Hansen MC, Potapov P V., Moore R, et al (2013) High-Resolution Global Maps of 21st-Century Forest Cover Change. Science (80-) 342:850–853. doi: 10.1126/science.1244693

Hauck M, Dulamsuren C, Heimes C (2008) Effects of insect herbivory on the performance of Larix sibirica in a forest-steppe ecotone. Environ Exp Bot 62:351–356. doi: 10.1016/j.envexpbot.2007.10.025

Heres AM, Camarero JJ, López BC, Martínez-Vilalta J (2014) Declining hydraulic performances and low carbon investments in tree rings predate Scots pine drought-induced mortality. Trees - Struct Funct 28:1737–1750. doi: 10.1007/s00468-014-1081-3

Hessl AE, Ariya U, Brown P, et al (2012) Reconstructing fire history in central Mongolia from tree-rings. Int J Wildl Fire 21:86–92. doi: 10.1071/WF10108

IPCC (2013) Climate Change 2013: The Physical Science Basis. Contribution of Working Group I to the Fifth Assessment Report of the Intergovernmental Panel on Climate Change. Intergov Panel Clim Chang Work Gr I Contrib to IPCC Fifth Assess Rep (AR5)(Cambridge Univ Press New York) 1535. doi: 10.1029/2000JD000115

IPCC (2007) Climate change 2007: the physical science basis. Intergov Panel Clim Chang 446:727–8. doi: 10.1038/446727a

Ishii R, Fujita N (2013) A Possible Future Picture of Mongolian Forest-Steppe Vegetation

Under Climate Change and Increasing Livestock: Results from a New Vegetation Transition Model at the Topographic Scale. In: The Mongolian Ecosystem Network. pp 65–82

Ishikawa M, Sharkhuu N, Zhang Y, et al (2005) Ground thermal and moisture conditions at the southern boundary of discontinuous permafrost, Mongolia. Permafr Periglac Process 16:209–216. doi: 10.1002/ppp.483

Jones HG (1998) Stomatal control of photosynthesis and transpiration. In: J. Exp. Bot. http://apps.isiknowledge.com/InboundService.do?product=WOS&action=retrieve&SrcApp=Papers&UT=000072842300013&SID=2BFJ517a6NHCk@68JDi&SrcAuth=mekentosj&mode=FullRecord&customersID=mekentosj&DestFail=http://access.isiproducts.com/custom_images/wok_failed_aut. Accessed 14 Mar 2017

Khishigjargal M, Dulamsuren C, Leuschner HH, et al (2014) Climate effects on inter- and intra-annual larch stemwood anomalies in the Mongolian forest-steppe. Acta Oecologica 55:113–121. doi: 10.1016/j.actao.2013.12.003

Khishigjargal M, Dulamsuren C, Lkhagvadorj D, et al (2013) Contrasting responses of seedling and sapling densities to livestock density in the Mongolian forest-steppe. Plant Ecol 214:1391–1403. doi: 10.1007/s11258-013-0259-x

Kullman L, Öberg L (2009) Post-Little Ice Age tree line rise and climate warming in the Swedish Scandes: a landscape ecological perspective. J Ecol 97:415–429. doi: 10.1111/j.1365-2745.2009.01488.x

Liu H, Park Williams A, Allen CD, et al (2013) Rapid warming accelerates tree growth decline in semi-arid forests of Inner Asia. Glob Chang Biol 19:2500–2510. doi: 10.1111/gcb.12217

Lkhagvadorj D, Hauck M, Dulamsuren C, Tsogtbaatar J (2013a) Pastoral nomadism in the forest-steppe of the Mongolian Altai under a changing economy and a warming climate. J Arid Environ 88:82–89. doi: 10.1016/j.jaridenv.2012.07.019

Lkhagvadorj D, Hauck M, Dulamsuren C, Tsogtbaatar J (2013b) Twenty Years After Decollectivization: Mobile Livestock Husbandry and Its Ecological Impact in the Mongolian Forest-Steppe. Hum Ecol 41:725–735. doi: 10.1007/s10745-013-9599-3

Lloyd AH, Bunn AG (2007) Responses of the circumpolar boreal forest to 20th century climate variability. Environ Res Lett 2:45013. doi: 10.1088/1748-9326/2/4/045013

Mcdowell N, Pockman WT, Allen CD, et al (2008) Mechanisms of Plant Survival and Mortality during Drought : Why Do Some Plants Survive while Others Succumb to Drought ? Published by : Wiley on behalf of the New Phytologist Trust Stable URL : http://www.jstor.org/stable/30149305 REFERENCES Linked refere. 178:719–739.

McDowell NG, Allen CD (2015) Darcy's law predicts widespread forest mortality under climate warming. Nat Clim Chang 5:669–672. doi: 10.1038/nclimate2641

McDowell NG, Beerling DJ, Breshears DD, et al (2011) The interdependence of mechanisms underlying climate-driven vegetation mortality. Trends Ecol Evol 26:523–532. doi: 10.1016/j.tree.2011.06.003

McDowell NG, Sevanto S (2010) The mechanisms of carbon starvation: how, when, or does it even occur at all? New Phytol 186:264–266. doi: 10.1111/j.1469-8137.2010.03232.x

Michaletz ST, Johnson EA (2008) A biophysical process model of tree mortality in surface fires. Can J For Res 38:2013–2029. doi: 10.1139/X08-024

Mühlenberg M, Batkhishig T, Dashzeveg T, et al (2006) Mongolia - lessons from tree planting initiatives in Mongolia. Washington, DC.

Onda Y, Kato H, Tanaka Y, et al (2007) Analysis of runoff generation and soil erosion processes by using environmental radionuclides in semiarid areas of Mongolia. J Hydrol 333:124–132. doi: 10.1016/j.jhydrol.2006.07.030

Peng C, Ma Z, Lei X, et al (2011) A drought-induced pervasive increase in tree mortality across Canada's boreal forests. Nat Clim Chang 1:467–471. doi: 10.1038/nclimate1293

Ryan MG, Yoder BJ (1997) Hydraulic limits to tree height and tree growth: what keeps trees from growing beyond a certain height? Bioscience 47:235–242. doi: 10.2307/1313077

Sala A, Piper F, Hoch G (2010) Physiological mechanisms of drought-induced tree mortality are far from being resolved. New Phytol 186:274–281. doi: 10.1111/j.1469-8137.2009.03167.x

Sala A, Woodruff DR, Meinzer FC (2012) Carbon dynamics in trees: Feast or famine? Tree Physiol 32:764–775. doi: 10.1093/treephys/tpr143

Sankey TT, Montagne C, Graumlich L, et al (2006) Lower forest–grassland ecotones and 20th Century livestock herbivory effects in northern Mongolia. For Ecol Manage 233:36–44. doi: 10.1016/j.foreco.2006.05.070

Sarris D, Christodoulakis D, Körner C (2007) Recent decline in precipitation and tree growth in the eastern Mediterranean. Glob Chang Biol 13:1187–1200. doi: 10.1111/j.1365-2486.2007.01348.x

Sevanto S, Mcdowell NG, Dickman LT, et al (2014) How do trees die? A test of the hydraulic failure and carbon starvation hypotheses. Plant, Cell Environ 37:153–161. doi: 10.1111/pce.12141

Sharkhuu N, Sharkhuu A (2012) Effects of Climate Warming and Vegetation Cover on Permafrost of Mongolia. Springer Netherlands, pp 445–472

Shuman JK, Shugart HH, O'Halloran TL (2011) Sensitivity of Siberian larch forests to climate change. Glob Chang Biol 17:2370–2384. doi: 10.1111/j.1365-2486.2011.02417.x

Sneath D (2004) Property Regimes and Sociotechnical Systems: Rights over Land in Mongolia's "Age of the Market." In: Property in Question : Value Transformation in the Global Economy. Bloomsbury Academic,

Soja AJ, Tchebakova NM, French NHF, et al (2007) Climate-induced boreal forest change: Predictions versus current observations. Glob Planet Change 56:274–296. doi: 10.1016/j.gloplacha.2006.07.028

Sugimoto A, Yanagisawa N, Naito D, et al (2002) Importance of permafrost as a source of water for plants in east Siberian taiga. Ecol Res 17:493–503. doi: 10.1046/j.1440-1703.2002.00506.x

Tei S, Sugimoto A, Yonenobu H, et al (2014) Growth and physiological responses of larch trees to climate changes deduced from tree-ring widths and δ13C at two forest sites in eastern Siberia. Polar Sci 8:183–195. doi: 10.1016/j.polar.2013.12.002

Terrier A, Girardin MP, Périé C, et al (2013) Potential changes in forest composition could reduce impacts of climate change on boreal wildfires. Ecol Appl 23:21–35. doi: 10.1890/12-0425.1

Thornthwaite CW (1948) An approach toward a rational classification of climate. Geogr Rev 38:55–94.

Tsogtbaatar J (2004) Deforestation and reforestation needs in Mongolia. For Ecol Manage 201:57–63. doi: 10.1016/j.foreco.2004.06.011

Tyree MT (2003) Hydraulic limits on tree performance: transpiration, carbon gain and growth of trees. Trees 17:95–100. doi: 10.1007/s00468-002-0227-x

Tyree MT, Zimmermann MH (2002) Xylem Structure and the Ascent of Sap. Springer Berlin Heidelberg, Berlin, Heidelberg

Verbyla D (2011) Browning boreal forests of western North America. Environ Res Lett 6:41003. doi: 10.1088/1748-9326/6/4/041003

Vicente-Serrano S, Beguería S, López-Moreno J (2010) A multiscalar drought index sensitive to global warming: The standardized precipitation evapotranspiration index. J Clim 23:1696–1718. doi: 10.1175/2009JCLI2909.1

Wigley TML, Briffa KR, Jones PD, et al (1984) On the Average Value of Correlated Time Series, with Applications in Dendroclimatology and Hydrometeorology. J Clim Appl Meteorol 23:201–213. doi: 10.1175/1520-0450(1984)023<0201:OTAVOC>2.0.CO;2

Zhao L, Wu Q, Marchenko SS, Sharkhuu N (2010) Thermal state of permafrost and active layer in Central Asia during the international polar year. Permafr Periglac Process 21:198–207. doi: 10.1002/ppp.688

Chapter 2

Age structure and trends in annual stem increment of *Larix sibirica* in two neighboring Mongolian forest-steppe regions differing in land use history

Elmira Khansaritoreh, Mahammad Eldarov, Kherlenchimeg Ganbaatar, Davaadorj Saindovdon, Christoph Leuschner, Markus Hauck, Choimaa Dulamsuren

Published in **Trees - Structure and Function** 2017, 31: 1973-1986

DOI: 10.1007/s00468-017-1601-z

2.1 Abstract

Climate warming increasingly limits the productivity of boreal forests via increased drought stress especially at the southern fringe of the biome. The southernmost boreal forests are exposed to more intensive human disturbance than most forests at more northern latitudes. We asked the question of how forest use through logging and moderate forest grazing interferes with the climate response of the annual radial stem increment. We conducted a case study in *Larix sibirica* stands of the Mongolian forest-steppe involving two neighboring forest regions (20 km distance) differing in logging and grazing intensity. One site was subjected to heavy logging until 25 years ago and low intensity of livestock grazing; another site was exposed to moderate selective logging and higher, but still moderate livestock numbers. While the differences in grazing had no detectable effect, former heavy logging led to younger and more even-aged forest stands. Forests at both sites showed recent increases in missing-ring frequency, which probably indicate increased drought vulnerability. Climate-response analysis indicated that heavy logging 25 years ago was associated with high sensitivity of stemwood formation to high summer (especially June) temperatures. These findings suggest that (i) recent logging under the conditions of climate warming has increased the sensitivity of tree growth to temperature in these southern boreal forests (ii) high replication at the stand level is needed to avoid bias in dendrochronological analyses in regions exposed to spatially heterogeneous logging intensities.

Key words

Boreal forest; Forest management; Climate response; Global warming; Drought limitation; Tree-ring analysis

2.2 Introduction

The boreal forest region differs from other forest biomes of the northern hemisphere by its cold climate and the limited amount of conversion of forest into agricultural land. During the short growing season, the productivity of boreal forests is usually limited by low summer temperatures, or indirectly via nutrient shortage due to slow organic matter decomposition (Jarvis and Linder 2000). Only recently, parts of the boreal forest turned from temperature and nitrogen limitation to water limitation as the result of climate warming-induced drought (Buermann et al. 2014). The forest-steppes at the continental southern margins of the boreal forest in Inner Asia and at the northern fringe of the Great Plains in North America differ from most of the central boreal forest belt insofar that drought has always been a key factor limiting tree growth (Gunin et al. 1999; Huang et al. 2010). Moreover, the forest-steppe located at the northern fringe of the temperate grassland belt has a long tradition of human land use mainly by mobile and sedentary pastoralists in Inner Asia (Outram et al. 2009) and a shorter history of livestock management in North America (Johnston 1970). Traditional forest use in the forest-steppe ecotone is usually not stand-replacing, as is modern forestry in most of the central boreal forest belt (Östlund et al. 1997; Hansen et al. 2013). Rather, timber harvest is dominated by haphazard selective logging, a practice that is continued in large parts of Inner Asia (Lkhagvadorj et al. 2013a; Dulamsuren et al. 2014). Fire is an additional important factor that affects forest stand dynamics and increases in significance due to rising temperatures and increased human activities (Park et al. 2009; Hessl et al. 2012).

Woodlands at the southern edge of the boreal forest belt have recently attracted increased attention in both Eurasia (Dulamsuren et al. 2013; Liu et al. 2013) and North America (Michaelian et al. 2011; Peng et al. 2011). This is because global warming-related drought has progressively reduced forest productivity and tree regeneration and is the cause of elevated tree mortality in the majority of studied places. Nonetheless, even within the southernmost fringe of the boreal forest contrasting examples have also been found where forests perform increasingly better due to climate warming, since temperature and not water is limiting at high elevation (D'Arrigo et al. 2000; Chen et al. 2012) or due to local increases in precipitation (Dulamsuren et al. 2010; Peng et al. 2011). The climatically induced spatial variation in trends of forest productivity, regeneration and tree mortality is additionally complicated by changes in the stand structure due to logging and forest grazing. These types of land use affect the competition for light, water and nutrients between trees by reducing stand density (Dulamsuren et al. 2014) and influencing the heat transfer to the soil and thus

trigger the melt of permafrost (Park et al. 2009). Furthermore, reduced competition by the ground vegetation as the result of high grazing pressure was found to facilitate seedling establishment. However, livestock grazing suppresses sapling growth and increases the saplings' mortality due to mechanical damage and feeding (Khishigjargal et al. 2013).

Tree-ring studies analyzing the climate response of annual stemwood formation seek to eliminate as much of the non-climatic variation from the tree-ring signal as possible in order to identify the climatic key effectors for the trees' productivity and to use this information for climate reconstruction (Briffa et al. 1996; Briffa 1999). While this practice is mandatory for the study of variations in climate, it reduces the options for analyzing the effects of external disturbances, including land use. We were interested in the combined effect of climate, selective logging and forest grazing on the age structure and stem increment of forests in the forest-steppe ecotone and thus used a combined approach with filtered and unfiltered tree-ring data. Therefore, we carried out a case study in the Mongolian forest-steppe ecotone at the southern edge of the Eurosiberian boreal forest to investigate the variability of age structure, stem increment, and tree mortality at a small spatial scale of some 20 km in stands of the same tree species with known differences in land-use history. At two locations, stands of *Larix sibirica* forest were studied with replicate plots differing in (1) the logging intensity until Mongolia's transition from planned to market economy in 1990, and (2) past and present density of livestock. The first site (site A) was exposed to higher logging intensity until 1990 as well as to lower past and present grazing pressure by livestock than the second site (site B; Table 2.1). At both sites, we distinguished plots at the lower forest border adjacent to steppe grassland from plots in the forest interior, since the forest edge is usually exposed to higher intensities of selective logging and livestock grazing (Khishigjargal et al. 2013; Lkhagvadorj et al. 2013a, b; Dulamsuren et al. 2014). With our study, we tested the hypotheses that (i) trees at the more heavily logged site A are less evenly distributed across age classes than trees at site B, (ii) mean sensitivity of tree-ring series to climate is higher at the less severely logged and thus less disturbed site B, (iii) stem increment at both sites is significantly limited by summer drought, and (iv) trees at both sites exhibit increasing missing-ring frequency since the late twentieth century. A major objective of these investigations was to analyze how severely spatial heterogeneity in land-use practices interferes with the climate response of forest productivity and forest health. As another outcome of our study we expected information on how strongly low replication on the stand level might bias the conclusions drawn from dendrochronological climate-response studies in the forest-steppe ecotone.

2.3 Materials and methods

2.3.1 Study area

Our study was carried out at the southern fringe of the Eurosiberian boreal forest in the forest-steppe of northwestern Mongolia, ca. 630 km west of Ulan Bator and 550 km southwest of Lake Baikal. Mongolia's forest-steppe is strongly dominated by Siberian larch (*Larix sibirica* Ledeb.); the species covers 75−80 % of Mongolia's boreal forest (Tsogtbaatar 2004; MNE 2012). The study was conducted in the northern Khangai Mountains, a large mountain range of central and western Mongolia, which represents a large proportion of Mongolia's forest-steppe landscape. The landscape is typically a vegetation mosaic of forests on north-facing slopes and grasslands on south-facing slopes and in dry valleys. The grasslands are home to pastoral nomad families that hold mixed flocks of livestock, including goats and sheep (most animals), cattle, yak, horses, and occasionally camels (Lkhagvadorj et al. 2013b). This livestock is not herded much and browses the forest, particularly forest edges, in addition to the grassland. Grazing intensity can considerably vary with the spatial distribution of nomad camps and water access, which thus differentially affects biodiversity (Hauck and Lkhagvadorj 2013; Hauck et al. 2014) and forest regeneration (Khishigjargal et al. 2013).

The climate in the Mongolian forest-steppe is highly continental and is imprinted by the stable Siberian High Pressure Cell in the cold winter and warm, short summers. The maximum annual precipitation of roughly 200−300 mm in most forest-steppe regions is mostly delivered in summer. The dominant bedrock type in the study region is siliceous rock, including granite and metamorphic rock (e.g. schist). The prevailing forest soils are Cambisols and Leptosols. The study area is located in the zone of discontinuous permafrost (Sharkhuu and Sharkhuu 2012).

2.3.2 Study sites and sample plot selection

The study sites were located in the Zavkhan province of Mongolia ca. 70−90 km southwest of the city of Tosontsengel (48°45' N, 98°16' E, 1700 m a.s.l.) at the border of the Tosontsengel and Ider administrative subunits of the Zavkhan province. Site A was located at 48°29−31' N, 97°52−54' E with plots distributed over an area of ca. 5 km^2, whereas plots at

site B were located at 48°20−22’ N, 97°41−47’ E and were distributed over an area of ca. 10 km^2 (Fig. S2.1; Table 2.1). Mean elevation of sample plots at site A (2026 m a.s.l., range 1975−2109 m a.s.l.) was 60 m higher than at site B (1966 m a.s.l., range 1917−2027 m a.s.l.). Climatically, the 60-m altitudinal distance implies a mean annual temperature 0.4 °C lower at site A if a temperature lapse rate of 6.5 °C km^{-1} is assumed. Site A was exposed to high logging intensity (selective logging and clear-cuts) due to a saw mill in Tosontsengel which operated until 1990 and was then abandoned as the result of the transformation of Mongolia’s economy from planned to market economy. Afterwards site A was subjected to unplanned occasional selective logging by the local population, as was site B before and after 1990. Site A was traditionally exposed to lower livestock grazing pressure than site B, because site B is located within a settlement area of pastoral nomads. There are no systematic differences in the fire regime of the two sites; variation in fire history in the Mongolian forest-steppe is usually on a small spatial scale due to the widespread logging and grazing influence and the isolated character of forest fragments (Hessl et al. 2012). Potential local variation in the fire history is overcome by high replication in our study.

Table 2.1 General characteristics of study sites A and B in the Khangai Mountains, near Tosontsengel, Mongolia

	Site A	Site B
Logging intensity	High intensity until 1990 (selective logging and clear cuts) Low-intensity selective logging after 1990	Low-intensity selective logging until and after 1990
Livestock grazing	Low	Moderate
Latitude	48°29−31’ N	48°20−22’ N
Longitude	97°52−54’ E	97°41−47’ E
Elevation (m a.s.l.)	1975−2109	1917−2027

A total of 17 plots per site or 34 plots for the entire study were investigated. Eleven replicate plots were selected in the forest interior at each site. Six of the 11 interior plots were randomly selected for establishing six additional neighboring plots occupying the forest edge position (Fig. S2.1 in the Electronic Supplementary Material). Plot size was 20 m × 20 m. All data on the age and stand structure provided in the paper refer only to the forest stands where both forest interior and forest edge plots were selected in order to allow direct comparison between habitats. On these 24 plots (six plots in the forest interior and six plots in the forest

edge per site), a total of 729 *L. sibirica* trees was sampled. Plots in the forest interior were located 50–100 m behind the forest line; plots at the forest edge had the outer limit at the mostly sharp lower (not temperature-driven) forest line at the border to steppe grassland. Each plot (or interior-edge plot pair, respectively) was located in a separate forest. Forests were selected using the rather regular distribution of forest and grassland in the Mongolian forest-steppe with the forests occurring as isolated patches on north-facing slopes. This way neighboring forests were selected within each site (Fig. S2.1). Plot location within a forest was selected randomly. As an exception from random selection, moist depressions were avoided, because they differ in tree growth characteristics from well-drained slopes.

2.3.3 Climate data

Air temperature and precipitation data were available from two manual weather stations run by Mongolia's meteorological agency. The weather station Ider (48°13' N, 97°22' E) is located ca. 30 km (site B) to 50 km (site A) southwest of our sample plots, whereas the weather station Tosontsengel is located ca. 80 km northeast of our plots. The Ider station is thus closer to our plots, but the weather station in Tosontsengel had a better data quality. Weather data in Tosontsengel cover the period from 1964 (precipitation: 1968) to 2012, whereas data from Ider were available from 1973 to 2010. In Tosontsengel, weather recording was disrupted in 1971 causing 2.9 % of missing values in the data set. The quality of the data set in Ider was much worse with 11.8 % and 12.3 % of missing values in the temperature and precipitation data, respectively. While missing temperature data for Ider could be reconstructed with the data from the Tosontsengel using linear regression for monthly mean values ($r = 0.67-0.92$, $P<0.001$), this was not possible for precipitation. We therefore used the data from Tosontsengel for the analysis of the climate response of tree-ring width. Mean annual, July, and January temperatures in Tosontsengel were -5.8, 14.8, and -31.2 °C, respectively, and mean annual precipitation was 224 mm. The less reliable data from Ider suggested somewhat lower precipitation and higher temperatures especially in winter.

2.3.4 Field and laboratory work for tree-ring analysis

Field work was carried out in August 2012. On the 34 plots, which were all monospecific stands of *L. sibirica*, all trees (ca. 1000 individuals) with a stem diameter (at 1.3 m height) of ≥3 cm were included in wood-core sampling for tree-ring analysis. In addition to these

samples from the 20 m × 20 m plots, living old trees located outside the plots were sampled as reference samples to establish long tree-ring chronologies. A total of 140 such trees were additionally sampled; data from these trees were not included in the analysis of age and stand structure. All cores were collected with a 5-mm increment borer (inner diameter). The cores were taken at 1.3 m above the ground in a direction parallel to the contour lines of the mountain slopes to avoid compression wood. Additional data, like trunk circumference, density of branches, dominance (dominant, subdominant and suppressed), and fire traces were recorded in the field.

The wood cores were mounted on wooden strips and the top of the core was shaved off with a microtome blade to make the growth rings visible; the contrast between annual tree rings was enhanced by dusting the surface with chalk dust. The tree-ring width was measured with a precision of 10 µm on a movable object table (Lintab 5, Rinntech, Heidelberg, Germany), the movements of which are electronically transmitted to a computer system equipped with Time Series Analysis and Presentation (TSAP)-Win software (Rinntech).

2.3.5 Evaluation of tree-ring data

The TSAP-Win software was also used for the evaluation of the tree-ring data. Trees were categorized into four age classes including ‘very old trees’ (>160 years), ‘old trees’ (101–160 years), ‘middle-aged trees’ (61–100 years) and ‘young trees’ (≤60 years). Age specifications represent the age of the cambium at 1.3 m above the ground. Tree age is higher than cambial age at 1.3 m, since the tree needs several years to reach that height. Based on the experience from other studies, tree age can be roughly estimated by adding 10 years to the cambial age (Körner et al. 2005; Sankey et al. 2006). The age of the very old trees (>160 cambial years) is partly underestimated by our method because in 4.6 % of these trees the pith was rotten in the center and the relevant wood cores were thus incomplete. Nevertheless, we kept these very old trees in our analysis, because this inaccuracy did not affect any of our conclusions.

The tree-ring series were controlled for missing and unrecognized false rings during cross-dating. Trees with similar growth trends were pooled separately into groups for calculating mean values of annual increment. Merging of tree-ring series to a chronology was based on the coefficient of agreement (‘Gleichläufigkeit’ [GL], Eckstein and Bauch 1969) and (standard) *t*-values. The GL- and *t*-values measure the similarity between tree-ring series in

the high- and low-frequency domain, respectively. Calculation of mean values was considered to be permitted for series with GL >65 % ($P \leq 0.05$) and t >3; with this approach, ca. 95 % of the individual tree-ring series could be incorporated in mean curves for annual stem increment. Trend lines were calculated using 5-year moving averages.

Tree-ring series were representative of the studied stands as shown by the calculation of the expressed population signal (EPS) using sums of squares of within-core variation and error sums of squares calculated in a two-way analysis of variance (ANOVA) (Wigley et al. 1984). The EPS calculated separately for the individual plots exceeded the 0.85-threshold in all cases; in most forest edge plots, however, this threshold was reached not reached before the late twentieth century (Table S2.1).

Original tree-ring series were standardized to extract the climate information and to remove the age-related trend in the data, which is the result of declining productivity at high tree age and the mere geometrical fact that, with increasing stem diameter, the wood is distributed over a larger circumference and thus leads to thinner tree rings (Fritts 1976; Cook 1985; Bräuning 1999). Standardization was achieved by calculating the annual tree-ring index (z_i) of year I, which was derived from the equation $z_i = w_i / m_i$, where w_i is observed tree-ring width and m_i is the moving 5-year average of year i (Dulamsuren et al. 2010). The large sample size in our study reduced the effect of stand-internal disturbances (e.g. the natural death of a neighboring tree) and stand-external disturbances (e.g. insect infestations, fire) or the influence of small-scale variation of site parameters on the tree-ring index.

The relationships between the annual tree-ring index and climate parameters (i.e. monthly mean temperature and monthly precipitation in the year of and prior to tree-ring formation) were analyzed separately for the different age classes using multiple regression analysis and including the complete period covered by the weather data record at the weather station in Tosontsengel. Multiple regression analysis was computed with SAS 9.4 software (SAS Institute Inc., Cary, North Carolina, U.S.A.). Standardized β coefficients were used to quantify the effect of temperature and precipitation in individual months in the climate-response analysis. Climate-response analysis was restricted to the tree-ring series of such forest stands where pairs of plots from the forest interior and forest edge were available (N=6) to enable direct comparison between these habitats.

In order to detect long-term (low-frequency) trends in annual radial stem increment as caused, for instance, by long-term changes in climate, regional growth curves (RGC) were established. In an RGC, the original (non-standardized) annual stem increment is related to tree age instead of the calendar year (Sarris et al. 2007; Dulamsuren et al. 2010). This procedure removes the inter-annual (high-frequency) variation in annual stem increment, but keeps the low-frequency variability, including the age-related trend. Changes in long-term site conditions that control the annual wood production can be inferred from the comparison of RGCs from different tree age classes by comparing the increment at the same cambial age. Comparing data from the same cambial age allows detecting long-term trends not related to tree age. The RGCs were only calculated for the two age classes that were occupied by most of the sample trees, i.e. old and middle-aged trees. Only subdominant trees were integrated in the RGCs, as dominant trees usually have better access to water than other trees. Suppressed trees were excluded, because their productivity is strongly affected by competition for light with other trees.

Mean sensitivity and autocorrelation coefficients (Fritts 1976) were calculated with TSAP-Win from raw increment data over the whole lifespan of each sample tree. Mean sensitivity is a measure for the inter-annual variation of tree-ring width and thus the putative influence of climate, which is usually the most strongly varying influential parameter between consecutive years; mean sensitivity is calculated as the difference in the tree-ring width of consecutive years divided by the mean tree-ring width of the two years. The first-order autocorrelation coefficient quantifies the dependence of tree-ring width on the stem increment in the previous year; first-order autocorrelation is the strength of the linear correlation of the tree-ring width in a given year with the tree-ring width in the previous year calculated for all consecutive years of a tree-ring series. High mean sensitivity in combination with low first-order autocorrelation coefficients is an indication of a large influence of climatic short-term variability on stemwood formation.

2.3.6 Statistics

Arithmetic means ± standard errors are presented throughout the paper. Data were tested for normality with the Shapiro-Wilk test. Pairwise differences (of non-normally distributed data) were tested for significance with Mann-Whitney's *U*-test. Multiple comparisons were done using Duncan's multiple range test. Two-way analysis of variance (ANOVA) was calculated

to quantify the effect of site location and habitat and the interaction between these parameters on age and stand structure. Degrees of freedom (df) for multiple tests are specified for model and error ($df_{model, error}$). All statistical tests were computed with SAS 9.4 software.

2.4 Results

2.4.1 Temperature and precipitation trends

Mean annual temperature at Tosontsengel weather station has increased by 2.4 °C or 0.50 °C decade^{-1} from 1964−2012 (Fig. 2.1a). In contrast to mean annual temperature, mean annual precipitation has remained unchanged since the 1960s (Fig. 2.1b). Significant increases in temperature occurred in all months except for December and January (Fig. 2.1c). The increases in monthly mean temperatures from February to November had slopes of similar magnitude. However, the temperature trends in the recent decades were of higher significance from July to September ($P \leq 0.001$) than in the rest of the year and most pronounced in July (r=0.60), which is the warmest month of the year. As with mean annual precipitation, most months did not show any significant trend for change in the amount of precipitation over time (Fig. 2.1d). Only in May, at the start of the growing season, precipitation showed a significant increase (r=0.32, P=0.01). This increase was partly compensated by a weak insignificant trend for decreasing precipitation in autumn, thus explaining the constant mean annual precipitation (Fig. 2.1b).

The qualitatively less reliable data from the weather station Ider showed an increase in temperature by 2.1 °C or 0.57 °C decade^{-1} from 1973−2010 (data not shown). For monthly mean temperatures, significant increases ($P \leq 0.05$) occurred from March to May and July to November. As in Tosontsengel, the most significant temperature trend over time was found for July (r=0.70, P<0.001). Mean annual precipitation remained constant from 1973−2010 (not shown). In the individual months, there were significant increases in precipitation in May (r=0.48, P=0.002) and from December to February (r=0.40−0.56; $P \leq 0.005$). These increases were associated with weak insignificant trends for declining precipitation from June to September and in April.

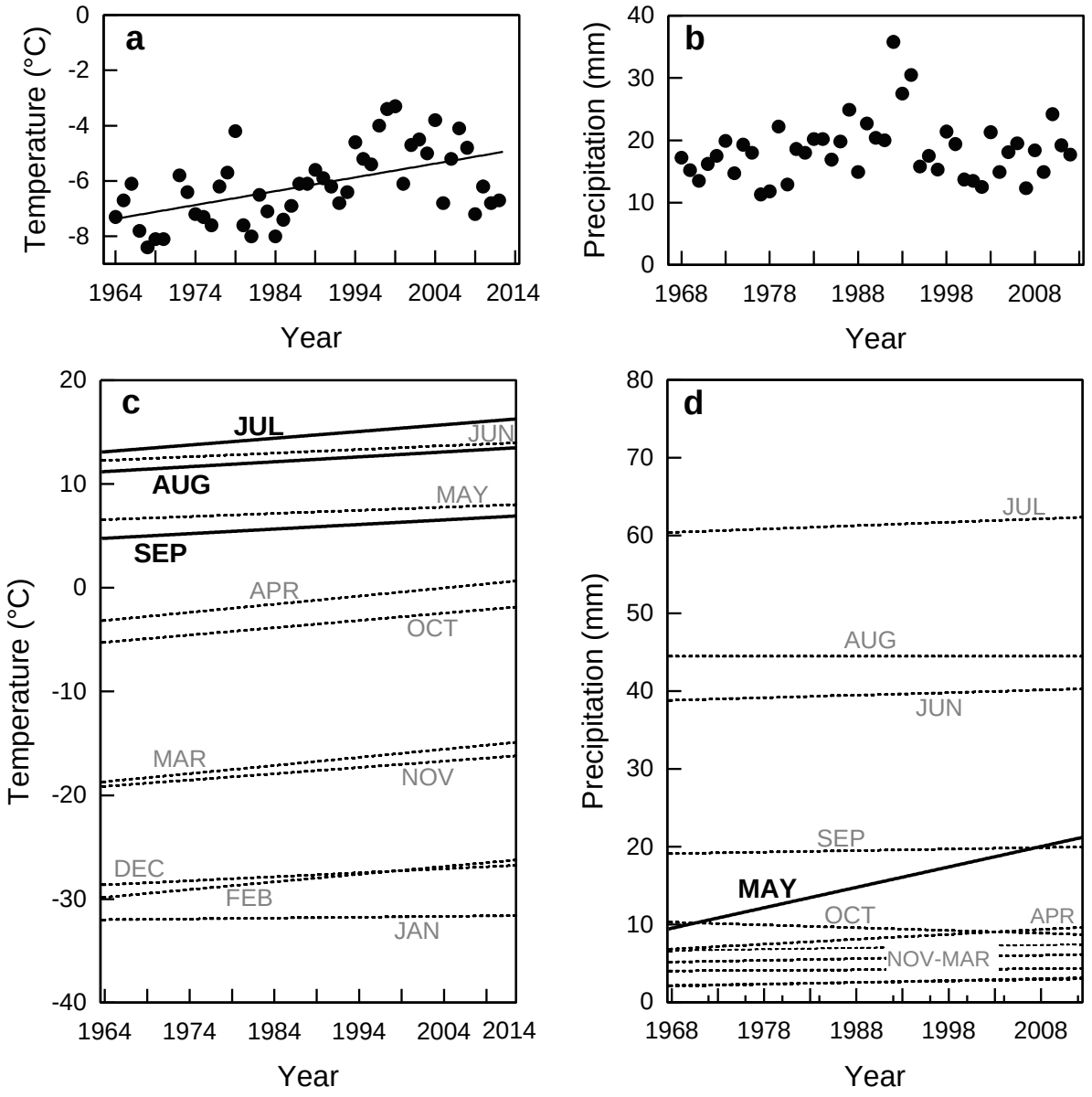

Fig. 2.1 Climate trends in Tosontsengel (48°45' N, 98°16' E, 1700 m a.s.l.), northwestern Mongolia: (a) increase in mean annual temperature ($y = 0.05x - 104.55$, r=0.54, P ≤0.001), (b) mean annual precipitation (no linear trend), (c, d) trends for monthly (c) mean temperature and (d) precipitation

2.4.2 Age and stand structure of the *Larix sibirica* forests

Both the location (site A vs. B) and the habitat (forest interior vs. edge) controlled the age structure, but not the stand structure (in terms of basal area and stand density) of the investigated larch forests (Table 2.2). Two-way ANOVA revealed a significant effect of the location on the percentage of the trees on a plot occurring in the individual age classes. The habitat had a significant effect on the relative abundance of very old and middle-aged trees.

Middle-aged trees represented the largest group of all sample trees (58 %, 421 out of 729 trees), followed by old trees (28 %), very old (8 %) and young trees (6 %). In the forest interior, very old trees were overrepresented and middle-aged trees underrepresented at site B compared to site A (Fig. 2.2). Furthermore, old trees showed an insignificant trend for higher relative abundance at site B. At the forest edges, the relative abundance of middle-aged trees was higher at site A than site B, whereas there was an insignificant trend in the opposite direction for old trees. Very old trees were very rare at forest edges of either location. Young trees were completely absent from site A, but contributed 10 % (forest interior) and 17 % (forest edge) to the total trees population at site B. This difference between sites was detected as being significant in the two-way ANOVA (Table 2.2), but not in the subsequent Duncan's multiple range test (Fig. 2.2).

Table 2.2 Results of two-way ANOVA ($df_{model, error}$=3, 20) analyzing the effect of location (site A vs. B) and habitat (forest interior vs. edge) on the percent of tree individuals in age classes as well as on mean and maximum tree ages, basal area, and stand density

	Total			Location		Habitat		Loc. × Hab.	
	R^2	*F*	*P*	*F*	*P*	*F*	*P*	*F*	*P*
Cambial age:									
>160 yr	0.55	8.2	<0.001	4.2	0.05	14.8	0.001	5.5	0.03
101−160 yr	0.28	2.6	0.08	5.2	0.03	2.5	0.13	0.0	1.00
61−100 yr	0.60	10.0	<0.001	19.9	<0.001	13.4	0.002	1.5	0.23
≤60 yr	0.20	1.7	0.20	5.0	0.04	0.0	0.89	0.0	0.89
Mean age	0.47	6.0	0.005	2.9	0.10	13.4	0.002	1.5	0.23
Max. age	0.32	3.1	0.05	2.0	0.18	7.3	0.01	0.1	0.75
Basal area	0.12	0.9	0.46	2.4	0.14	0.4	0.54	0.0	1.00
Stand density	0.03	0.2	0.88	0.3	0.61	0.3	0.58	0.1	0.77

In terms of absolute numbers, most larch trees forming the interior forest stands at site B have established throughout the complete nineteenth and twentieth centuries (Fig. 2.3b). Most trees growing at the more heavily logged site A established in the early twentieth century (Fig. 2.3a); tree establishment also occurred throughout the nineteenth century, but the number of tree individuals left from that time in today's forest stands at site A was small. At the forest edges, most trees established during the first half of the twentieth century at both sites A and B (Fig. 2.3c, d). At site B, some trees established earlier in the second half of the nineteenth century, whereas trees that germinated during the nineteenth century were virtually absent from site A. Trees that established before the nineteenth century are not included in Fig. 2.3, but occurred at both sites (a total of 8 trees in A and 2 trees in B). The oldest trees at sites A and B had a cambial age of at least 286 and 407 years, respectively.

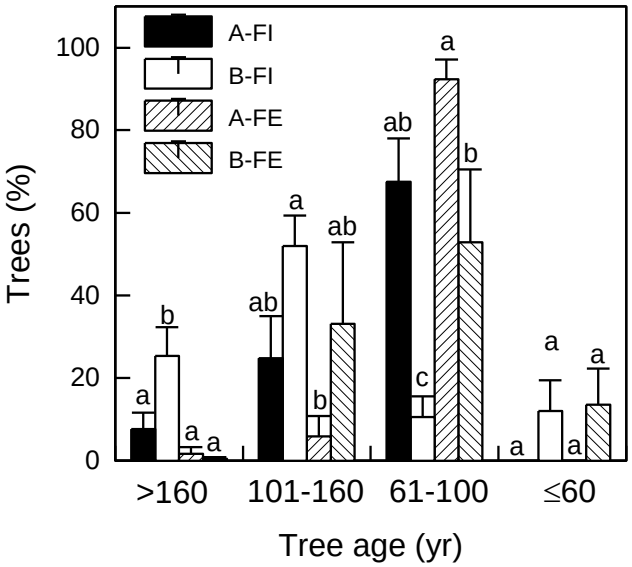

Fig. 2.2 Distribution of sample trees in age classes (cambial age at 1.3 m) in the forest interior (FI) and at the forest edge (FE) of sites A and B. Within the same age class, bars (±SE) sharing a common letter represent means that do not differ significantly ($P \leq 0.05$, Duncan's multiple range test, $df_{model, error}=3, 20$)

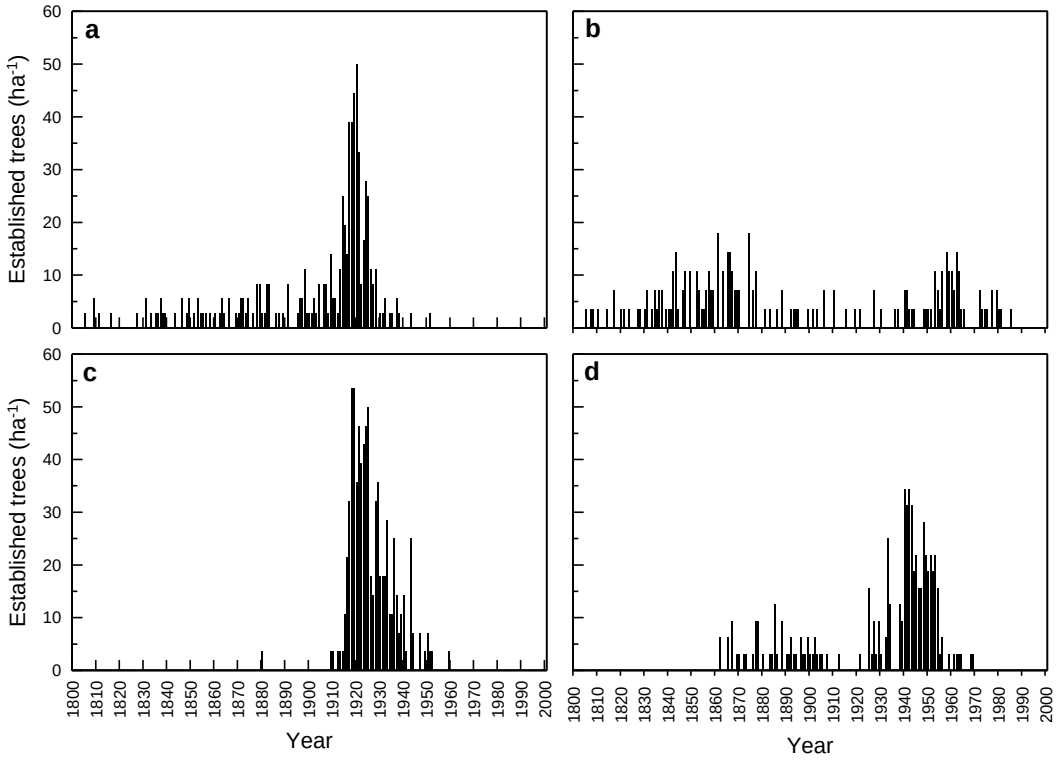

Fig. 2.3 Chronology of the establishment of the present *L. sibirica* populations during the 19th and 20th centuries in (a, b) the forest interior and (c, d) the forest edge of sites A (a, c) and B (b, d). Numbers of trees established before 1800 are not shown

Plot-wise mean and maximum ages were more strongly influenced by the habitat than by the location (Tables 2.1, 2.2). Trees tended to be younger at the edges than in the interior of the forests, though this difference was only significant for mean age at site B in Duncan's multiple range test. There was also a tendency for greater tree age at site B than A, but this trend was only significant for the mean age of trees growing in the forest interior.

Stand basal area and stand density did not differ between sites A and B or between forest interior and forest edge according to the results of both two-way ANOVA (Table 2.2) and Duncan's multiple range test (Table 2.3). However, there were tendencies towards higher values for both parameters at site A compared to site B and in the forest interior compared to the forest edge.

Table 2.3 Mean and maximum ages of *L. sibirica* trees as well as basal area and stand density in the forest interior and at the forest edge of sites A and B[a]

	Site A		Site B	
	FI	FE	FI	FE
Mean age (yr)	113±4 a	91±3 a	139±14 b	95±11 a
Max. age (yr)	214±18 ab	136±27 a	272±42 b	172±39 ab
Basal area (m^{-2} ha)	62±9 a	57±10 a	47±12 a	43±7 a
Stand density (trees ha^{-1})	1196±84 a	1146±238 a	1154±256 a	992±107 a

[a] Within a row, means (±SE) sharing a common letter do not differ significantly ($P \leq 0.05$, Duncan's multiple range test, $df_{model, error}$=3, 20)

2.4.3 Climate-response of the tree-ring index

Climate-response analysis refers to the last part of our tree-ring chronologies since 1964, in an interval of the chronologies with high sample numbers (Fig. 2.4). Mean sensitivity was higher and first-order autocorrelation was lower at the less intensely logged site B than at site A (Table 2.4). Trees from the forest interior that were more than 100 years old had a tendency to be less sensitive than other trees. Climate-response analysis revealed a trend towards weaker correlation of the tree-ring index with monthly mean temperatures and precipitation from middle-aged trees (Table 2.5) to old trees to very old trees at site A (Table S2.2), but not at site B (Table S2.3).

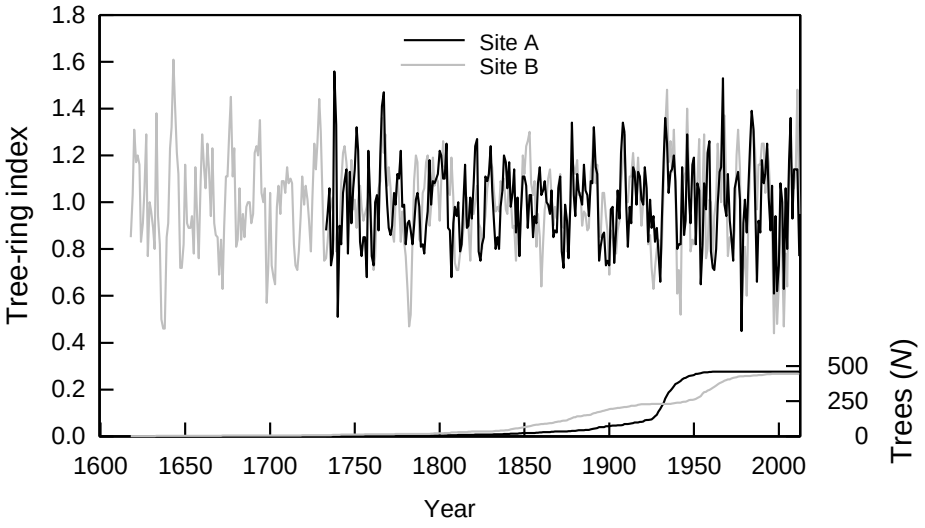

Fig. 2.4 Tree-ring index for *L. sibirica* from the forest interior of sites A and B

Table 2.4 Mean sensitivity and first-order autocorrelation coefficients of *L. sibirica* trees of different age classes from the forest interiors (FI) and the forest edges (FE) of sites A and B

	Mean sensitivity			Autocorrelation		
	Site A	Site B		Site A	Site B	
All trees	0.34±0.00	0.39±0.00	***	0.77±0.01	0.73±0.01	***
>160 yr, FI	0.26±0.01	0.38±0.01	***	0.77±0.02	0.73±0.01	*
>160 yr, FE	−	0.35±0.00		−	0.72±0.02	
101−160 yr, FI	0.27±0.01	0.39±0.01	***	0.81±0.01	0.75±0.01	***
101−160 yr, FE	0.28±0.01	0.37±0.01	***	0.83±0.02	0.76±0.01	**
61−100 yr, FI	0.36±0.01	0.40±0.01	*	0.78±0.01	0.73±0.02	**
61−100 yr, FE	0.35±0.01	0.40±0.01	***	0.75±0.01	0.71±0.01	**
≤60 yr, FI	−	0.43±0.02		−	0.62±0.03	
≤60 yr, FE	−	0.44±0.01		−	0.76±0.01	

The climate-response analysis yielded similar, but weaker correlations for temperature at site B than at site A (Tables 2.4, S2.1, S2.2). The tree-ring index decreased with increasing June and April temperatures of the current growing season and with increasing December and January temperatures at both sites. However, correlations in June were weaker and fewer at site B than at site A and never exceeded the level of marginal significance ($P \leq 0.10$). Positive correlation with May temperature was widespread at site A, but lacking at site B. Sporadic positive correlation of the tree-ring index was found with August temperature of the current year at both sites. On a few plots, stem increment decreased with June and July temperature of the previous summer.

Table 2.5 Response of the tree-ring index of *L. sibirica* trees of middle-aged trees (60−99 years) from the forest interior and forest edge at sites A and B to monthly temperature and precipitation of the year of and the year prior to tree-ring formation[a]

	Temperature											Precipitation									
	Prior year				Current year							Prior year					Current year				
	3	5	6	12	1	2	3	4	5	6	8	4	5	7	8	12	1	2	3	7	8
Site A:																					
FE1									●	□								○			
FE2	○								○	■				●				○			□
FE3					■	●		■	●	■			○					●		○	
FE4					□	○		■	○	■		○			●						
FE5			□	■	□			□	●	■				●				○	○		■
FE6	○				□	●		□	●	□								○			
FI1				■												□	●	○			■
FI2	○								○		●										
FI3	●								○	■						■		□			■
FI4				□	□			□	●	□						■	○				□
FI5								□										○			
FI6	○				□			■	●									○			
Site B:																					
FE1									□					●		□	■		○		
FE2						□		□					○	●		□			○		
FE3		■	□			■												●			
FE4																					
FE5																					
FE6	○					■		■		□				○			□	○			
FI1								■							○					○	
FI2																					
FI3								□					●				□		●		
FI4																					
FI5																					
FI6																					

[a] Correlation significant ($P \leq 0.05$): ● positive, ■ negative correlation; marginally significant ($P \leq 0.10$): ○ positive, □ negative correlation. Months are identified with numbers 1 to 12. FE1−6, forest edge plots no. 1−6; FI1−6, forest interior plots no. 1−6

Correlations between growing season precipitation and the tree-ring index tended to be stronger and more frequent at site B than A (Tables 2.4, S2.1, S2.2). Both sites shared sporadic positive correlations of tree-ring index with July and August precipitation of the previous summer. At site B, positive correlations with June precipitation of the summer prior to tree-ring formation were also found. Further positive correlations were found with April and May precipitation of the previous year, which were, however, stronger at site B than at site A. Precipitation of the current summer was more often correlated with annual stem increment at site B than A. Positive correlation with current June precipitation occurred, albeit sporadically, throughout all age classes at site B, but was completely absent in the data from site A. In a few cases, the tree-ring index was positively correlated with July precipitation and negatively correlated with August precipitation at both sites. In terms of winter precipitation, tree-ring indices were inversely correlated with December precipitation at both sites, whereas positive correlation of the tree-ring index with January and February precipitation (mostly only marginally significant at $P \leq 0.10$) was limited to site A.

2.4.4 Tree-ring width as dependent on time and tree age

Regional growth curves (RGC) revealed that middle-aged trees grew more slowly than old trees at the same cambial age at site A (Fig. S2.2a). The cumulative radial stem increment differed by ca. 20 mm at a cambial age of 75 years ($P<0.001$, *U*-test). At site B, middle-aged trees grew even faster than old trees, though the difference between age classes was less than 10 mm ($P=0.004$, *U*-test). At both sites, trees at the forest edge grew faster at the same cambial age than trees in the forest interior (Fig. S2.3). The original tree-ring data plotted against the calendar year for middle-aged trees representing the largest age class, however, showed that the edge trees' lead in the annual increment has decreased since the 1970s at both sites A and B (Fig. S2.4).

2.4.5 Frequency of missing rings

Missing-ring frequency increased dramatically at the end of the twentieth century and in the early twenty-first century at both sites A and B (Fig. 2.5). The highest percentage of missing rings in the total tree-ring series was found in 2003.

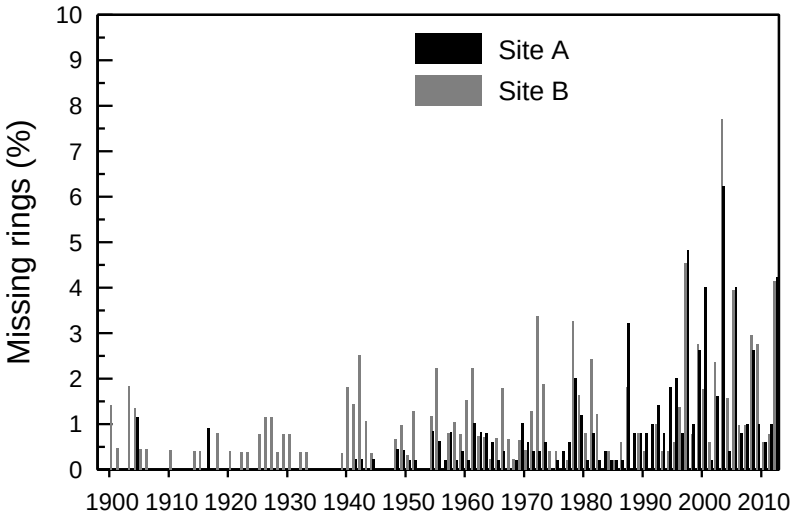

Fig. 2.5 Frequency of trees with missing rings from 1900−2012 for merged data from the forest interior and the forest edge at sites A and B

2.5 Discussion

The larch forests at site A were situated merely some 20 km from neighboring site B. Though these sites shared largely identical topography, elevation, climate, and edaphic characteristics, they clearly differed in the age structure of their forest stands. These differences are certainly the result of heavy logging during the twentieth century at site A, but only sporadic timber harvest at site B. Logging resulted in the removal of old (cambial age of 101−160 years) and very old (>160 years) *L. sibirica* trees from site A. Decreasing numbers of old trees due to timber harvest and deforestation are a global phenomenon and critical for forest biodiversity (Lindenmayer et al. 2012). The strong overrepresentation of middle-aged trees (61−100 years) at site A is the direct consequence of the removal of older trees, which opened space for the next tree generation; the presently middle-aged trees were obviously too small to be attractive for timber harvesting during the period of heavy logging until 1990. The complete lack of young trees (<60 years) at site A is probably also the result of logging, since clear-cutting reduces seed availability and in addition increases soil temperature and reduces soil moisture both immediately by heat storage in the more exposed soil surface and in the long term by the melting of permafrost (Park et al. 2009). Since permafrost is currently on retreat in the Inner Asian forest-steppe due to climate warming (Jin et al. 2007; Sharkhuu and Sharkhuu 2012), its regeneration is not likely under the present climatic conditions. The germination success and seedling survival of *L. sibirica* in the forest-steppe are hampered by high soil temperatures and low soil moisture during the growing season (Dulamsuren et al. 2008). Slower growth of middle-aged relative to old trees at the same age (Fig. S2.2) despite reduced competition due to logging at site A is probably also the result of warmer and drier site conditions. In contrast to site A, sporadic logging in recent decades at site B led to growth releases (Fig. S2.4) and even slightly higher cumulative increment at the same tree age in middle-aged than in old trees. This finding indicates that a dramatic deterioration of the water supply due to increased heat transfer to the soil and permafrost melting has apparently not occurred at the generally less intensely logged site B.

Despite the strong influence of timber harvest on the age structure of the larch stands at site A, the past logging intensity hardly exerted an effect on structural stand characteristics. Although former intense logging has replaced forest stands of heterogeneous age structure with more evenly-aged stands in agreement with our first hypothesis, stand density and basal

area were similar at the present stage of forest development. The dominance of middle-aged trees, however, increases homogeneity in the vertical stand structure, which was not systematically analyzed. The disturbance by former heavy logging activities was reflected by a significant reduction of mean sensitivity and an increase in first-order autocorrelation of tree-ring width. This observation is consistent with our second hypothesis. A reduction of climate sensitivity is likely to have occurred after logging as the result of growth releases due to reduced competition among the remaining trees (Martin-Benito et al. 2011; D'Amato et al. 2013; Dulamsuren et al. 2014).

The results of climate-response analysis could substantiate a high sensitivity of tree-ring index to summer drought only at the heavily logged site A, which is only supportive of the third hypothesis for this site. Since global climate warming has caused a strong recent increase of temperature in the study area, which is, like in many regions of semi-arid Inner Asia, far above the global average (Batima et al. 2005; IPCC 2013), the susceptibility of stem increment to summer drought has apparently caused an increase in missing-ring frequency in the recent past in support of our fourth hypothesis. In contrast to the results of climate-response analysis, increased missing-ring frequencies were found at both study sites. Increased missing-ring frequency has already been observed elsewhere in the Mongolian forest-steppe (Khishigjargal et al. 2014; Khansaritoreh et al. 2017) and other parts of Inner Asia (Liang et al. 2016). Missing-ring frequency is not related to tree age (Lorimer et al. 1999; Khishigjargal et al. 2014; Liang et al. 2016) and thus attributable to climate warming. Missing rings evidence a marked reduction of vitality in these forests and clearly suggest that *L. sibirica* is primarily limited by water availability in this region and thus not by low summer temperatures and probably also not by low nitrogen availability (Chapin et al. 2010; Yarie and Van Cleve 2010). Water limitation of forest productivity was to be expected given the position of the studied forests in the forest-steppe ecotone, but this stressor is increasingly shared by boreal forests even at higher latitudes (Buermann et al. 2014; Tei et al. 2014). The observed peak in the frequency of missing ring in 2003 after three dry and warm years (Fig. 2.1) supports our conclusions.

An interesting detail concerning the putative increased limitation of stem increment by increased summer drought in our study area is the comparison of tree-ring series from the interior and the edges of *L. sibirica* forests (Fig. S2.4). Trees at both sites showed higher radial stem increment at forest edges than in the interior in the mid-twentieth century, but

similar growth rates since the late twentieth century when climate warming accelerated at the global level (IPCC 2013). Apparently, the trees profited from the lower stand density and thus lower intraspecific competition for resources at the forest edge through higher productivity in the cooler mid-twentieth century, but are now equally constrained by summer drought in both habitats. This finding could indicate that the more light-exposed, warmer and better nutrient-supplied forest edges (Dulamsuren and Hauck 2008; Hauck et al. 2012) have recently switched from the limitation by several site factors to merely water-limited systems as the result of climate warming (Chapin et al. 2010).

Although stem increment at both sites was limited by summer drought, the sites exhibited a consistent difference in the details of climate response of tree-ring width. Sensitivity of stemwood formation to summer drought may manifest in correlations of tree-ring width with both summer temperature (negative correlation) and precipitation (positive correlation) (D'Arrigo et al. 2004; Wilmking and Myers-Smith 2008; Dulamsuren et al. 2011; Tei et al. 2014). While the tree-ring index in the formerly heavily logged site A decreased with June temperature, but was never correlated with precipitation, the tree-ring index at site B increased with June precipitation (Tables 2.4, S2.1, S2.2). Correlations with June temperature occurred only sporadically at site B and were merely marginally significant ($P \leq 0.10$). However, even the correlations of the tree-ring index with June precipitation at site B were less frequent than the correlation of tree-ring index of middle-aged trees with June temperature at site A. Since the environmental conditions were comparable between sites A and B and the geographic separation between these sites was small, it is plausible to assume that the different age structure of the *L. sibirica* stands was the key factor that controlled the trees' sensitivity to temperature and precipitation in summer. Middle-aged tree populations are generally more productive than stands that are dominated by old and senescent trees (Schulze et al. 1999; Bond-Lamberty et al. 2004; Girardin et al. 2011). The higher productivity is usually associated with higher water consumption (Bond-Lamberty et al. 2009; Jassal et al. 2009) and constraints due to water shortage increase with stand density (Smith and Long 2001). Therefore, it is plausible to assume that growth of the dominantly middle-aged forests at site A is more sensitive to increases in the atmospheric vapor pressure deficit. Increased summer temperatures under the semi-arid climate of the Inner Asian forest-steppes cause elevated saturation deficits and thus should lead to reduced stomatal conductance and carbon assimilation (Li et al. 2006; Dulamsuren et al. 2009). Correspondingly, increasing summer temperatures at constant precipitation were shown to

cause reductions in the annual stem increment in *L. sibirica* forests in the forest-steppe of eastern Kazakhstan (Dulamsuren et al. 2013). These findings from Kazakhstan suggest decreasing wood formation and probably net primary production by a trend of increasing atmospheric saturation deficits due to climate warming. The positive correlations of the tree-ring index with June temperature combined with a growing frequency of missing rings suggests a similar mechanism in the forests at site A dominated by middle-aged trees, especially since the most relevant correlations were found for middle-aged trees.

The sporadic increases of the tree-ring index with increasing June precipitation and decreasing June temperature at site B with a higher share of old and very old (or in other words overmature and thus less productive) trees could be the result of weaker limitation of net primary production by summer drought than at site A. The assumed weaker drought impact is explicable by lower water consumption of a less productive canopy. Furthermore, permafrost degradation after clear-cut in the formerly more heavily logged site A could cause the presently higher susceptibility of the forests at site A to summer drought than at site B, since soil layers influenced by permafrost can reduce the susceptibility to summer drought by supplying water in addition to the current precipitation (Sugimoto et al. 2003; Li et al. 2006). Unfortunately, we do not have data on the local permafrost distribution in our study regions.

The positive correlation of the tree-ring index with the mean temperature of May, the month when snowmelt typically takes places, at site A, but not at site B, could also be the result of an improved water budget at site A, since high temperatures at snowmelt foster wood formation by increasing the trees' water supply (Sugimoto et al. 2003; Tei et al. 2014). On the other hand, high water consumption in spring through evapotranspiration can also aggravate drought stress later in summer, as the soil water reserves are consumed earlier (Buermann et al. 2013; Parida and Buermann 2014). Earlier rapid spring onset is often combined with superficial snowmelt over the frozen soil and leads to higher water loss by surface runoff than in late springs (Barnett et al. 2005), thereby further aggravating summer water shortage . Apparently trees at site B were not severely limited by summer drought until the recent decades. This is suggested by the fact that presently middle-aged trees at site B revealed faster growth than that formerly seen in the old trees when they had the same age. In the recent past, the missing-ring frequency as an indicator of drought-related stress has increased, even at site B.

The existing differences in the livestock grazing pressure between sites A and B were apparently not effective at influencing the age structure of the studied *L. sibirica* stands, since young trees were found at the more intensely grazed site B, but not at site A. The impact of livestock grazing must therefore be subordinate compared to the effect of timber harvest. The livestock grazing pressure in our study region, the western Khangai Mountains, is generally moderate (Hauck and Lkhagvadorj 2013; Lkhagvadorj et al. 2013a, b). Heavy livestock grazing can exert a significant influence on the age structure of forest stands in the forest-steppe by suppressing regeneration (Sankey et al. 2006). The effect on the recent regeneration was not investigated in our study, since a detailed analysis from a heavily grazed region of the Mongolian forest-steppe already showed that grazing facilitates seedling establishment through the reduction of competition by opening gaps in the ground vegetation (Khishigjargal et al. 2013). However, the abundance and vitality of sapling-sized trees is reduced, since these trees are the preferential food of goats (Khishigjargal et al. 2013), which increasingly dominate the Mongolian livestock (Lkhagvadorj et al. 2013a, b). Despite the proximity of the study sites and the replicate plots, effects of disturbances (e.g. fire, insect infestations) might have differed between individual plots in the centuries covered by our tree-ring data. Such potential differences might explain parts of the within-site variability found in the results of the climate-response analysis.

2.6 Conclusions

Differences in the logging history of *L. sibirica* forests in close proximity (ca. 20 km) with comparable site conditions exerted strong influences on the age structure of these forest stands. This difference was the probable cause of deviations in the climate response of the tree-ring index between site A that was heavily logged until 25 years ago and site B that was continuously used for moderate selective logging. The more heavily logged site A was apparently more susceptible to increased summer temperatures and thus drought than site B. The observed differences in the results of the climate-response analysis on a small spatial scale demonstrate the importance of high replication on the stand level for the generalizability of dendrochronological results in the Inner Asian forest-steppe, which is characterized by high spatial heterogeneity in terms of forest structure and land-use intensity. Our results also suggest that heavy logging might aggravate the detrimental impact of climate warming on forests in the drought-prone forest-steppes of Inner Asia.

Author contribution statement

CD and MH conceived of and designed the study; CD, KG, DS and MH performed field work; EK, CD, and ME conducted tree-ring measurements and analyzed these data. EK, CD, MH and CL wrote the manuscript.

Acknowledgments

The study was supported by a grant of the Volkswagen Foundation to M. Hauck, Ch. Dulamsuren and Ch. Leuschner for the project "Forest regeneration and biodiversity at the forest-steppe border of the Altai and Khangai Mountains under contrasting developments of livestock numbers in Kazakhstan and Mongolia". E. Khansitoreh received an Erasmus Mundus Scholarship in the Salam 2 program. We are thankful to the director of the Tarvagatai Nuruu National Park, Ms. D. Tuya, for her support during field work.

Conflicts of interest

The authors declare that they have no conflict of interest.

References

Barnett TP, Adam JC, Lettenmaier DP (2005) Potential impacts of a warming climate on water availability in snow-dominated regions. Nature 438:303-309

Batima P, Natsagdorj L, Gombluudev P, Erdenetsetseg B (2005) Observed climate change in Mongolia. Assess Impact Adapt Clim Change Work Pap 12:1-26

Bond-Lamberty B, Wang C, Gower ST (2004) Net primary production and net ecosystem production of a boreal black spruce wildfire chronosequence. Glob Change Biol 10:473-487

Bond-Lamberty B, Peckham SD, Gower ST, Ewers BE (2009) Effects of fire on regional evapotranspiration in the central Canadian boreal forest. Glob Change Biol 15:1242-1254

Bräuning A (1999) Zur Dendroklimatologie Hochtibets während des letzten Jahrtausends. Dissert Bot 312:1-164

Briffa KR (1999) Interpreting high-resolution proxy climate data – the example of dendroclimatology. In: Storch H, Navarra A (Eds.) Analysis of climate variability. Springer, Berlin, pp 77-94

Briffa KR, Jones PD, Schweingruber FH, Karlén W, Shiyatov SG (1996) Tree-ring variables as proxy-climate indicators: problems with low-frequency signals. In: Jones PD, Bradley RS, Jouzel J (Eds.) Climatic variations and forcing mechanisms of the last 2000 years. Springer, Berlin, pp 9-41

Buermann W, Parida BR, Jung M, Burn DH, Reichstein M (2013) Earlier springs decrease peak summer productivity in North American boreal forests. Environ Res Lett 8 (024027):1-10

Buermann W, Parida BR, Jung M, MacDonald GM, Tucker CJ, Reichstein M (2014) Recent shift in Eurasian boreal forest greening response may be associated with warmer and drier summers. Geophys Res Lett, doi: 10.1002/2014GL059450

Chapin FS, McGuire AD, Ruess RW et al. (2010) Resilience of Alaska's boreal forest to climatic change. Can J For Sci 40:1360-1370

Chen F, Yuan YJ, Wei WS, Fan ZA, Zhang TW, Shang HM, Zhang RB, Yu SL, Ji CR, Qin L (2012) Climatic responses of ring width and maximum latewood density of *Larix sibirica* in the Altay Mountains reveals recent warming trends. Ann For Sci 69:723-733

Cook ER (1985) A time series analysis approach to tree ring standardization. PhD thesis, Univ. Arizona, Tucson

D'Amato AW, Bradford JB, Fraver S, Palik BJ (2013) Effects of thinning on drought vulnerability and climate response in north temperate forest ecosystems. Ecol Appl 23:1735-1742

D'Arrigo RD, Jacoby GC, Pederson N, Frank D, Buckley B, Baatarbileg N, Mijiddorj R, Dugarjav R (2000) Mongolian tree-rings, temperature sensitivity and reconstructions of Nothern Hemisphere temperature. Holocene 10:669-672

D'Arrigo RD, Kaufmann RK, Davi N, Jacoby GC, Laskowski C, Myneni RB, Cherubini P (2004) Thresholds for warming-induced growth decline at elevational tree line in Yukon Territory, Canada. Glob Biogeochem Cycl 18 (GB3021):1-7

Dulamsuren Ch, Hauck M (2008) Spatial and seasonal variation of climate on steppe slopes of the northern Mongolian mountain taiga. Grassl Sci 54:217-230

Dulamsuren Ch, Hauck M, Mühlenberg M (2008) Insect and small mammal herbivores limit tree establishment in northern Mongolian steppe. Plant Ecol 195:143-156

Dulamsuren Ch, Hauck M, Bader M, Osokhjargal D, Oyungerel Sh, Nyambayar S, Runge M, Leuschner C (2009) Water relations and photosynthetic performance in *Larix sibirica* growing in the forest-steppe ecotone of northern Mongolia. Tree Physiol 29:99-110

Dulamsuren Ch, Hauck M, Khishigjargal M, Leuschner HH, Leuschner C (2010) Diverging climate trends in Mongolian taiga forests influence growth and regeneration of *Larix sibirica*. Oecologia 163:1091-1102

Dulamsuren Ch, Hauck M, Leuschner HH, Leuschner C (2011) Climate response of tree-ring width in *Larix sibirica* growing in the drought-stressed forest-steppe ecotone of northern Mongolia. Ann For Sci 68:275-282

Dulamsuren Ch, Wommelsdorf T, Zhao F, Xue Y, Zhumadilov BZ, Leuschner C, Hauck M (2013) Increased summer temperatures reduce the growth and regeneration of *Larix sibirica* in southern boreal forests of eastern Kazakhstan. Ecosystems 16:1536-1549

Dulamsuren Ch, Khishigjargal M, Leuschner C, Hauck M (2014) Response of tree-ring width to climate warming and selective logging in larch forests of the Mongolian Altai. J Plant Ecol 7:24-38

Eckstein D, Bauch J (1969) Beitrag zur Rationalisierung eines dendrochronologischen Verfahrens und zur Analyse seiner Aussagesicherheit. Forstwiss Centralbl 88:230-250

Fritts HC (1976) Tree rings and climate. Academic Press, London

Girardin MP, Bernier PY, Gauthier S (2011) Increasing potential NEP of eastern boreal North American forests constrained by decreasing wildfire activity. Ecosphere 2 (25):1-23

Gunin PD, Vostokova EA, Dorofeyuk NI, Tarasov PE, Black CC (1999) Vegetation dynamics of Mongolia. Kluwer, Dordrecht

Hauck M, Lkhagvadorj D (2013) Epiphytic lichens as indicators of grazing pressure in the Mongolian forest-steppe. Ecol Indic 32:82-88

Hauck M, Javkhlan S, Lkhagvadorj D, Bayartogtokh B, Dulamsuren Ch, Leuschner C (2012) Edge and land-use effects on epiphytic lichen diversity in the forest-steppe ecotone of the Mongolian Altai. Flora 207:450-458

Hauck M, Dulamsuren Ch, Bayartogtokh B, Ulykpan K, Burkitbaeva UD, Otgonjargal E, Titov SV, Enkhbayar T, Sundetpaev AK, Beket U, Leuschner C (2014) Relationships between the diversity patterns of vascular plants, lichens and invertebrates in the Central Asian forest-steppe ecotone. Biodivers Conserv 23:1105-1117

Hansen MC, Potapov PV, Moore R et al. (2013) High-resolution global maps of 21st-century forest cover change. Science 342:850-853

Hessl AE, Ariya U, Brown P, Byambasuren O, Green T, Jacoby G, Kennedy Sutherland E, Nachin B, Maxwell RS, Pederson N, De Grandpré L, Saladyga T, Tardif JC (2012) Reconstructing fire history in central Mongolia from tree-rings. Int J Wildland Fire 21:86-92

Huang J, Tardif JC, Bergeron Y, Denneler B, Berninger F, Girardin MP (2010) Radial growth response of four dominant boreal tree species to climate along a latitudinal gradient in the eastern Canadian boreal forest. Glob Change Biol 16:711-731

IPCC (2013) Climate change 2013: the physical science basis. Contribution of working group I to the fifth assessment report of the Intergovernmental Panel on Climate Change. Cambridge University Press, Cambridge

Jarvis P, Linder S (2000) Constraints to growth of boreal forests. Nature 405:904-905

Jassal RS, Black TA, Spittlehouse DL, Brümmer C, Nesic Z (2009) Evapotranspiration and water use efficiency in different-aged Pacific Northwest Douglas-fir stands. For Ecol Manag 149:1168-1178

Jin H, Yu Q, Lü L, Guo D, He R, Yu S, Sun G, Li Y (2007) Degradation of permafrost in the Xing'anling Mountains, northeastern China. Permafrost Periglac Process 18:245-258

Johnston A (1970) A history of rangelands of western Canada. J Range Manag 23:3-8

Khansaritoreh E, Dulamsuren Ch, Klinge M, Ariunbaatar T, Bat-Enerel B, Batsaikhan G, Ganbaatar Kh, Saindovdon D, Yeruult Y, Tsogtbaatar J, Tuya D, Leuschner C, Hauck M (2017) Higher climate warming sensitivity of Siberian larch in small than large forest

islands in the fragmented Mongolian forest steppe. Glob Change Biol, doi: 10.1111/gcb.13750

Khishigjargal M, Dulamsuren Ch, Lkhagvadorj D, Leuschner C, Hauck M (2013) Contrasting responses of seedling and sapling densities to livestock density in the Mongolian forest-steppe. Plant Ecol 214:1391-1403

Khishigjargal M, Dulamsuren Ch, Leuschner HH, Leuschner C, Hauck M (2014) Climate effects on inter- and intra-annual larch stemwood anomalies in the Mongolian forest-steppe. Acta Oecol 55:113-121

Körner C, Sarris D, Christodoukalis D (2005) Long-term increase in climatic dryness in the East-Mediterranean evidenced for the island of Samos. Reg Environ Change 5:27-36

Lkhagvadorj D, Hauck M, Dulamsuren Ch, Tsogtbaatar J (2013a) Pastoral nomadism in the forest-steppe ecotone of the Mongolian Altai under a changing economy and a warming climate. J Arid Environ 88:82-89

Lkhagvadorj D, Hauck M, Dulamsuren Ch, Tsogtbaatar J (2013b) Twenty years after decollectivization: mobile livestock husbandry and its ecological impact in the Mongolian forest-steppe. Human Ecol 41:725-735

Li SG, Tsujimura M, Sugimoto A, Sasaki L, Yamanaki T, Davaa G, Oyunbaatar D, Sugita M (2006) Seasonal variation in oxygen isotope composition of waters for a montane larch forest in Mongolia. Trees 20:122-130

Liang EY, Leuschner C, Dulamsuren Ch, Wagner B, Hauck M (2016) Global warming-related tree growth decline and mortality on the north-eastern Tibetan Plateau. Climatic Change 134:163-176

Lindenmayer DB, Laurance WF, Franklin JF (2012) Global decline in large old trees. Science 338:1305-1306

Liu H, Williams AP, Allen CD, Guo D, Wu X, Anenkhonov OA, Liang EY, Sandanov DV, Yin Y, Qi Z, Badmaeva NK (2013) Rapid warming accelerates tree growth decline in semi-arid forests of Inner Asia. Glob Change Biol 19:2500-2510

Lorimer CG, Dahir SE, Singer MT (1999) Frequency of partial and missing rings in *Acer saccharum* in relation to canopy position. Plant Ecol 143:189-202

Martin-Benito D, Kint V, del Río M, Muys B, Cañellas I (2011) Growth completion and productivity: Past trends and future perspectives. For Ecol Manag 262:1030-1040

Michaelian M, Hogg EH, Hall RJ, Arsenault E (2011) Massive mortality of aspen following severe drought along the southern edge of the Canadian boreal forest. Glob Change Biol 17:2084-2094

MNE (2012) Forest resources of Mongolia. Mongolia Ministery of Environment and Green Development, Government Agency of Forests, Ulan Bator (in Mongolian).

Östlund L, Zackrisson O, Axelsson A-L (1997) The history and transformation of a Scandinavian boreal forest landscape since the 19th century. Can J For Sci 27:1198-1206

Outram AK, Stear NA, Bendrey R, Olsen S, Kasparov A, Zaibert V, Thorpe N, Evershed RP (2009) The earliest horse harnessing and milking. Science 323:1332-1335

Parida BR, Buermann W (2014) Increasing summer drying in North American ecosystems in response to longer nonfrozen periods. Geophys Res Lett, doi: 10.1002/2014GL060495

Park YE, Lee DK, Stanturf JA, Woo SY, Zoyo D (2009) Ecological indicators of forest degradation after forest fire and clear-cutting in the Siberian larch (*Larix sibirica*) stand of Mongolia. J Korean Forestry Soc 98: 609-617

Peng C, Ma Z, Lei X, Zhu Q, Chen H, Wang W, Liu S, Li W, Fang X, Zhou X (2011) A drought-induced pervasive increase in tree mortality across Canada's boreal forest. Nature Clim Change 1:467-471

Sankey TT, Montagne C, Graumlich L, Lawrence R, Nielsen J (2006) Lower forest-grassland ecotones and 20th century livestock herbivory effects in northern Mongolia. For Ecol Manag 233:36-44

Sarris D, Christodoukalis D, Körner C (2007) Recent decline in precipitation and tree growth in the eastern Mediterranean. Glob Change Biol 13:1187-1200

Schulze E-D, Lloyd J, Kelliher FM (1999) Productivity of forests in the Eurosiberian boreal region and their potential to act as a carbon sink – a synthesis. Glob Change Biol 5:703-722

Sharkhuu N, Sharkhuu A (2012) Effects of climate warming and vegetation cover on permafrost of Mongolia. In: Werger MJA, van Staalduinen MA (Eds.) Ecological problems and livelihoods in a changing world. Springer, Dordrecht, pp 445-472.

Smith FW, Long JN (2001) Age-related decline in forest growth: an emergent property. For Ecol Manag 144:175-181

Sugimoto A, Naito D. Yanagisawa N, Ichiyanagi K, Kurita N, Kubota J, Kotake T, Ohata T, Maximov TC, Fedorov AN (2003) Characteristics of soil moisture in permafrost observed in East Siberian taiga with stable isotopes of water. Hydrol Process 17:1073-1092

Tei S, Sugimoto A, Yonenobu H, Ohta T, Maximov TC (2014) Growth and physiological responses of larch trees to climate changes deduced from tree-ring widths and $\delta^{13}C$ at two forest sites in eastern Siberia. Polar Sci 8:183-195

Tsogtbaatar J (2004) Deforestation and reforestation needs in Mongolia. For Ecol Manag 201:57-63

Wigley TML, Briffa KR, Jones PD (1984) On the average value of correlated time series, with applications in dendroclimatology and hydrometeorology. J Clim Appl Meteorol 23:201-213

Wilmking M, Myers-Smith I (2008) Changing climate sensitivity of black spruce (*Picea mariana* Mill.) in a peatland-forest landscape in Interior Alaska. Dendrochronologia 25:167-175

Yarie J, Van Cleve K (2010) Long-term monitoring of climatic and nutritional affects on tree growth in interior Alaska. Can J For Sci 40:1325-1335

Supporting information

Table S2.1 Expressed population signal (EPS) in tree-ring series from the replicate plots from the forest interior (FI) and forest edge (FE) at site A and B included in the climate-response analysis[a]

Plot	Site A	Site B
FI1	≥0.88 (1880)	≥0.89 (1950)
FI2	≥0.86 (1890)	≥0.97 (1965)
FI3	≥0.90 (1910)	≥0.85 (1855)
FI4	≥0.89 (1895)	≥0.88 (1890)
FI5	≥0.85 (1915)	≥0.88 (1860)
FI6	≥0.90 (1885)	≥0.93 (1890)
FE1	≥0.98 (1905)	≥0.86 (1885)
FE2	≥0.97 (1970)	≥0.98 (1975)
FE3	≥0.97 (1950)	≥0.86 (1905)
FE4	≥0.93 (1960)	≥0.96 (1891)
FE5	≥0.88 (1965)	≥0.88 (1900)
FE6	≥0.98 (1970)	≥0.97 (1970)

Table S2.2 Response of the tree-ring index of *L. sibirica* trees of different age classes from the forest interior and forest edge at site A to monthly temperature and precipitation of the year of and the year prior to tree-ring formation[a]

	Temperature											Precipitation									
	Prior year				Current year							Prior year					Current year				
	3	5	6	12	1	2	3	4	5	6	8	4	5	7	8	12	1	2	3	7	8
Very old trees (>160 years):																					
FE1																					
FE2																					
FE3																					
FE4																					
FE5																					
FE6																					
FI1																					
FI2	○						○										○				
FI3																					
FI4																					
FI5																					
FI6					■	○		■	●	●		○			●			○			
Old trees (101-160 years):																					
FE1	●					○		■		■		○		●							
FE2																					
FE3																					
FE4																					
FE5																					
FE6																					
FI1				□		○	○	□			○	○				●					
FI2	○	□					○	■		□				●							
FI3								■		■								●			
FI4						●		■	○		○	○	○		○	●		○			
FI5	○							■			●						○	○			
FI6																					
Middle-aged trees (60-99 years):																					
FE1									●	□								○			
FE2	○								○	■				●				○			□
FE3					■	●		■	●	■			○					●		○	
FE4					□	○		■	○	■		○			●						
FE5			□	■	□			□	●	■				●				○	○		■
FE6	○				□	●		□	●	□								○			
FI1				■												□	●	○			■
FI2	○								○		●										
FI3	●								○	■						■		□			■
FI4				□	□			□	●	□						■	○				□
FI5								□										○			
FI6	○				□			■	●									○			

[a] Correlation significant ($P \leq 0.05$): ● positive, ■ negative correlation; marginally significant ($P \leq 0.10$): ○ positive, □ negative correlation. Months are identified with numbers 1 to 12. FE1−6, forest edge plots no. 1−6; FI1−6, forest interior plots no. 1−6

Table S2.3 Response of the tree-ring index of *L. sibirica* trees of different age classes from the forest interior and forest edge at site B to monthly temperature and precipitation of the year of and the year prior to tree-ring formation[a]

	Temperature										Precipitation										
	Prior year						Current year				Prior year							Current year			
	3	4	6	7	11	12	1	4	6	8	4	5	6	7	8	9	12	3	6	7	8
Very old trees (>160 years):																					
FE1						■	□		□		○		●	●	●		□	○			
FE2																					
FE3																					
FE4																					
FE5																					
FE6																					
FI1																					
FI2				○	□			□			●										
FI3							■						●	●	○		□	○			
FI4								□		●											
FI5				■		□											□		○		
FI6																					
Old trees (101-160 years):																					
FE1								□													
FE2																					
FE3						□	□	□					○	●	○						
FE4								■						○		□			●		
FE5													●	●	○	□					
FE6																					
FI1								□													
FI2														○							
FI3												●	●			■	■		○		
FI4								■		○											
FI5														○			□		○		
FI6																					
Middle-aged trees (60-99 years):																					
FE1									□					●		□	■		○		
FE2						□		□				○		●		□			○		
FE3		■	□			■												●			
FE4																					
FE5																					
FE6	○					■	■		□					○			□	○			
FI1							■								○					○	
FI2																					
FI3								□				●					□		●		
FI4																					
FI5																					

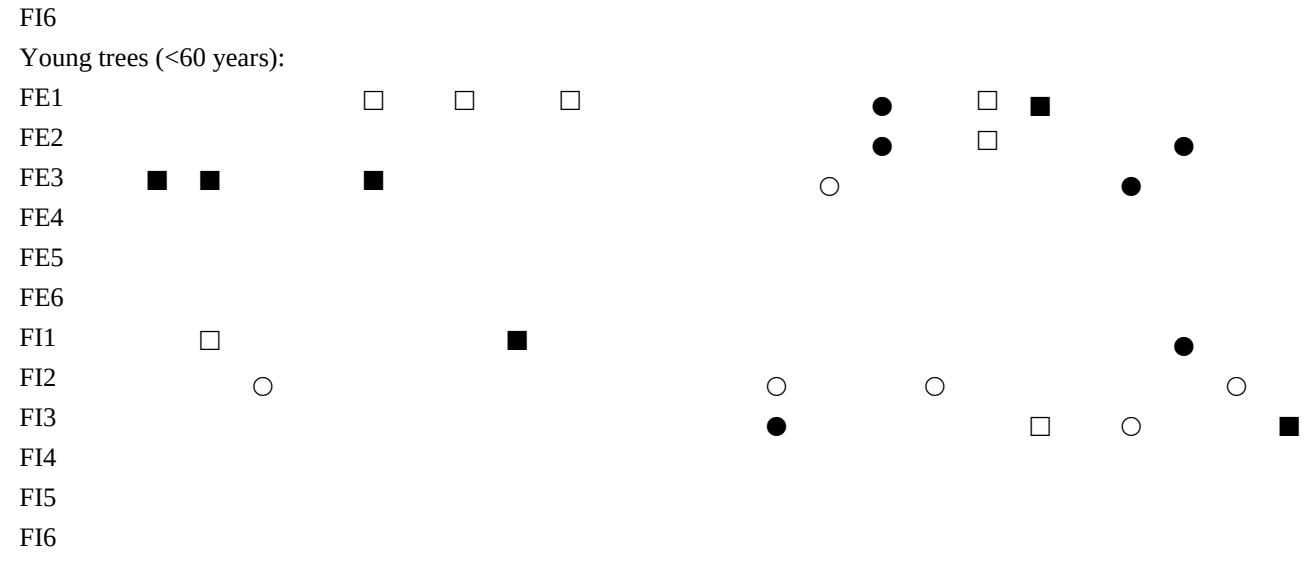

[a] Correlation significant ($P \leq 0.05$): ● positive, ■ negative correlation; marginally significant ($P \leq 0.10$): ○ positive, □ negative correlation. Months are identified with numbers 1 to 12. FE1−6, forest edge plots no. 1−6; FI1−6, forest interior plots no. 1−6

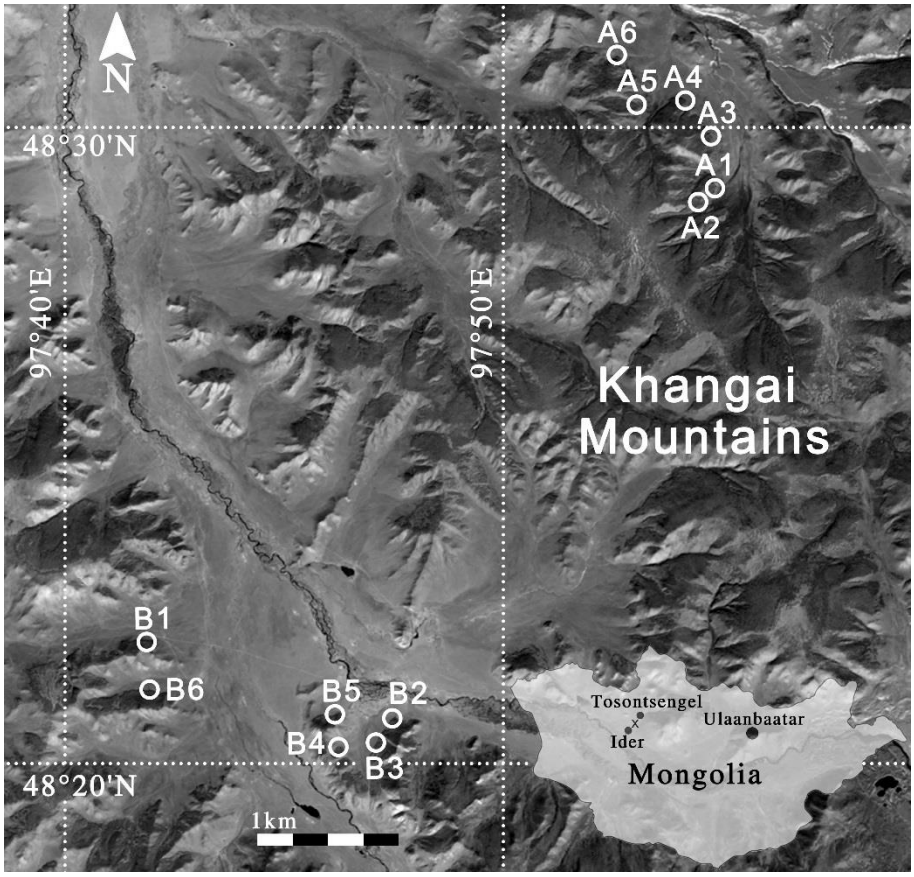

Fig. S2.1 Location of study sites A and B in north-western Mongolia with replicate plots used for the analysis of age and stand structure of *L. sibirica* forests. Each dot represents a pair of neighboring plots from the forest interior and the forest edge

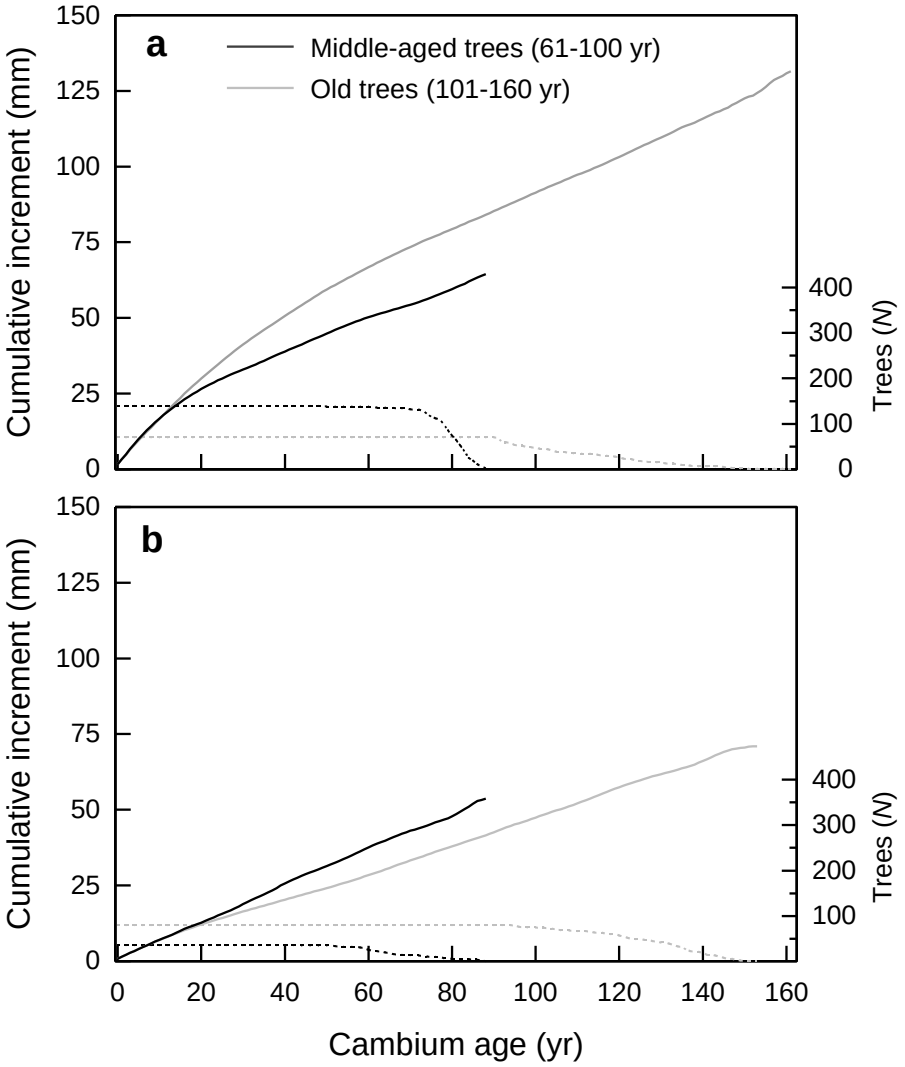

Fig. S2.2 Cumulative regional growth curves (RGC) for middle-aged and old trees of *L. sibirica* from the forest interior of sites A (a) and B (b)

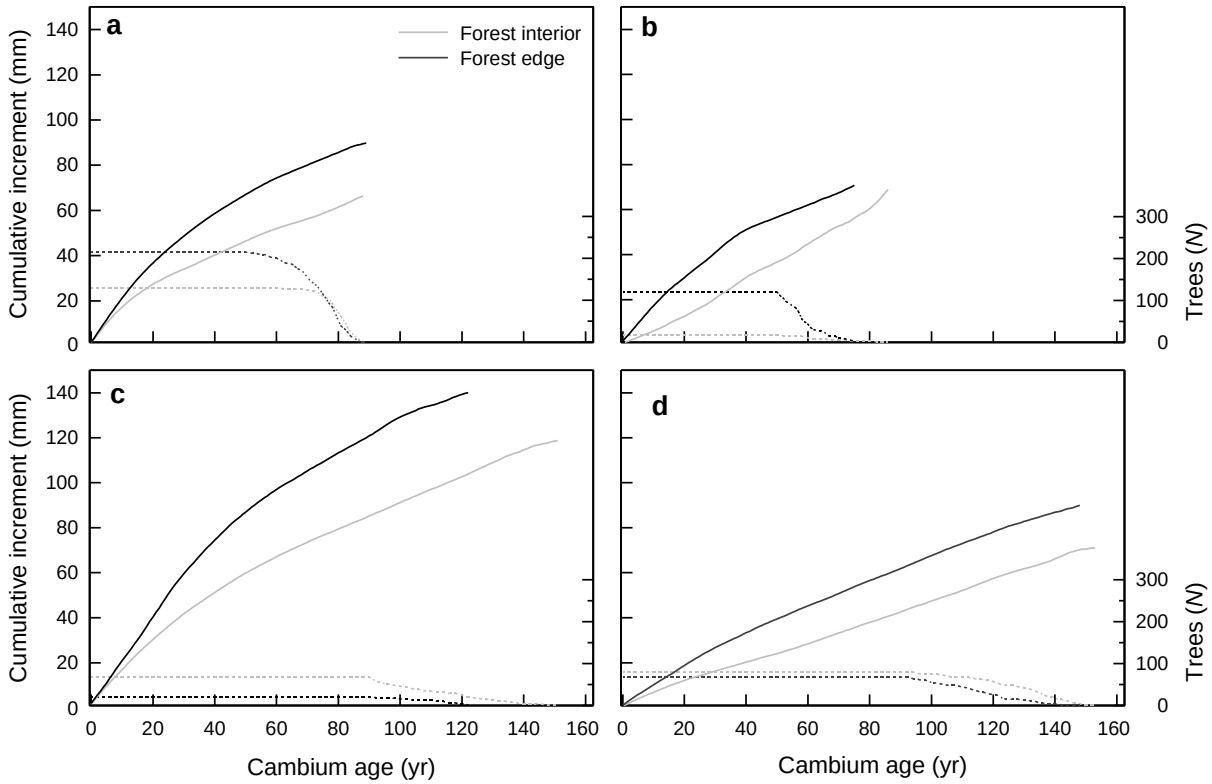

Fig. S2.3 Cumulative regional growth curves (RGC) showing the difference in the cumulative stem increment for (a, b) middle-aged and (c, d) old trees of *L. sibirica* from (a, c) sites A and (b, d) B

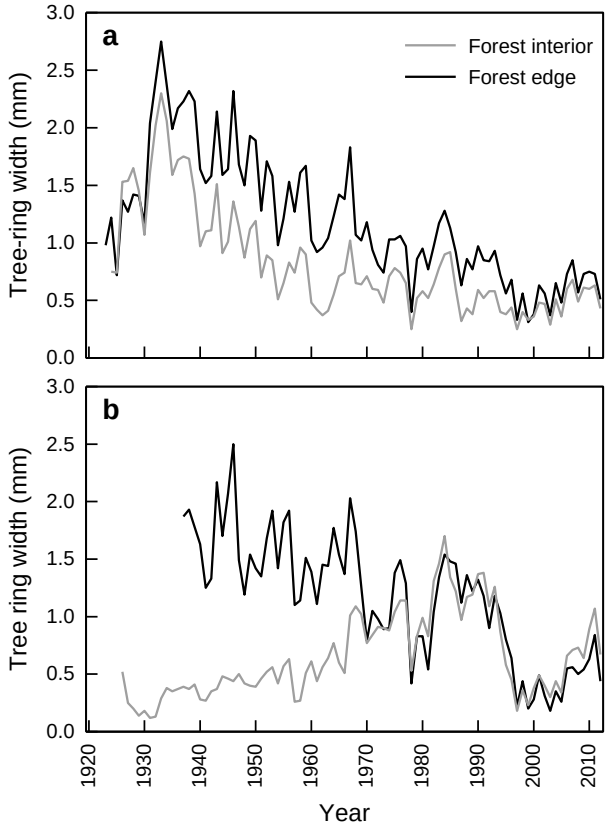

Fig. S2.4 Tree-ring width of middle-aged trees at the forest interior and the forest edge at sites (a) A and (b) B

Chapter 3

Higher climate warming sensitivity of Siberian larch in small than large forest islands in the fragmented Mongolian forest steppe

Elmira Khansaritoreh, Choimaa Dulamsuren, Michael Klinge, Tumurbaatar Ariunbaatar, Banzragch Bat-Enerel, Ganbaatar Batsaikhan, Kherlenchimeg Ganbaatar, Davaadorj Saindovdon, Yolk Yeruult, Jamsran Tsogtbaatar, Daramragchaa Tuya, Christoph Leuschner, Markus Hauck

Published in **Global Change Biology** 2017, 23:3675-3689

DOI: 10.1111/gcb.13750

3.1 Abstract

Forest fragmentation has been found to affect biodiversity and ecosystem functioning in multiple ways. We asked whether forest size and isolation in fragmented woodlands influences the climate warming sensitivity of tree growth in the southern boreal forest of the Mongolian *Larix sibirica* forest-steppe, a naturally fragmented woodland embedded in grassland, which is highly affect by warming, drought and increasing anthropogenic forest destruction in recent time. We examined the influence of stand size and stand isolation on the growth performance of larch in forests of four different size classes located in a woodland-dominated forest-steppe area and small forest patches in a grassland-dominated area. We found increasing climate sensitivity and decreasing first-order autocorrelation of annual stemwood increment with decreasing stand size. Stemwood increment increased with previous year's June and August precipitation in the three smallest forest size classes, but not in the largest forests. In the grassland-dominated area, the tree growth dependence on summer rainfall was highest. Missing ring frequency has strongly increased since the 1970s in small, but not in large forests. In the grassland-dominated area, the increase was much greater than in the forest-dominated landscape. Forest regeneration decreased with decreasing stand size and was scarce or absent in the smallest forests. Our results suggest that the larch trees in small and isolated forest patches are far more susceptible to climate warming than large in continuous forests pointing to a grim future for the forests in this strongly warming region of the boreal forest that is also under high land use pressure.

Keywords: habitat fragmentation, boreal forest, Siberian larch (*Larix sibirica*), global warming, deforestation, tree-ring analysis, missing rings, forest regeneration

3.2 Introduction

Effects of global climate warming on boreal forests have been reported from different areas of this vegetation belt (Lloyd & Bunn, 2007). Rising temperatures can either lead to increased productivity and the advancement of treelines if low summer temperatures are limiting, or result in decreased productivity and even increased rates of tree mortality, if the vegetation is limited by moisture availability. Buermann et al. (2014) showed that moisture limitation has become increasingly relevant in the recent past. Climate-response analyses of tree-ring width (Barber et al., 2000) as well as analyses of drought-induced missing ring frequency (Khishigjargal et al., 2014), tree mortality (Peng et al., 2011), forest regeneration (Bond-Lamberty et al., 2014), and treeline position (Kullman & Öberg, 2009) have been published repeatedly that elucidate the response of boreal forest trees to different climatic trends.

Interaction of other factors with the climate warming sensitivity of boreal forests is less well studied. Probably most attention has been paid to the interaction of climate warming with fire and their combined effect on vegetation. While increased drought intensity increases fire frequency and intensity (Girardin et al., 2009), the replacement of conifers by broadleaved pioneer stands following the disturbance reduces the likelihood and the effect of forest fires (Terrier et al., 2013). The impact of insect herbivores on boreal forests is usually thought to increase negative effects of climate warming, since herbivore life cycles are accelerated and overwinter survival is increased (Ayres & Lombardero, 2000). The ability to defend herbivores of conifers are affected by drought, since a reduced turgor of xylem parenchyma cells decreases, though not the production of resin, but the pressure gradient along which it is transported to wounded tissue (Rossner & Hannrup, 2004). Climate warming can also establish new herbivore-host plant relationships through asynchronous range shifts (Hódar & Zamora, 2004).

The structure of forest stands also interacts with climate warming, as stand structure influences the competition between trees for water. Therefore, stand density is generally inversely correlated with water availability (McDowell & Allen, 2015). This was also shown in the boreal forest of Mongolia, where trees at forest edges with reduced stand density had less tense water relations and higher tree-ring widths than in the forest interior (Dulamsuren et al., 2010; Chenlemuge et al., 2015). The influence of other stand-structural characteristics on the climate warming sensitivity of forests is much less explored.

We addressed the question how forest fragmentation interacts with the sensitivity of moisture-limited boreal forest stands to global climate warming. The forest-steppe ecotone of Mongolia is characterized, like other forest-steppe ecotones in mountainous terrain, by a mosaic of boreal forest patches at the moistest places on north-facing mountain slopes and grasslands on south-facing slopes. This natural pattern creates forest islands of varying size, while the forest stands have been additionally fragmented by human activities due to industrial logging, forest fires, and the combined impact of wood extraction and forest grazing by mobile pastoralists (Erdenechuluun, 2006; Lkhagvadorj et al. 2013a). Hansen et al. (2013) identified Mongolia as one of the world's countries with the highest rates of recent net loss of forest area.

Forest fragmentation results in the reduction of stand size and also in the isolation of forest stands. The effects of forest fragmentation or habitat isolation in general have mostly been studied with respect to changes in biodiversity (Robinson et al., 1992; Fahrig, 2003). In addition to isolation effects, forest fragmentation enhances edge effects with increasing temperature extremes and a drier microclimate found in forest islands as compared to the interior of continuous forest stands (Saunders et al., 1991; Debinski & Holt, 2000). Fragmentation may also affect the nutrient status of soil and plants mediated via differences in microclimate, atmospheric inputs, and differences in decomposition rate (Bierregaard et al., 1992; Didham, 1997).

There are several potential factors in small forest patches of the Mongolian forest-steppe that could differ from the conditions in continuous forests and might influence the trees' vigor and productivity. These factors include microclimate, since temperature should reach more extreme maxima and minima in small forests, whereas air humidity and soil moisture should be higher and less variable in the interior of continuous forests (Chen et al., 1995, 1999). Due to the characteristic type of land use in the Mongolian forest-steppe with mobile pastoralists, who house with their livestock in the grasslands around the forests and make their living off the use of local ecosystem services, forest stand size can also be assumed to influence land use intensity. Small forests are likely to be more severely affected by forest grazing which contributes to the suppression of forest regeneration (Khishigjargal et al., 2013). Furthermore, pastoralists in Mongolia satisfy their needs for fuel and construction wood preferentially from forests in the neighborhood of their dwellings and from forest edges in particular

(Dulamsuren et al., 2014). This practice should result in higher anthropogenic disturbance of the stand structure with decreasing stand size.

To study the putatively complex interaction of forest fragmentation with productivity and stand structure, we conducted tree-ring analyses and stand surveys in forests of Siberian larch (*Larix sibirica*) of varying stand size in the Mongolian forest-steppe (Fig. S3.1 in the Supporting Information). The objective of our study was to test the hypotheses that (1) decreasing stand size increases climate sensitivity and thus the susceptibility to summer drought of radial stem increment, (2) the frequency of drought-induced missing rings increases with decreasing stand size, and (3) forest regeneration success increases with increasing stand size. In addition to stands of varying size, we compared forest islands of the same size in a forest-dominated subregion with isolated stands in a grassland-dominated subregion to test the hypothesis (4) that forests in the grassland-dominated landscape are more sensitive to variation in climate, since climatic parameters can be expected to be more variable here than in forest-dominated areas of the forest-steppe ecotone. Validation of our hypotheses would imply that forest fragmentation would aggravate the already widespread drought-induced reductions in forest productivity in moisture-limited boreal forests.

3.3 Materials and methods

3.3.1 Study area

Field work was carried out in August 2014 near Tosontsengel (Zavkhan province, 48°45’ N, 98°16’ E, 1700 m a.s.l.) in the forest-steppe of Mongolia, c. 630 km W of Ulan Bator and 550 km SW of Lake Baikal. The Inner Asian forest-steppe regions form the southernmost part of the spacious Eurosiberian boreal forest region. Except for some temperature-limited forests that are mostly located near the alpine treeline (Jacoby et al., 1996; Chen et al., 2012; Dulamsuren et al., 2014), most studied forests in the forest-steppe ecotone are drought-limited and thus susceptible to rising temperatures (e.g. Davi et al., 2010; Dulamsuren et al., 2010a, 2013; Liu et al., 2013). Drought limitation was evidently predominant in this area since a long time, because the forest border in the Central Asian steppe region is located in a north-south precipitation gradient, where water shortage is the principal factor limiting tree growth (Gunin et al., 1999).

The southern boreal forests in Mongolia (c. 73,800 km², Dulamsuren et al., 2016) consist mostly of stands strongly dominated by Siberian larch (*Larix sibirica* Ledeb.). Therefore, we selected monospecific *L. sibirica* forests for our study. Forest stands in the study area were subjected to industrial timber harvest in the second half of the twentieth century until 1990, but were used for unsystematic selective logging by the rural population afterwards. The forest-steppe area is home to mobile pastoralists, who keep mixed herds of sheep, goats, cattle, yak, and horses on common pastures. Livestock is not much herded and animals preferentially graze on grassland, but also penetrate into the forests along the edges and further into the interior, when the forest islands are small (Lkhagvadorj et al., 2013b).

The dominant bedrock type in the study region is siliceous rock, including granite and metamorphic rock (e.g. schist). In addition, cover beds of aeolian sand of up to several meters thickness occur upon the lower slope positions. The prevailing forest soils are Cambisols and Leptosols. The study area is located in the zone of discontinuous permafrost (Sharkhuu & Sharkhuu, 2012).

3.3.2 Climate of the study region

According to weather data available since 1964 (temperature) and 1968 (precipitation), the climate near Tosontsengel is highly continental with long cold winters and short summers, resulting in a subzero mean annual air temperature of -5.8 °C (July 14.8°C, January -31.2 °C). Mean annual precipitation is as low as 224 mm and peaks in July. Air temperature in Tosontsengel has increased by 0.44 K decade^{-1} since the 1960s, whereas mean annual precipitation did not show any trend. In this period, monthly temperatures have increased in all months, except in December and January; the strongest increase was found from July to September. The seasonal distribution of precipitation has changed to a certain degree with a shift from autumn to spring (May).

3.3.3 Study design

We selected forests of four different size classes (classes F1 to F4, Table 3.1) in a subregion of our study area with high forest-to-grassland ratio (Fig. 3.1) to analyze the influence of patch size on tree growth patterns. In the smallest size class, we also selected forest stands in a subregion with low forest-to-grassland ratio (class G1). Forest-dominated and grassland-dominated subregions (Fig. S3.1) were compared in order to analyze the influence of the degree of isolation on forest productivity and stand structure. Such influences could be mediated by differences in microclimate and land use intensity. Three replicates were studied for each plot type (F1 to F4 and G1) yielding a total of 15 sampled forests. The F-type plots were selected from clusters where all four size classes were represented in order to reduce potential effects of physiographic heterogeneity within the study area. The clusters were evenly distributed over the forest-dominated subregion, while the individual forest patches of the different size classes were randomly selected within each cluster. The plots in the grassland-dominated subregion were also randomly selected among the available forest stands of the smallest size class. Selection of clusters and plots was based on remote sensing analysis of forest distribution in the study region. Forest stands that recently had changed their size class were not selected as sample plots (see below). Plots of 20 m × 20 m were selected in the interior of each forest stand and the geographic position was determined by GPS. Selection was by random, though moist depressions, which are not characteristic for

most of the forest area, were avoided. The outermost 30 m of the forests were excluded from the plot search to avoid bias by direct edge effects. As a result from this random selection procedure, the plots were not necessarily located right in the center of the forest stands (Table 3.1). To account for spatial heterogeneity in the forest islands, two plots were selected per forest stand and tree-ring chronologies were pooled for these subplots (Fig. 3.2). These subplots were selected randomly within a radius of 100 m from the first randomly selected subplot, still following the rule that a minimum distance of 30 m from the nearest forest edge had to be kept.

Table 3.1 Plot types selected to study the effect of forest stand size and isolation

Class	Forest size (km^2)	Forest-to-grassland ratio	Realized size (km^2)	Distance to lower forest line (m)	Elevation (m a.s.l.)
F1	<0.1	High	0.04±0.00	98±27	1943±98
F2	0.1−1.0	High	0.15±0.04	173±13	1923±45
F3	1.1−5.0	High	2.9±0.8	153±42	1946±46
F4	>5.0	High	30.2±7.6	297±20	1978±42
G1	<0.1	Low	0.09±0.02	82±24	1981±45

Arithmetic means ±SE. 'Realized size' specifies the forested area of the specific stands selected for sampling in contrast to size classes ('forest size') that were used for defining the plot types.

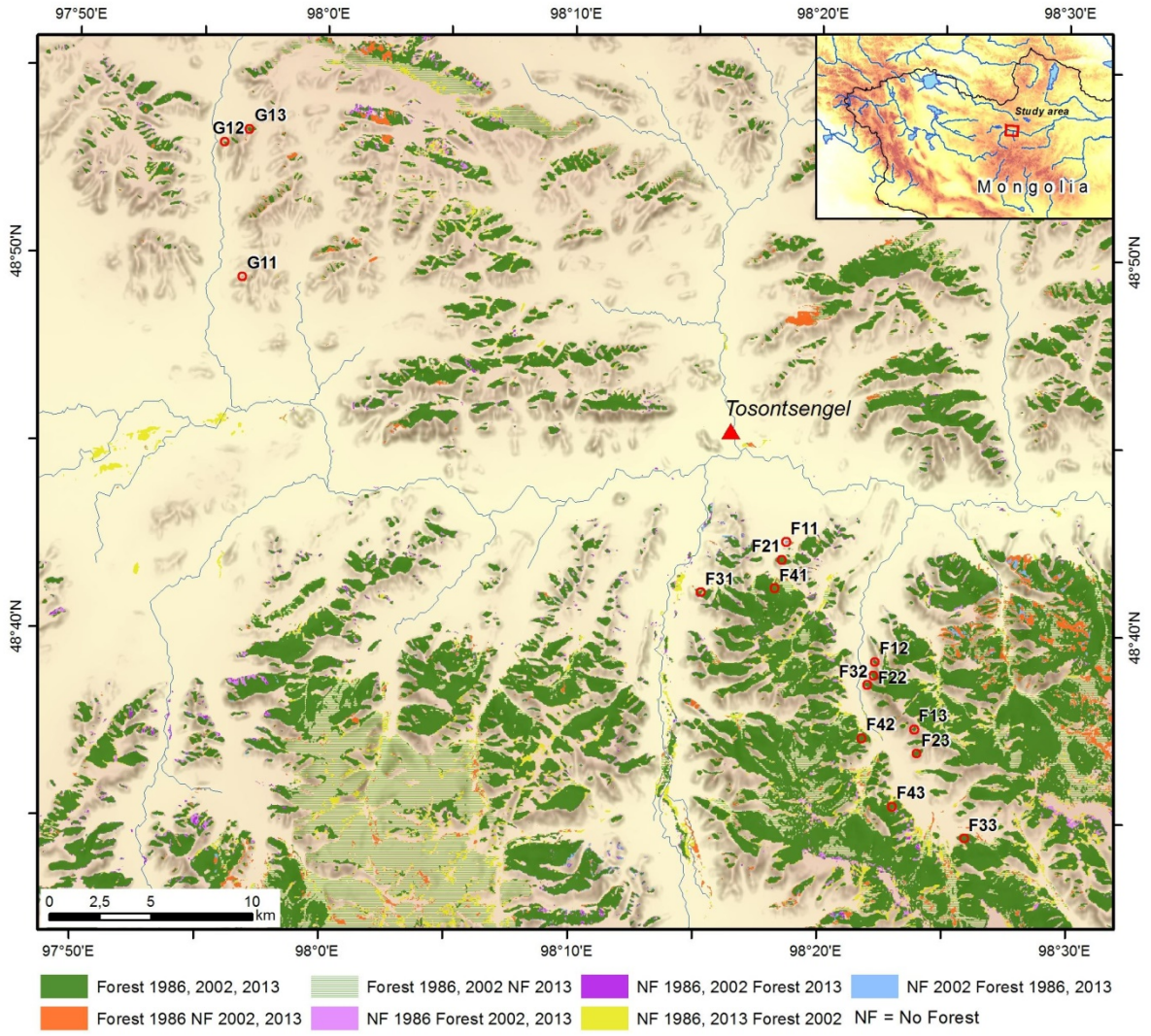

Fig. 3.1 Study area near Tosontsengel, Mongolia with distribution of clusters of forest stands of different size (increasing from F1/G1 to F4) in subregions with high (F1 to F4, south-eastern part of the study area) or low (G1, north-western part) forest-to-grassland ratio. Forest area changes between 1986 (Landsat 5, July 23), 2002 (Landsat 7, June 9), and 2013 (Landsat 8, September 19) are indicated by different signatures. The last digit in the stand numbers specifies plot clusters 1-3.

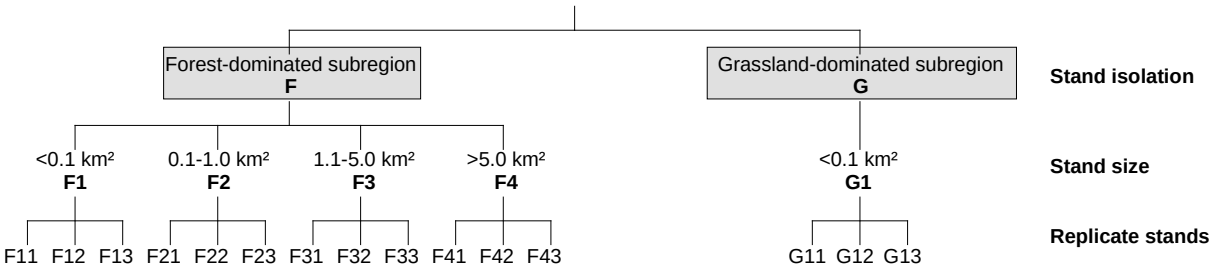

Fig. 3.2 Plot design for studying the effect of stand isolation (forest-dominated vs. grassland-dominated area) and, within the forest-dominated subregion, stand size on *Larix sibirica* stands. Two plots of 20 m × 20 m were studied per replicate stand; data per stand were averaged.

3.3.4 Structural characteristics and humus layer depth of the studied forest stands

Stand structure was studied in order to assess how well the studied stands of the different plot types were comparable in terms of basic structural characteristics. The different plot types (F1-F4, G1) did not differ significantly in their stand density (c. 1100-1880 trees ha^{-1}) and basal area (30-44 m^2 ha^{-1}) or in the mean (107-157 years) and maximum ages (c. 270-340 years) of *L. sibirica* trees (Duncan's multiple range; Table S3.1). None of the aforementioned parameters increased or decreased with stand size, except for mean tree age in the forest-dominated subregion, which showed a tendency for decrease with stand size. This trend was the result of the increasing occurrence of young (≤60 year-old) trees with stand size; trees ≤60 years were even absent from the smallest stands (<0.1 km^2) of the forest-dominated subregion (F1). Forests in the grassland-dominated subregion of the same size (G1) had high numbers of ≤60-year-old trees (Table S3.1). For the other tree age classes, no change in abundance with forest size was detected. The stand types did not differ significantly in the depth of the organic layer (c. 2 cm), nor of the Ah horizon (c. 7-11 cm; Table S3.1).

3.3.5 Stand microclimate

Below-canopy microclimate was measured to characterize the temperature, humidity and moisture conditions of in dependence of stand size and stand isolation. Air temperature and relative air humidity were recorded in every sample plot using HOBO U23 ProV2 sensors (Onset Computer Cooperation, Bourne, Massachusetts, U.S.A.). The sensors were placed on the northern side of three randomly selected trees at c. 150 cm above the ground. Temperature and relative air humidity were logged hourly for one year from August 2014 to July 2015. Soil temperature was recorded with tempmate B4 Miniature Hygrologgers (imec Messtechnik, Heilbronn, Germany) in one randomly selected plot cluster within the smallest (F1) and the largest (F4) forest stands for the same period. Sensors were placed in soil profiles at 1 cm, 50 cm, 100 cm, 150 cm, and 200 cm depth in the F1 plot and at 1 cm, 50 cm, 100 cm, 125 cm, 150 cm, and 175 cm in the F4 plot. In the F4 plot, sensors were not installed up to 200 cm depth, because deep permafrost hampered the installation. Soil temperature was recorded twice a day at 3:00 AM and 3:00 PM.

3.3.6 Remote sensing analysis of forest distribution

The remote sensing analysis of forest distribution was performed with ArcGIS 3.2. The aim of the analysis was to determine stand sizes and to study the temporal dynamics of forest stand sizes to avoid that the results from tree-ring analysis were influenced by recent fluctuations in stand size. The forest distribution in the study area was determined by supervised classification of a Spot 6 multispectral satellite image of September 14, 2014. The spatial resolution of this image of 1.6 m × 1.6 m enabled a detailed delineation of forest stands and isolated trees. The classification result was visually corrected and transformed into vectored data. The size of the single polygons bordering the closed forests was used to calculate the forest areas. To proof the spatial permanence of the investigated forests during the last 30 years, a change detection analysis was performed using three different Landsat satellite images: Landsat 5 TM of July 23, 1986; Landsat 7 ETM+ from June 9, 2002; Landsat 8 OLT/TIRS of September 19, 2013. Initially the forest distribution of every satellite image was delineated by supervised classification. The computed forest areas of every time slice were subtracted from each other to analyze potential area changes. The spatial resolution of Landsat images of 30 m × 30 m induces a minor inaccuracy depending on the relative portion of trees in one pixel. Therefore, single trees cannot be detected and the borders of closed forests can slightly alternate between the different classifications. However, closed forests are generally satisfactorily distinguished. Although there was forest disturbance by fire in the surrounding region, a significant change in forested area during the studied period can be ruled out for the investigated sites.

3.3.7 Field and laboratory methods related to tree-ring analysis and stand surveys

Tree-ring analysis, including the analysis for the climate response of tree-ring width, for missing rings and for forest regeneration, formed the central part of our study. Wood cores from all *L. sibirica* trees (1755 individuals) with a stem diameter of ≥3 cm, were collected with an increment borer with an inner diameter of 5 mm at 1.3 m height above the ground. Samples were taken parallel to the contour lines of the mountain slopes to avoid compression wood. In order to use more reference samples to establish long-term tree-ring chronologies, old trees growing in the neighborhood of the plots were also sampled (in total 135 trees; F1: 29, F2: 46, F3: 32, F4: 6, G1: 22 trees). These trees were included in the tree-ring chronologies, but not in the analysis of age and stand structure. Only 1198 trees were

included in tree age analyses, since incomplete cores (primarily due to rotten pith) had to be excluded. Additional data, such as trunk circumference, tree height, dominance (dominant, subdominant and suppressed), and fire scars were recorded in the field. The recent regeneration of *L. sibirica* was analyzed by counting seedlings and saplings (stem diameter <3 cm at 1.3 m height, or trees not reaching 1.3 m height) of 5 different height classes (<50 cm, 50-100 cm, 100-150 cm, 150-200 cm, >200 cm) in the field. Stem cross-sections were collected from randomly selected individuals of each size class to assess sapling age. For analyzing the effect of selective logging, tree stumps were counted. We distinguished visually between stumps remaining from logged trees and those originating from natural mortality.

Wood cores were mounted on wooden strips with grooves to hold the cores and then they were cut lengthwise with a microtome. The contrasts between annual tree rings were brought out with chalk. The tree-ring width was measured to an accuracy of 10 µm using a Lintab 5 measuring system (Rinntech, Heidelberg, Germany). The shifts of a movable object table were electronically transmitted to a computer system equipped with Time Series Analysis and Presentation (TSAP)-Win software (Rinntech). Stem cross-sections of saplings were soaked in distilled water for one week and then cut with a sliding microtome (Hn 40, Reichert-Jung, Nußloch, Germany) into 20-25 µm thick sections. Tree rings were counted on images from sections stained with safranin and alcian blue.

3.3.8 Evaluation of tree-ring data

Tree-ring data were evaluated with the TSAP-Win software. We classified trees into four age classes including 'very old trees' (>160 years), 'old trees' (101-160 years), 'middle-aged trees' (61-100 years), and 'young trees' (≤60 years) according to their cambial age at 1.3 m above the ground. For identifying the year of establishment, 10 years were added to cambial age. Thirty-eight percent of very old trees and 8% of old trees had rotten piths so that their year of establishment could not be determined.

Tree-ring series were cross-dated to check the quality of the tree-ring counts and to identify missing rings (i.e. years without stemwood formation). Tree-ring series integrated in a mean curve had to have a coefficient of agreement ('Gleichläufigkeit' [GL], Eckstein & Bauch, 1969) >65% and a (standard) *t*-value >3. These criteria were met by c. 90% of the samples. The applied parameters measure the similarity between tree-ring series in the high- (GL) and low-frequency (*t*) domains, respectively. Trend lines were calculated applying 5-year moving averages. Standardization of tree-ring series to remove the age-dependent decline of tree-ring width (Carrer & Urbinati, 2004; Helama et al., 2004) was done by applying the equation $z_i = w_i/m_i$, where z_i is the tree-ring index, w_i is the tree-ring width, and m_i is the 5-year moving average of year *i* (Dulamsuren et al., 2010b). High replication on the tree level was applied to minimize the effect of stand-internal disturbances (e.g. the natural death of a neighboring tree) and stand-external disturbances (e.g. insect infestations, fire, selective logging), tree-specific characteristics resulting from genetic variation, and the effect of small-scale variation of site parameters on the tree ring index. The expressed population signal (EPS; Wigley et al. 1984) was calculated to quantify how well our tree-ring series represented the stem increment dynamics of the studied stands (Table S3.3). The EPS was calculated separately for age classes using Arstan software (Cook & Holmes 1984). Good representation by a given tree-ring series is accepted at EPS >0.85.

Climate-response analysis was conducted separately for the different age classes in each patch size using monthly means of temperature and precipitation from the complete interval covered by the climate station in Tosontsengel. The strength and direction of the correlation were quantified with standardized beta coefficients. All tree-ring series that could be correctly cross-dated and that were complete for the period where climate data were available were included (1514 trees). This number included the tree-ring series with missing rings. In

addition to climate-response analysis, principal component analysis (PCA) was calculated for the tree-ring index in variation of monthly temperature and precipitation values.

While the tree-ring index removes much of the long-term (low-frequency) variation of annual stem increment, regional growth curves (RGC) were applied to remove age-related long-term trends, but to keep all other long-term trends in annual stem increment (Sarris et al., 2007; Dulamsuren et al. 2010b). In RGC, the cumulative annual stem increment is plotted versus age (and not the calendar year). Long-term trends that are not related to tree age are detected by comparing the stem increment between different age classes of trees at a given age.

Raw increment data over the whole lifespan of each tree was used to calculate the mean sensitivity and the autocorrelation coefficient of the tree-ring series. The sensitivity is a measure for the intensity of climate signals in the tree-ring series. The autocorrelation coefficient provides information of the physiological buffering capacity of trees. Mean sensitivity was calculated as the difference in the tree-ring width of consecutive years divided by the mean tree-ring width of the two years. First-order autocorrelation, which analyzes the linear correlation of tree-ring width in a given year with tree-ring width in the previous year, was calculated for all consecutive years of each tree-ring series. High autocorrelation, despite inter-annual variations in climate, suggests that the tree is able to compensate for climatically unfavorable conditions with its stored carbohydrates.

3.3.9 Statistical analyses

Arithmetic means ± standard errors are presented throughout the paper. Data were tested for normal distribution with the Shapiro-Wilk test. Multiple comparisons were made with Duncan's multiple range test. Degrees of freedom (df) for multiple tests are specified for model and error (df_{model}, $_{error}$). These tests were computed with SAS 9.4 software (SAS Institute Inc., Cary, North Carolina, U.S.A.); linear multiple regression analyses for climate-response analysis and PCA were calculate with R software (R Development Core Team).

3.4 Results

3.4.1 Forest size and isolation effects on microclimate

The small forest stands in the forest-dominated subregion (F1, F2), and the smallest stands (F1) in particular, had a more extreme climate with higher annual amplitudes than the large forests (F3, F4). The small stands were characterized by lower minimum and higher maximum air temperatures and lower relative air humidity than the large stands (Fig. 3.3, Table S3.2). Since cold temperatures prevail in the Mongolian forest-steppe with its short growing season, mean annual temperature was also lower in the small than in the large stands. The forest stands in the grassland-dominated subregion had lower mean, minimum, and maximum air temperatures than the forests in the forest-dominated subregion. The smallest forests in the forest-dominated subregion (F1) had lower values of relative air humidity than all other forests (Fig. 3.3). The forests in the grassland-dominated subregion (G1) were colder than those in the forest-dominated area (Fig. 3.3), although there was no difference in elevation (Table S3.1). This difference referred primarily to maximum temperature.

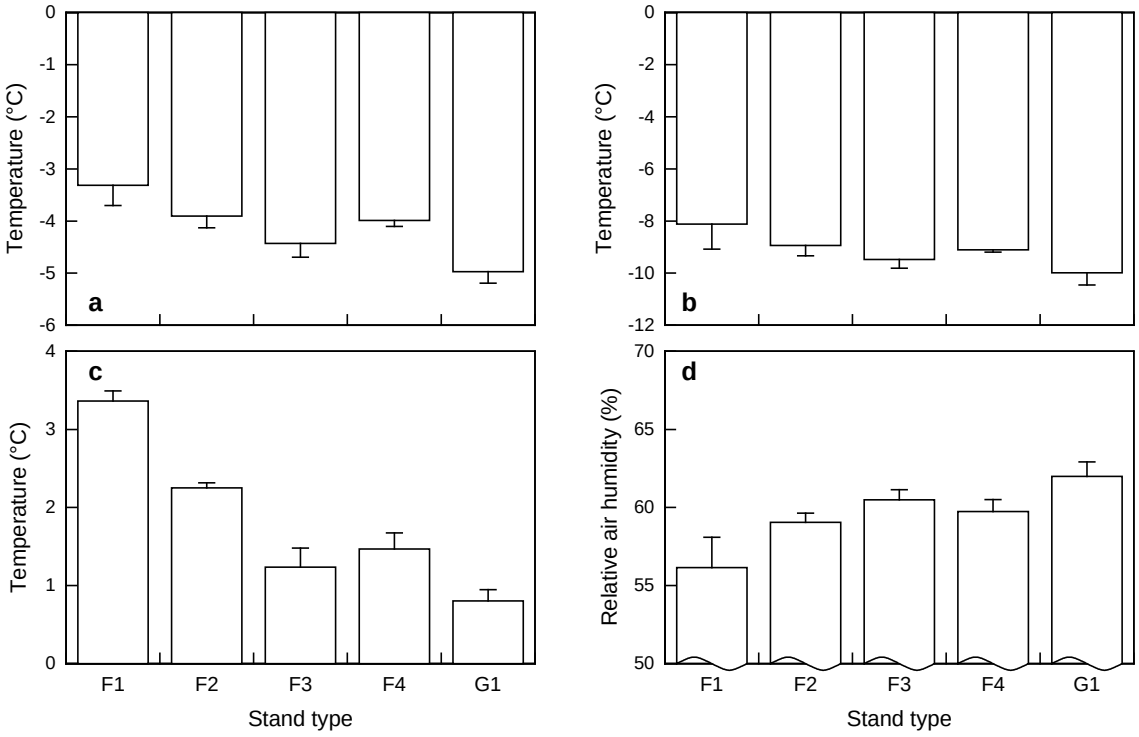

Fig. 3.3 (a) Mean, (b) minimum, and (c) maximum air temperatures, and (d) relative air humidity in forest stands of different size (increasing from F1/G1 to F4) in subregions with high (F1 to F4, south-eastern part of the study area) or low (G1, north-western part) forest-to-grassland ratio based on measurements from August 2014 to July 2015.

Mean soil surface temperature was much lower in the small (F1: -4.1±0.5 °C at 1 cm depth) than in the large (F4: -2.7±0.4 °C) forest (Fig. 3.4). Below 1 m depth, mean soil temperatures of the two forests became similar due to the significant temperature increase with increasing soil depth in the small forest, whereas mean soil temperature increased much less with depth in the large forest. Maximum soil temperatures sharply increased and minimum soil temperatures sharply decreased towards the surface in both forests, with the maximum and minimum temperatures in the large forest being consistently somewhat higher than in the small forest. Despite lower soil temperatures in small than in the large forests, spring melt of soil water occurred later by 6 days at 1 cm, and 33 days at 50 cm depth in the large forest (Fig. S3.2). The difference at 50 cm depth corresponded to a melt of soil water in mid-May (F4) instead of mid-April (F1), which was attributable to a more rapid warming of the air in the small forest in spring (data not shown). A possible explanation for this faster spring warming in the small forests could be lower snow accumulation due to higher wind exposure. In mid-summer, ice crystals were found at much greater depth in the small (at c. 2 m depth) than in the large forest (c. 75-125 cm depth).

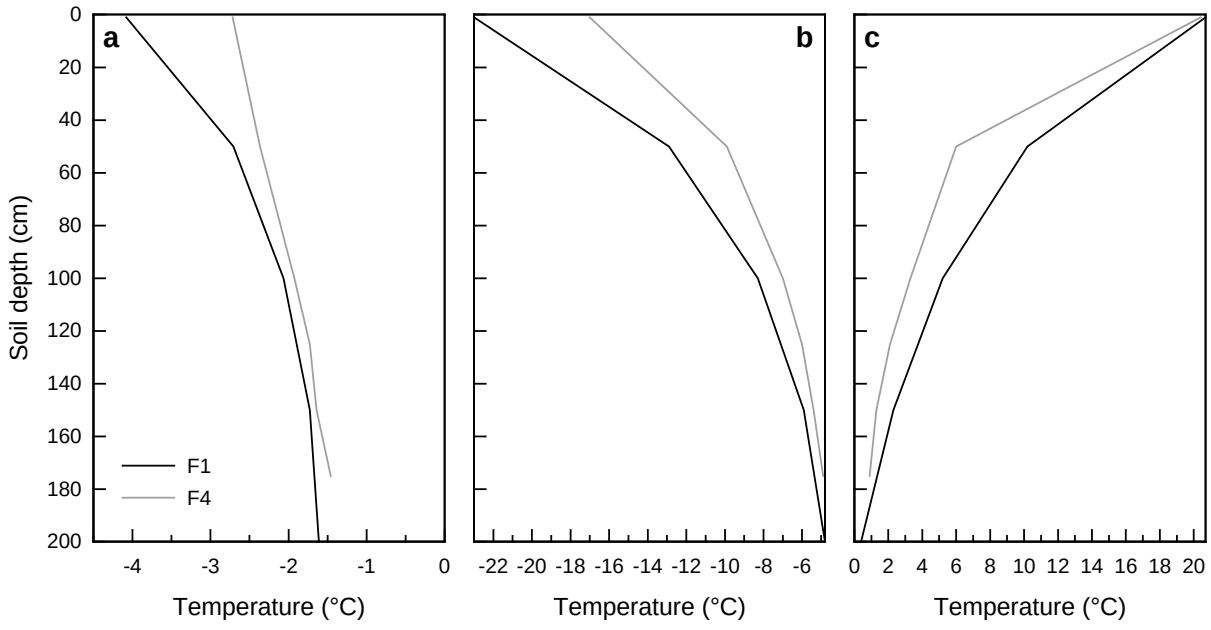

Fig. 3.4 (a) Mean, (b) minimum, and (c) maximum soil temperature as a function of soil depth in <0.1 km^2 (F1) and >5 km^2 large (F4) *L. sibirica* stands in the forested subregion based on measurements from August 2014 to July 2015.

3.4.2 Climate response of annual stem increment in variation of stand size

Mean sensitivity, first-order autocorrelation as well as the results of the climate-response analysis of annual radial stem increment in *L. sibirica* depended on forest stand size. Mean sensitivity decreased from roughly 40% in the smallest forests to c. 30% in the largest forests in all age classes (Table 3.2). First-order autocorrelation increased from c. 0.6 to 0.8 in more than 100-year old trees from small to large forests. Similar trends were also visible in less than 100-year old trees, but were not significant.

The results of the climate-response analysis were also influenced by stand size (Table 3.3). Trees more than 60 years old were more sensitive to low summer precipitation and high summer temperatures in small forest stands (size classes F1 to F3) than in large forests of >5 km^2 size (F4). These relationships mostly referred to the climatic conditions in the year prior to stemwood formation. The tree-ring index in the trees of size classes F1 to F3 was mostly positively correlated with previous year's June precipitation. In the few cases, where this correlation was not significant ($P \leq 0.05$), there were correlations that were at least marginally significant ($P \leq 0.10$). Several significant positive correlations were also found with previous year's August precipitation in the size classes F1 to F3. In the small forests of classes F1 and F2, significant increases of the tree-ring index occurred with decreasing July temperature of the year before tree-ring formation were detected in a few cases. The summer climate of the current year was much less influential. Young trees (≤60 years) showed different and less consistent responses to temperature and precipitation.

Promotion of stem increment by the previous year's summer precipitation was also suggested by PCA (Fig. 3.5). June and August precipitation of the previous year explained ≥70% of the variation of the tree-ring index. Stand types were increasingly associated with high values of precipitation with decreasing stand size.

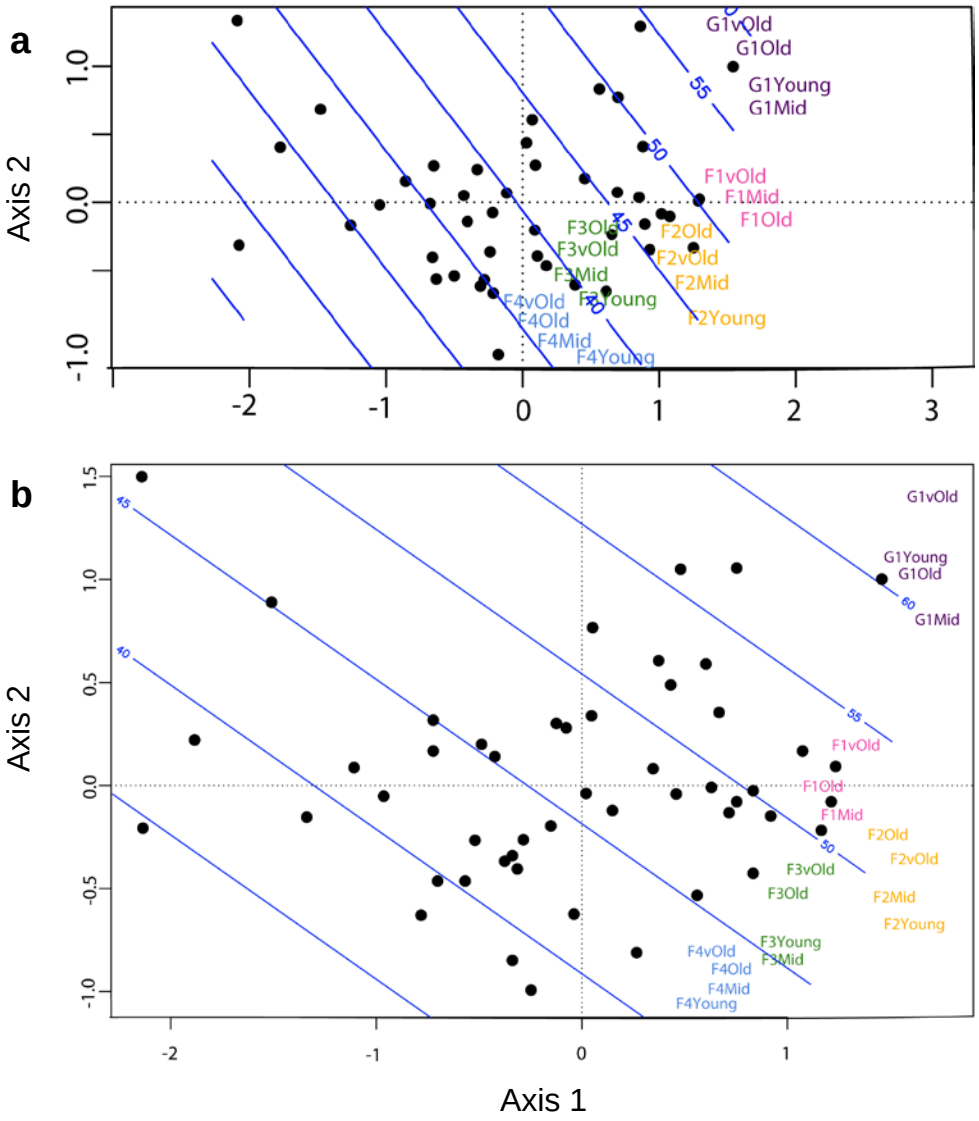

Fig. 3.5 PCA for the tree-ring index of *L. sibirica* saplings in stands of increasing size (from F1/G1 to F4) in the forest (F)- and grassland (G)-dominated subregions in variation of (a) June and (b) August precipitation of the previous year. Dots represent individual years from 1964 to 2014 and contour lines represent levels of precipitation. Explained variance: (a) 72 % (axis 1), 8 % (axis 2); (b) 70 % (axis 1), 9 (axis 2). Total variance: (a) 40.45, (b) 38.59.

3.4.3 Effect of forest stand isolation on the climate response of annual stem increment

Forest-to-grassland ratio had no significant effect on mean sensitivity and first-order autocorrelation (Table 3.2). The former was similarly high and the latter as low in the G1 as in the F1 plots. Annual stem increment in the trees from G1 plots increased with increasing summer precipitation of the year prior to tree-ring formation (Table 3.3). In contrast to the F1 plots, this increase was not limited to June and August, but also concerned the most

precipitation-rich month July, at least in trees that were more than 100 years old. PCA results suggested that the tree-ring index in the G1 plots was associated even more strongly with high summer precipitation than in the F1 (and any other F) plots.

Table 3.2 Mean sensitivity and first-order autocorrelation of tree-ring width in dependence on forest stand size, isolation and tree age

	≤60 yr	61−100 yr	101−160 yr	≥161 yr
Mean sensitivity:				
F1	-	0.42±0.01 ab	0.45±0.01 a	0.42±0.01 a
F2	0.38±0.02 ab	0.38±0.01 ab	0.39±0.01 ab	0.38±0.01 ab
F3	0.33±0.02 ab	0.39±0.01 ab	0.36±0.01 ab	0.35±0.01 ab
F4	0.30±0.01 a	0.31±0.01 a	0.29±0.01 b	0.32±0.01 b
G1	0.55±0.01 b	0.49±0.01 b	0.47±0.01 a	0.44±0.01 a
Autocorrelation coefficient:				
F1		0.61±0.03 a	0.63±0.01 a	0.64±0.01 a
F2	0.61±0.03 a	0.71±0.01 a	0.69±0.01 ab	0.68±0.01 a
F3	0.68±0.02 a	0.74±0.01 a	0.77±0.01 bc	0.70±0.02 a
F4	0.72±0.02 a	0.79±0.01 a	0.80±0.01 c	0.82±0.01 b
G1	0.70±0.01 a	0.70±0.01 a	0.65±0.02 ab	0.70±0.02 a

Arithmetic means ±SE. Within a column, means of mean sensitivity or autocorrelation, respectively, sharing the same letter do not differ significantly ($P \leq 0.05$, Duncan's multiple range test, $df_{model, error} = 4, 10$).

Table 3.3 Response of the tree-ring index of *L. sibirica* trees of different age groups to monthly temperature and precipitation of the year of and the year prior to tree-ring formation

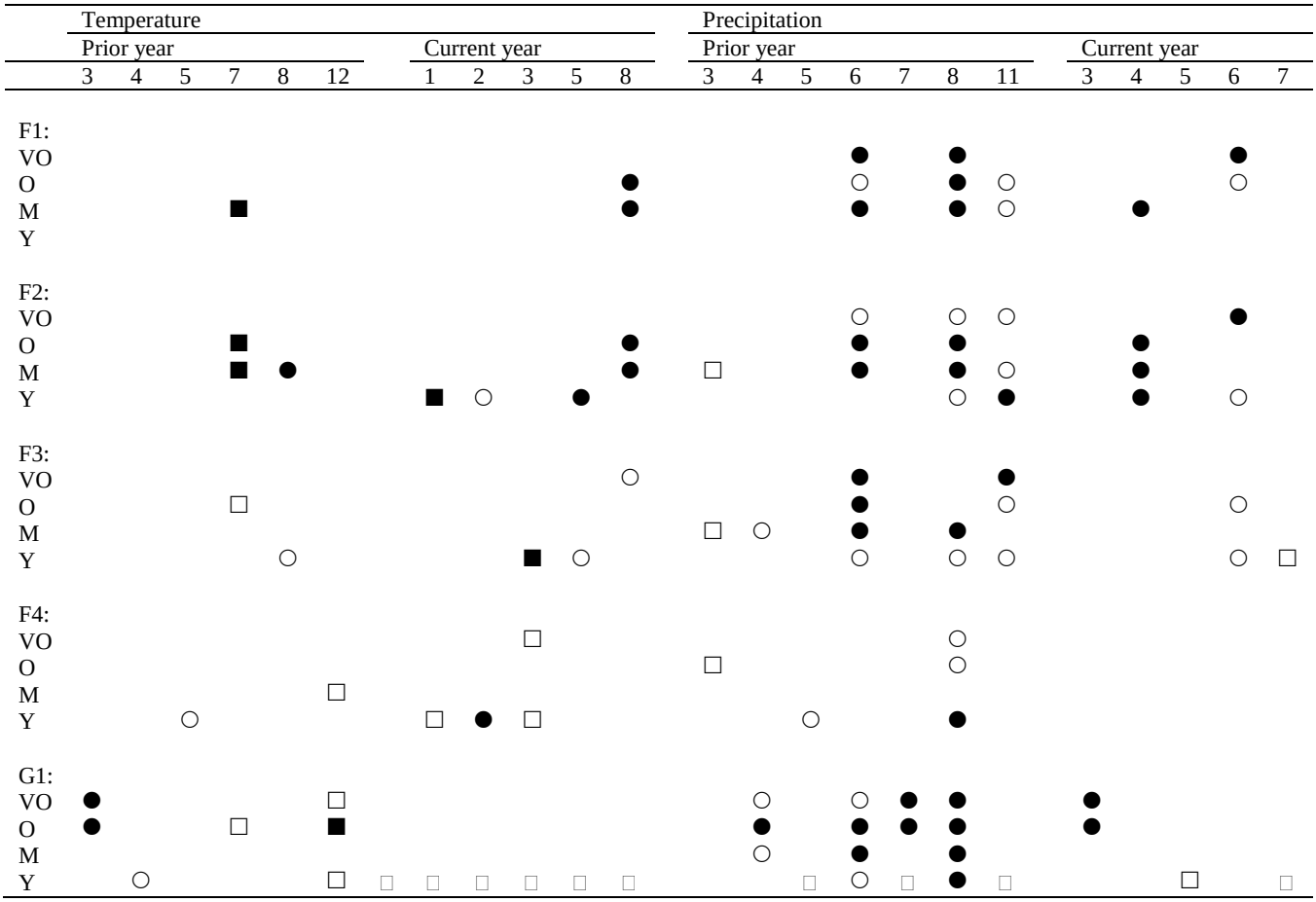

Correlation significant ($P \leq 0.05$): ● positive, ■ negative correlation; marginally significant ($P \leq 0.10$): ○ positive, □ negative correlation. Months are identified with numbers 1 to 12. Forest stands increasing in size (from F1/G1 to F4) in the forest (F)- and grassland (G)-dominated subregions. VO, very old trees (>160 years); O, old trees (101-160 years); M, middle-aged trees (61-100 years); Y, young trees (<60 years).

3.4.4 Variation of tree-ring width

The interannual variation of annual radial stem increment showed high synchronicity across the different locations as evidenced by the largely parallel variation of the tree-ring indices in trees from forests of different size and degree of isolation (Figs. S3.3, S3.4). Calculated for a long period (1900-2014) mean tree-ring width amounted to 0.3-0.4 mm and did not significantly differ between forest stand types. However, tree-ring width differed between the large forests of >5 km^2 (F4) and the smaller forest stands (F1-F3) in individual periods (Fig. 3.6). These increment data in Fig. 3.6 are displayed for different age classes to reduce effects of age-dependent growth variation. From the late eighteenth to the mid twentieth century,

trees of stand type F1-F4 mostly shared the same positive and negative peaks in annual tree-ring width, but at different amplitudes. Mean tree-ring width reached far higher values in periods of favorable growth conditions in small forests (F1-F3) than in large forests, but was on a similar scale during intervals with slow growth. Since the late twentieth century, however, mean tree-ring width in the large forests of >5 km^2 (F4) exceeded that in the smaller forests for up to 160-year old trees (Fig. 3.6). Very old trees (>160 years of cambial age) showed similar stem increment across the differently-sized stands in recent time, but had repeated pulses of higher increment in the <5km^2-sized forest than in the larger forests before (Fig. 3.6d).

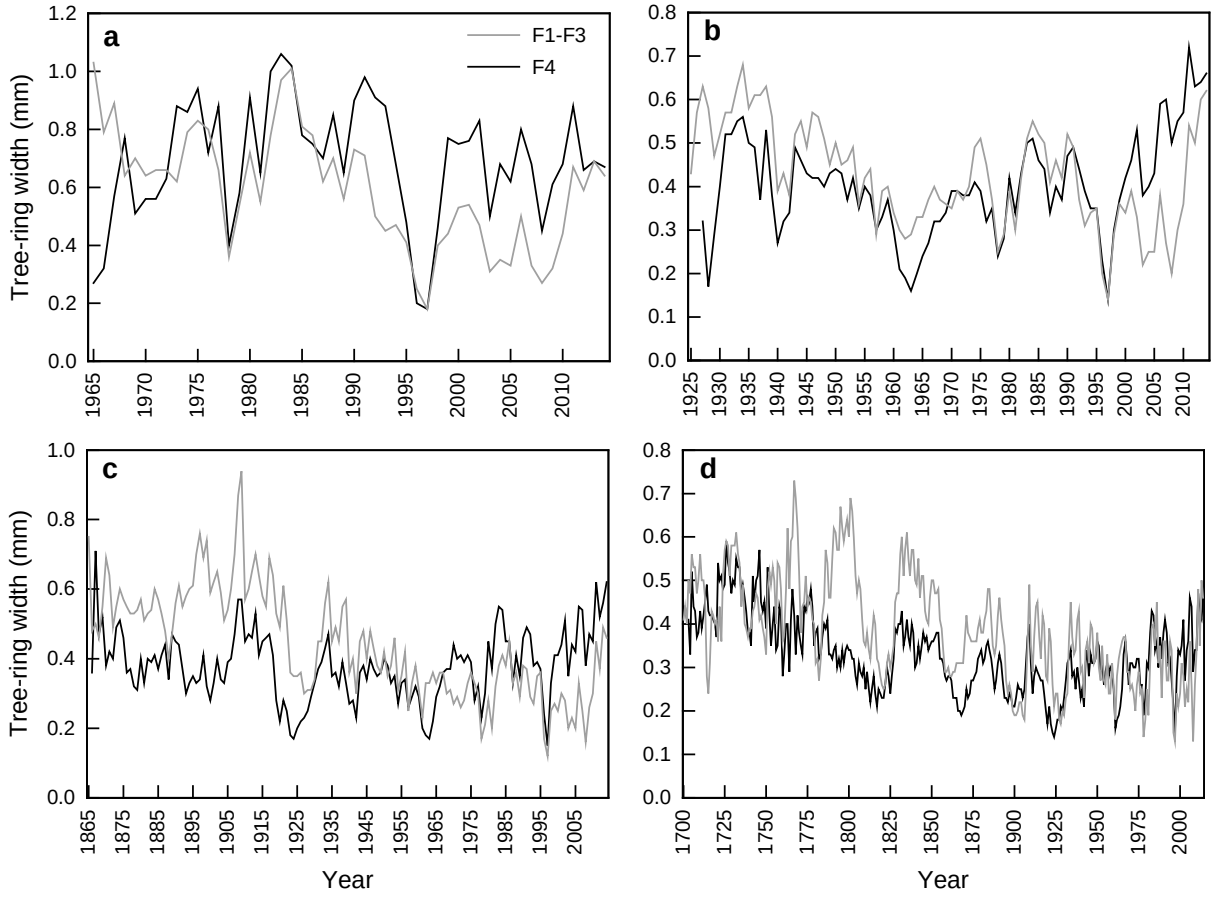

Fig. 3.6 Mean tree-ring width in *L. sibirica* trees from forest stands of >5 vs. <5 km^2 size (stand type F4 vs. F1-F3) in the forest-dominated subregion in trees of a cambial age of (a) ≤60 years, (b) 61-100 years, (c) 101-160 years, and (d) >160 years. Note different scale on the y-axis. Number of samples (F4; F1-F3): (a) 99; 44; (b) 56; 171; (c) 67; 425; (d) 72; 327 trees.

Cumulative RGC revealed that middle-aged trees (cambial age 61-100 years) grew faster in recent decades than old trees (101-160 years) did in the past at younger age in the F1 plots, but not in the other forests (Fig. S3.5). Middle-age trees in the small forests (F1, F2, G1) and all trees in the largest forests (F4) recently showed an upward curvature in the graph for cumulative stem increment indicating growth releases.

3.4.5 Missing ring frequency

From 1900-2014, annual mean frequency of missing rings (Table 3.4) was lower in the forests of >5 km^2 size (F4) than in the smaller forests (F1-F3, G1). There was a marked increase in missing ring frequency after 1970 in all forests of <5 km^2 size. Frequency increased by the factor 2.4-3.3 in the larch stands of the forest-dominated subregion (F1-F3), but by the factor 7.9 in the grassland-dominated subregion (G1). In contrast, the large forests of >5 km^2 size in the forest-dominated subregion showed only a slight (insignificant) increase in missing ring frequency by the factor 1.2.

Table 3.4 Missing ring frequency (in %) in *L. sibirica* trees from stands of different size (increasing from F1 to F4) in subregions with high (F1 to F4) or low (G1) forest-to-grassland ratio before and after 1970

Class	1900-1969	1970-2014	Increase
F1	1.31±0.14	3.96±0.44 *	302 %
F2	1.21±0.89	2.87±0.37 *	237 %
F3	1.23±0.15	4.00±0.41 *	325 %
F4	0.87±0.12	1.04±0.14	120 %
G1	0.71±0.13	5.60±1.01 *	789 %

Arithmetic means ±SE. Asterisks indicate significant difference between periods ($P \leq 0.05$, *U*-test).

3.4.6 Forest regeneration and tree stump density

Forest regeneration increased with stand size (Fig. 3.7). The large forests of >5 km^2 size (F4) exhibited considerably higher sapling densities than the smaller forests (F1-F3, G1). In the F1 plots, no seedlings and saplings were found at all, whereas few saplings occurred in the small forest patches in the grassland-dominated subregion (G1).

A trend toward increasing frequency of downed tree trunks with stand size was not significant due to high variation between plots of the same stand class (Fig. S3.6a, b). While downed deadwood was absent from the smallest forests (F1, G1), there were 133±46 downed tree trunks per ha in the largest forest stands (F4). The density of tree stumps did not differ between the stand types (Fig. S3.6c). However, there was an insignificant trend to higher stump-to-live-tree ratios in the smallest (F1, G1) compared to the larger forest stands (Fig. S3.6d).

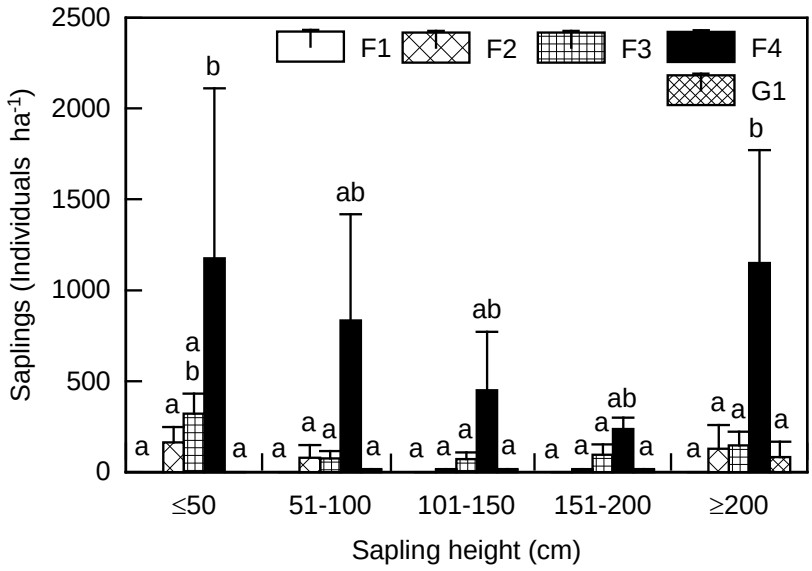

Fig. 3.7 Density of *L. sibirica* saplings in stands of increasing size (from F1/G1 to F4) in the forest (F)- and grassland (G)-dominated subregions. Means (±SE) sharing a common letter do not differ significantly ($P \leq 0.05$, Duncan's multiple range test, $df_{model, error} = 23, 51$).

3.5 Discussion

Our results suggest that small forest stand size increases the sensitivity of annual stem increment to climate warming in the studied *L. sibirica* stands at the southern fringe of the boreal forest in the Mongolian forest-steppe ecotone. In agreement with our first hypothesis, mean sensitivity of tree-ring width increased with decreasing stand size, whereas first-order autocorrelation decreased. These opposing trends give evidence of the trees' apparently reduced capacity to withstand unfavorable weather conditions and maintain the photosynthetic activity of the canopy with negative consequences for stemwood production in small forest stands. Positive correlation between the tree-ring index and summer precipitation in small and medium-sized forests of <5 km^2 size (size classes F1-F3), but not in large forest stands of >5 km^2, suggests that more intense drought exposure is indeed the cause of the higher climate sensitivity of stemwood production in small forests. A likely causal chain is drought-induced reduction of stomatal conductance and resulting reduction in carbon assimilation (Dulamsuren et al., 2009). Our measurements of temperature and relative humidity, demonstrating both more extreme maximum and minimum temperatures and reduced humidity in the small forest stands, indicate that the small forests were drier and warmer in summer than the large stands. A warmer and drier summer microclimate in forest fragments has repeatedly been reported from woodland regions around the world and has been attributed to edge effects. The smaller the forest patch, the larger is the proportion of the forest's interior area that is influenced by the microclimate of the open land in the surroundings (Chen et al., 1995).

While the edge effect causes higher mean temperatures inside small forest patches in subtropical to warm-temperate regions (Saunders et al., 1991), higher maximum and lower minimum temperatures in the cold-temperate high-elevation forest-steppe of Mongolia result in a reduction of mean annual temperature with decreasing forest size. This pattern is attributable to the long winter in Mongolia's forest-steppe region, which largely determines mean annual temperature that lies below freezing point in many regions of the country (Hauck et al., 2016). The generally lower temperatures in the grassland-dominated forest-steppe compared to the forest-dominated landscape may result from higher wind speeds (Kelliher et al., 1993) and from the higher albedo of grasslands than of boreal forests especially in winter (Li et al., 2015; Helbig et al., 2016). Furthermore, the higher aerodynamical roughness of forests compared to grasslands causes a greater potential to heat

the air (Baldocchi & Vogel, 1997). Lee et al. (2011) quantified the warming effect of forests for the boreal forest biome north of 45° N as to be 0.85 K for mean air temperature. The forest-to-grassland ratio has primarily an effect on maximum temperatures, which contrasts with the effect of forest size on the microclimate. Though the effect of forest vs. grassland vegetation on microclimate is undisputed, spatial microclimatic variation due differences in microtopography, of course, also influences forest distribution by excluding trees from dry and hot sites.

The cooling effect of reduced forest stand size during winter can also explain the higher mean and minimum soil temperatures recorded in large (F4) as compared to small (F1) forests. This stand size effect apparently caused deeper freezing in the permafrost soil of the small forests compared to the large forests, a result which might contradict intuitive expectations, but which is in agreement with more frequent frost events at the edge than in the interior of forests as postulated by Geiger (1965) and Saunders et al. (1991). While stand-replacing disturbance by clear-cut or fire is widely reported to deteriorate permafrost (Jin et al., 2007), forest fragmentation without alteration of forest cover, as was studied by us in the Mongolian forest-steppe, apparently does at least not completely destruct the permafrost in the forest islands. Our microclimate measurements refer to below-canopy climate and are, thus, relevant to permafrost conditions, but differ from the microclimate above and within the microclimate (Pomeroy & Dion, 1996; Baldocchi & Vogel, 1997), which is more influential on the trees' stomatal conductance. Differences in organic layer thickness were not found between stand types and thus could not have contributed to the variation in soil temperature.

A two- to three-fold increase in missing ring frequency in the forest <5 km^2 size (F1-F3), but not in the forests >5 km^2 (F4), since the 1970s is in line with the greater climate sensitivity of the trees in small forests. Missing rings are induced by drought during the growing season (Lorimer et al., 1999; Khishigjargal et al., 2014; Liang et al., 2016). The absence of a trend for increased frequency of missing rings with late twentieth century warming in the large forests thus suggests less tense water relations than in the small forests. This result matches with the absence of significant correlations of mature tree's stem increment with summer precipitation and temperature in large forests. While climate sensitivity increased gradually with decreasing forest size, the dependence of missing ring frequency on stand size was non-linear, with low frequency only in large continuous forests (F4). Our second hypothesis supposing a gradual change of missing ring frequency with forest size was thus not fully

supported. It has been shown that missing ring frequency is in general not dependent on tree age (Lorimer et al., 1999), suggesting that the recently increased occurrence of missing rings in the forests of <5 km^2 was not an effect of potential changes in stand age structure over time.

Forest regeneration increased with stand size in agreement with our third hypothesis. It is plausible to assume that this is due to a combined effect of higher moisture availability and much lower grazing pressure in the interior of large forests than in small stands. Seed germination and seedling establishment of *L. sibirica* in the forest-steppe ecotone are known to benefit from low soil temperature and high soil moisture (Dulamsuren et al., 2008), while light seems to be of minor importance. Grazing livestock, albeit beneficial for the initial establishment of seedlings owing to the reduction of competition by the ground vegetation, is strongly limiting for sapling survival, since larch saplings are a preferred diet of cashmere goats (Khishigjargal et al., 2013). Goats avoid the interior of large forests, but are regularly found at forest edges and in the interior of small forest patches surrounded by grassland. Both climate and livestock densities have become more unfavorable for the regeneration of *L. sibirica* in the recent past, since climate has become warmer (Dagvadorj et al., 2009) and the number of goats has more than tripled since the early 1990s (Lkhagvadorj et al., 2013b).

Missing ring frequency was also influenced by the isolation of the forest stands. The small forest stands in the grassland-dominated landscape (G1) exhibited a nearly eightfold increase in missing ring frequency since the 1970s. This increase was far higher than in forests of the same size (F1) in the forest-dominated landscape. Positive correlation of annual stem increment with the previous year's June, July, and August precipitation in the G1 forests, but only with June and August precipitation in the F1 (and F2, and F3) forests, is in line with the large increase in missing ring frequency. These findings, which support our fourth hypothesis, suggest that trees in the grassland-dominated forest-steppe suffered from more intense drought stress than trees in the forest-dominated subregion, irrespective of forest size. Unfortunately, we do not have physiological data that would corroborate this assumption. Since mean temperatures were even lower in the G1 than the F1 plots, we can only speculate, that higher wind speeds in the open grassland-dominated landscape (not measured) caused higher evapotranspiration rates than in the landscape with more forest area. Detailed measurements of microclimate variability and permafrost distribution in forest-steppe regions

of variable forest-grassland ratios would be needed to interpret the observed differences in the trees' climate warming response.

An interesting detail of our results emerges from the comparison of mean tree-ring widths of larch trees growing in forests of either less than or more than 5 km^2 size (Fig. 3.6). Trees in the large stands (F4) grew recently faster than trees in small forests (F1-F3), whereas the opposite trend was visible in the preceding 200 years. We hypothesize that this recent switch could be due to intensified permafrost melt in large forests. The active layer was located at lower depth in the soil profile and reached higher temperatures in the large than in the small forests during summer, when melted permafrost is most critical for the water supply of the vegetation (Sugimoto et al., 2003; Lopez et al., 2010).

Our results strongly support our initial assumption that both forest size and isolation are important determinants of the climate-warming response of *L. sibirica* trees in the forest-steppe ecotone. Nevertheless, there are other factors that were not investigated in this study, which likely interfere with the relationship between forest fragmentation and warming sensitivity. Major disturbances like fire, insect calamities, and logging cause strong changes in stand structure, microclimate, and permafrost distribution (Gromtsev, 2002; Zyryanova et al., 2007), and are thus likely to affect the sensitivity of forests to climate warming. Though we have no systematic data of forest fires from our sample plots, it was obvious during field work that fire had not been restricted to small forest patches, but even had occurred in the large forests, which are more often visited by people for the collection of berries and pine nuts. Selective logging as is commonly practiced in Mongolia leads to reduced stand density, which improves the water supply of the remaining trees (Dulamsuren et al., 2010a; Chenlemuge et al., 2015) and thus should increase their tolerance to drought episodes. Clear-cuts and large forest fires, however, cause permafrost melt with a transient increase, but long-term decrease, of soil moisture (Yoshikawa et al., 2003). We tried to control for these factors as much as possible in our investigation by clustering the stands of different size in our sampling design. Selective logging is usually more intense in small forests than in the interior of large forest stands in the Mongolian forest-steppe (Dulamsuren et al., 2014). Logging should, therefore, have had a more positive effect on tree water relations in the small stands than in the large forests. Since we found a stronger response to climate warming in small forests, it is not likely that logging had a decisive impact on the observed differences in climate-warming sensitivity in our study. This conclusion is supported by the fact that stand

density, basal area, and tree stump frequency did not differ significantly between the plot types, although there was an insignificant trend for higher stump-to-live-tree ratios in the smallest forests (F1, G1) than in the other stands.

Our findings suggest that the progressive fragmentation of the southern boreal forest in the Inner Asian forest-steppe due to the combined effect of logging, fire, and forest grazing (Erdenechuluun, 2006; Hansen et al., 2013) reinforces the sensitivity of the remaining forest to climate warming. The southern fringe of the boreal forest in Inner Asia is one of the world's regions with most intense climate warming (IPCC, 2013) and is already a key region of global warming-related decline of forest health (Dulamsuren et al., 2010a, 2013; Liu et al., 2013). The same is true for oroboreal coniferous forests south of the continuous boreal forest belt in Inner Asia (Liang et al., 2016). The potential negative impact of forest fragmentation on the climate warming tolerance of these forests has not been addressed in the literature so far. It is likely that negative feedbacks of forest size and forest stand isolation on the climate warming tolerance of forests are common in drought-limited forest ecosystems around the world. Today, these forests are suffering from drought-induced forest mortality in many regions on earth. While this process has received considerable attention (Allen et al., 2010), the interaction of other factors with the tolerance of these forests to climate warming is not sufficiently studied.

Acknowledgments

The study was supported by a grant of the Volkswagen Foundation to M. Hauck, Ch. Dulamsuren and Ch. Leuschner for the project "Forest regeneration and biodiversity at the forest-steppe border of the Altai and Khangai Mountains under contrasting developments of livestock numbers in Kazakhstan and Mongolia". E. Khansitoreh received an Erasmus Mundus Scholarship in the Salam 2 program. We are thankful to the staff of the Tarvagatai Nuruu National Park for their support during field work.

References

Allen CD, Macalady AK, Chenchouni H *et al.* (2010) A global overview of drought and heat-induced tree mortality reveals emerging climate change risks for forests. *Forest Ecology and Management*, **259**, 660-684.

Ayres MP, Lombardero MJ (2000) Assessing the consequences of global change for forest disturbance from herbivores and pathogens. *Science of the Total Environment*, **262**, 263-286.

Baldocchi DD, Vogel CA (1997) Seasonal variation of energy and water vapor exchange rates above and below a boreal jack pine forest canopy. *Journal of Geophysical Research*, **102**, 28939-28951.

Barber VA, Juday GP, Finney BP (2000) Reduced growth of Alaskan white spruce in the twentieth century from temperature-induced drought stress. *Nature*, **405**, 668-673.

Bierregaard BO, Lovejoy TE, Kapos V, dos Santos AA, Hutchings RW (1992) The biological dynamics of trophic rainforest fragments: a prospective comparison of fragments and continuous forest. *BioScience*, **42**, 859-866.

Bond-Lamberty B, Rocha AV, Calvin K, Holmes B, Wang C, Goulden ML (2014) Disturbance legacies and climate jointly drive tree growth and mortality in an intensively studied boreal forest. *Global Change Biology*, **20**, 216-227.

Buermann W, Parida B, Jung M, MacDonald GM, Tucker CJ, Reichstein M (2014) Recent shift in Eurasian boreal forest greening response may be associated with warmer and drier summers. *Geophysical Research Letters*, doi: 10.1002/2014GL059450.

Bunn AG (2008) A dendrochronology program library in R (dplR). *Dendrochronologia*, **26**, 115-124.

Carrer M, Urbinati C (2004) Age-dependent tree-ring growth responses to climate in *Larix decidua* and *Pinus cembra*. *Ecology*, **85**, 730-740.

Chen F, Yuan YJ, Wei WS, Fan ZA, Zhang TW, Shang HM, Zhang RB, Yu SL, Ji CR, Qin L (2012) Climatic responses of ring width and maximum latewood density of *Larix sibirica* in the Altay Mountains reveals recent warming trends. *Annals of Forest Science*, **69**, 723-733.

Chen J, Franklin JF, Spies TA (1995) Growing-season microclimatic gradients from clearcut edges into old-growth Douglas-fir forests. *Ecological Applications*, **5**, 74-86.

Chen J, Saunders JC, Crow TR, Naiman RJ, Brosofske KD, Mroz GD, Brookshire BL, Franklin JF (1999) Microclimate in forest ecosystem and landscape ecology. *BioScience*, **49**, 288-297.

Chenlemuge T, Dulamsuren Ch, Hertel D, Schuldt B, Leuschner C, Hauck M (2015) Hydraulic properties and fine root mass of *Larix sibirica* along forest edge-interior gradients. *Acta Oecologica*, **63**, 28-35.

Cook ER, Holmes RL (1984) *Program ARSTAN User Manual.* Laboratory of Tree-Ring Research, University of Arizona, Tucson, Arizona.

Dagvadorj D, Natsagdorj L, Dorjpurev J, Namkhainyam B (2009) *Mongolian Assessment Report on Climate Change 2009.* Ministry of Environment, Nature and Tourism, Mongolia, Ulan Bator.

Davi N, Jacoby G, Fang K, Li J, D'Arrigo R, Baatarbileg N, Robinson D (2010) Reconstructing drought variability for Mongolia based on a large-scale tree-ring network: 1520−1993. *Journal of Geophysical Research*, **115**, D22103, doi: 10.1029/2010JD013907.

Debinski DM, Holt RD (2001) A survey and overview of habitat fragmentation experiments. *Conservation Biology*, **14**, 342-355.

Didham R (1997) The influence of edge effects and forest fragmentation on leaf-litter. In: *Tropical Forest Remnants: the Ecology, Conservation, and Management of Fragmented Communities* (eds Laurance WF, Bierregaard BO), pp. 55-70. University of Chicago Press, Chicago.

Dulamsuren Ch, Hauck M, Mühlenberg M (2008) Insect and small mammal herbivores limit tree establishment in northern Mongolian steppe. *Plant Ecology*, **195**, 143-156.

Dulamsuren Ch, Hauck M, Bader M, Osokhjargal D, Oyungerel Sh, Nyambayar S, Runge M, Leuschner C (2009) Water relations and photosynthetic performance in *Larix sibirica* growing in the forest-steppe ecotone of northern Mongolia. *Tree Physiology*, **29**, 99-110.

Dulamsuren Ch, Hauck M, Leuschner C (2010a) Recent drought stress leads to growth reductions in *Larix sibirica* in the western Khentey, Mongolia. *Global Change Biology*, **16**, 3024-3035.

Dulamsuren Ch, Hauck M, Khishigjargal M, Leuschner HH, Leuschner C (2010b) Diverging climate trends in Mongolian taiga forests influence growth and regeneration of *Larix sibirica*. *Oecologia*, **163**, 1091-1102.

Dulamsuren Ch, Wommelsdorf T, Zhao F, Xue Y, Zhumadilov BZ, Leuschner C, Hauck M (2013) Increased summer temperatures reduce the growth and regeneration of *Larix sibirica* in southern boreal forests of eastern Kazakhstan. *Ecosystems*, **16**, 1536-1549.

Dulamsuren Ch, Khishigjargal M, Leuschner C, Hauck M (2014) Response of tree-ring width to climate warming and selective logging in larch forests of the Mongolian Altai. *Journal of Plant Ecology*, **7**, 24-38.

Dulamsuren Ch, Klinge M, Degener J, Khishigjargal M, Chenlemuge Ts, Bat-Enerel B, Yeruult Yo, Saindovdon D, Ganbaatar K, Tsogtbaatar J, Leuschner C, Hauck M (2016) Carbon pool densities and a first estimate of the total carbon pool in the Mongolian forest-steppe. *Global Change Biology*, **22**, 830-844.

Erdenechuluun T (2006) *Wood Supply in Mongolia: the Legal and Illegal Economies. Mongolia Discussion Papers*. World Bank, Washington, DC.

Fahrig L (2003) Effects of habitat fragmentation on biodiversity. *Annual Review of Ecology, Evolution, and Systematics*, **34**, 487-515.

Geiger R (1965) *The Climate near the Ground*. Harvard University Press, Cambridge.

Girardin MP, Ali AA, Carcaillet C, Mudelsee M, Drobyshev I, Hély C, Bergeron Y (2009) Heterogenous response of circumboreal wildfire risk to c000limate change since the early 1900s. *Global Change Biology*, **15**, 2751-2769.

Gromtsev A (2002) Natural disturbance dynamics in the boreal forests of European Russia: a review. *Silva Fennica*, **36**, 41-55.

Gunin PD, Vostokova EA, Dorofeyuk NI, Tarasov PE, Black CC (1999) *Vegetation Dynamics of Mongolia*. Kluwer, Dordrecht.

Hansen MC, Potapov PV, Moore R *et al.* (2013) High-resolution global maps of 21st-century forest cover change. *Science*, **342**, 850-853.

Hauck M, Dulamsuren Ch, Leuschner C (2016) Anomalous increase in winter temperature and decline in forest growth associated with severe winter smog in the Ulan Bator basin. *Water, Air and Soil Pollution*, **227**, article 261, 1-10.

Helama S, Lindholm M, Timonen M, Eronen M (2004) Detection of climate signal in dendrochronological data analysis: a comparison of tree-ring standardization methods. *Theoretical and Applied Climatology*, **79**, 239-254.

Helbig M, Wischnewski K, Kljun N, Chasmer LE, Quinton WL, Detto M, Sonnentag O (2016) Regional atmospheric cooling and wetting effect of permafrost thaw-induced boreal forest loss. *Global Change Biology*, doi:10.1111/gcb.13348.

Hódar JA, Zamora R (2004) Herbivory and climatic warming: a Mediterranean outbreaking caterpillar attacks a relict, boreal pine species. *Biodiversity and Conservation*, **13**, 493-500.

IPCC (2013) *Climate Change 2013: the Physical Science Basis. Contribution of Working Group I to the Fifth Assessment Report of the Intergovernmental Panel on Climate Change.* Cambridge University Press, Cambridge.

Jacoby GC, D'Arrigo RD, Davaajamts T (1996) Mongolian tree-rings and 20th-century warming. *Science*, **273**, 771-773

Jin H, Yu Q, Lü L, Guo D, He R, Yu S, Sun G, Li Y (2007) Degradation of permafrost in the Xing'anling Mountains, northeastern China. *Permafrost and Periglacial Processes*, **18**, 245-258.

Kelliher FM, Leuning R, Schulze E-D (1993) Evaporation and canopy characteristics of coniferous forests and grasslands. *Oecologia*, **95**, 153-163.

Khishigjargal M, Dulamsuren Ch, Lkhagvadorj D, Leuschner C, Hauck M (2013) Contrasting responses of seedling and sapling densities to livestock density in the Mongolian forest-steppe. *Plant Ecology*, **214**, 1391-1403.

Khishigjargal M, Dulamsuren Ch, Leuschner HH, Leuschner C, Hauck M (2014) Climate effects on inter- and intra-annual larch stemwood anomalies in the Mongolian forest-steppe. *Acta Oecologica*, **55**, 113-121.

Kullman L, Öberg L (2009) Post-Little Ice Age tree line rise and climate warming in the Swedish Scandes: a landscape ecological perspective. *Journal of Ecology*, **97**, 415-429.

Lee XL, Goulden ML, Hollinger DY *et al.* Observed increase in local cooling effect of deforestation at higher latitudes. *Nature*, **479**, 384-387.

Li Y, Zhao M, Motesharrei S, Mu Q, Kalnay E, Li S (2015) Local cooling and warming effects of forests based on satellite observations. *Nature Communications*, **6**, doi:10.1038/ncomms7603.

Liang EY, Leuschner C, Dulamsuren Ch, Wagner B, Hauck M (2016) Global warming-related tree growth decline and mortality on the north-eastern Tibetan Plateau. *Climatic Change*, **134**, 163-176.

Liu H, Williams AP, Allen CD *et al.* (2013) Rapid warming accelerates tree growth decline in semi-arid forests of Inner Asia. *Global Change Biology*, **19**, 2500-2510.

Lkhagvadorj D, Hauck M, Dulamsuren Ch, Tsogtbaatar J (2013a) Pastoral nomadism in the forest-steppe of the Mongolian Altai under a changing economy and a warming climate. *Journal of Arid Environments*, **88**, 83-89.

Lkhagvadorj D, Hauck M, Dulamsuren Ch, Tsogtbaatar J (2013b) Twenty years after decollectivization: mobile livestock husbandry and its ecological impact in the Mongolian forest-steppe. *Human Ecology*, **41**, 725-735.

Lloyd AH, Bunn AG (2007) Responses of the circumpolar boreal forest to 20th century climate variability. *Environmental Research Letters*, **2**, doi:10.1088/1748-9326/2/4/045013.

Lopez ML, Shirota T, Iwahana G, Koide T, Maximov TC, Fukuda M, Saito H (2010) Effect of increased rainfall on water dynamics of larch (*Larix cajanderi*) forest in permafrost regions, Russia: an irrigation experiment. *Journal of Forest Research*, **15**, 365-373.

Lorimer CG, Dahir SE, Singer MT (1999) Frequency of partial and missing rings in *Acer saccharum* in relation to canopy position. *Plant Ecology*, **143**, 189-202.

McDowell NG, Allen CD (2015) Darcy's law predicts widespread forest mortality under climate warming. *Nature Climate Change*, **5**, 669-672.

Peng C, Ma Z, Lei X, Zhu Q, Chen H, Wang W, Liu S, Li W, Fang X, Zhou X (2011) A drought-induced pervasive increase in tree mortality across Canada's boreal forest. *Nature Climate Change*, **1**, 467-471.

Pomeroy JW, Dion K (1996) Winter radiation extinction and reflection in a boreal pine canopy: measurements and modelling. *Hydrological Processes*, **10**, 1591-1608.

Robinson GR, Holt RD, Gaines MS, Hamburg SP, Johnson ML, Fitch HS, Martinko EA (1992) Diverse and contrasting effects of habitat fragmentation. *Science*, **257**, 524-526.

Rosner S, Hannrup B (2004) Resin canal traits relevant for constitutive resistance of Norway spruce against bark beetles: environmental and genetic variability. *Forest Ecology and Management*, **200**, 77-87.

Sarris D, Christodoukalis D, Körner C (2007) Recent decline in precipitation and tree growth in the eastern Mediterranean. *Global Change Biology*, **13**, 1187-1200.

Sauders DA, Hobbs RJ, Margules CR (1991) Biological consequences of ecosystem fragmentation: a review. *Conservation Biology*, **5**, 18-32.

Sharkhuu N, Sharkhuu A (2012) Effects of climate warming and vegetation cover on permafrost of Mongolia In: *Ecological Problems and Livelihoods in a Changing World* (eds Werger MJA, van Staalduinen MA), pp 445-472, Springer, Dordrecht.

Sugimoto A, Naito D. Yanagisawa N, Ichiyanagi K, Kurita N, Kubota J, Kotake T, Ohata T, Maximov TC, Fedorov AN (2003) Characteristics of soil moisture in permafrost observed in East Siberian taiga with stable isotopes of water. *Hydrological Processes*, **17**, 1073-1092.

Terrier A, Girardin MP, Périé C, Legendre P, Bergeron Y (2013) Potential changes in forest composition could reduce impacts of climate change on boreal wildfires. *Ecological Applications*, **23**, 21-35.

Wigley TML, Briffa KR, Jones PD (1984) On the average value of correlated time series, with applications in dendroclimatology and hydrometeorology. *Journal of Climate and Applied Meteorology*, **23**, 201-213.

Yoshikawa K, Bolton WR, Romanovsky VE, Fukuda M, Hinzman LD (2003) Impacts of wildfire on the permafrost in the boreal forests of Interior Alaska. *Journal of Geophysical Research*, **108**, D1 (8148), 1-14

Zyryanova OA, Yaborov VT, Tchikhacheva TL, Koike T, Makoto K, Matsuura Y, Fuyuki S, Zyryanov VI (2007) The structure and biodiversity after fire disturbance in *Larix gmelinii* (Rupr.) Rupr. forests, northeastern Asia. *Eurasian Journal of Forest Research*, **10**, 19-29.

Supporting information

Table S3.1 Density, age structure, and humus layer thickness of the studied *L. sibirica* stands differing in size and isolation

	F1	F2	F3	F4	G1
Number of sample trees:					
>160 yr	81(53)	62 (54)	33(46)	67(28)	20 (15)
101−160 yr	79 (8)	112(15)	195 (6)	60 (5)	49 (8)
61−100 yr	16(0)	75(0)	70 (0)	54 (0)	44 (0)
≤60 yr	0	12 (0)	19 (0)	98 (0)	52(0)
Mean age (yr)	157±9 a	146±12 a	143±13 a	130±11 a	107±18 a
Max. age (yr)	303±34 a	299±29 a	342±43 a	331±18 a	270±27 a
Basal area (m^{-2} ha^{-1})	40±5 a	41±7 a	44±5 a	34±8 a	30±2 a
Stand density (trees ha^{-1})	1100±31 a	1450±53 a	1883±33 a	1387±36 a	1667±89 a
Thickness of soil horizons containing high amounts of organic matter:					
Organic layer (cm)	1.9±0.3 a	2.0±0.4 a	2.1±0.7 a	1.9±0.6 a	1.8±0.9 a
Ah horizon (cm)	6.8±0.4 a	7.2±1.2 a	6.2±1.1 a	11.3±2.7 a	9.1±0.3 a

F1/G1, <0.1 km^2; F2, 0.1-1.0 km^2, F3, 1.1-5.0 km^2; F4, >5.0 km^2 in forest (F)- or grassland (G)-dominated subregion. Tree age specifications refer to cambial age; numbers in brackets refer to trees sampled outside the sample plots that were incorporated in the tree-ring chronologies, but not in specifications of stand structural and stand age characteristics. Arithmetic means ± SE. Within a row, means sharing a common letter, do not differ significantly ($P \leq 0.05$, Duncan's multiple range test, $df_{model, error} = 4, 10$).

Table S3.2 January and June/July mean, minimum, and maximum air temperatures, and relative humidity in forest stands of different size (increasing from F1/G1 to F4) in subregions with high (F1 to F4, south-eastern part of the study area) or low (G1, north-western part) forest-to-grassland ratio.

	F1	F2	F3	F4	G1
January 2015					
Mean *T* (°C)	-3.7±0.7 a	-4.3±0.8 a	-4.7±0.8 a	-4.5±0.7 a	-5.1±0.8 a
Min. *T* (°C)	-8.5±0.7 a	-10.1±0.7 ab	-9.3±0.7 ab	-9.7±0.7 b	-9.5±0.7 ab
Max. *T* (°C)	2.9±0.8 a	1.9±0.8 b	1.0±0.9 b	1.0±0.8 b	0.7±0.9 b
RH (%)	67±1 a	73±1 b	77±1 bc	76±1 bc	77±1 c
June/July 2015					
Mean *T* (°C)	15.5±0.5 a	15.5±0.4 a	15.5±0.4 a	15.2±0.4 a	15.9±0.4 a
Min. *T* (°C)	9.7±0.4 a	8.9±0.5 a	9.3±0.5 a	9.1±0.4 a	8.7±0.5 a
Max. *T* (°C)	23.5±0.6 ab	23.1±0.6 ab	22.7±0.5 ab	22.4±0.6 a	24.4±0.6 b
RH (%)	47±3 a	48±3 a	48±2 a	49±3 a	46±2 a

F1/G1, <0.1 km^2; F2, 0.1-1.0 km^2, F3, 1.1-5.0 km^2; F4, >5.0 km^2 in forest (F)- or grassland (G)-dominated subregion. Within a row, means sharing a common letter, do not differ significantly ($P \leq 0.05$, Duncan's multiple range test, $df_{model, error} = 4, 145$).

Table S3.3 Expressed population signal (EPS) of the studied *L. sibirica* stands for trees of different age classes

Age class	F1	F2	F3	F4	G1
>160 yr	0.92 (1815)	0.92 (1805)	0.89 (1785)	0.87 (1830)	0.96 (1860)
101−160 yr	0.94 (1900)	0.93 (1881)	0.93 (1900)	0.91 (1915)	0.94 (1978)
61−100 yr	0.84 (1960)	0.97 (1960)	0.96 (1960)	0.92 (1960)	0.96 (1970)
≤60 yr	−	0.96 (1985)	0.95 (1985)	0.97 (1985)	0.97 (1985)

F1/G1, <0.1 km^2; F2, 0.1-1.0 km^2, F3, 1.1-5.0 km^2; F4, >5.0 km^2 in forest (F)- or grassland (G)-dominated subregion. Tree age specifications refer to cambial age. Numbers in brackets specify the year from which on the given EPS is reached

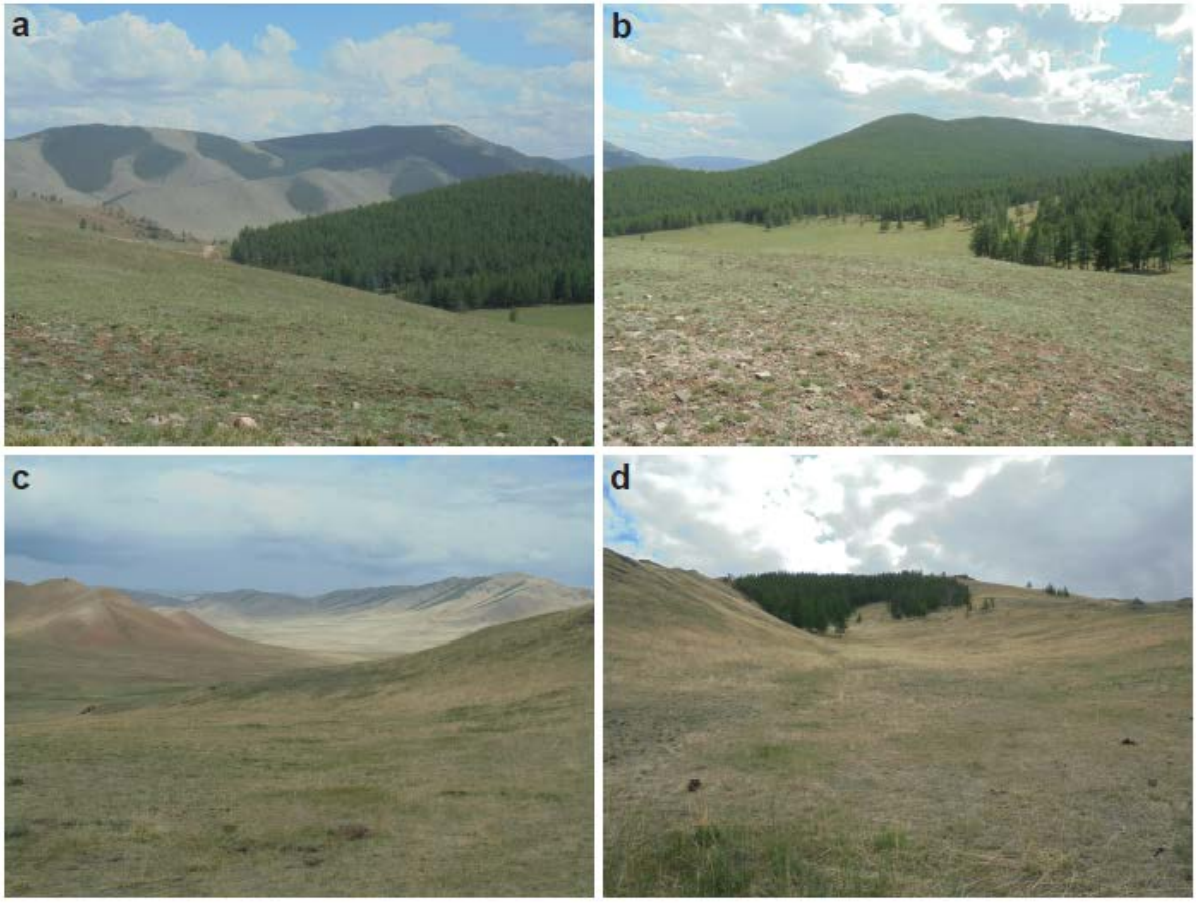

Fig. S3.1 *Larix sibirica*-dominated forest-steppe near Tosontsengel, Mongolia: (**a**) Forest stands of varying size and (**b**) large forest of c. 15 km^2 in the forest-dominated area. (**c**) Grassland-dominated area with small forest patches on the mountain slope in the background. (**d**) Small forest island (<0.1 km^2) in the grassland-dominated area.

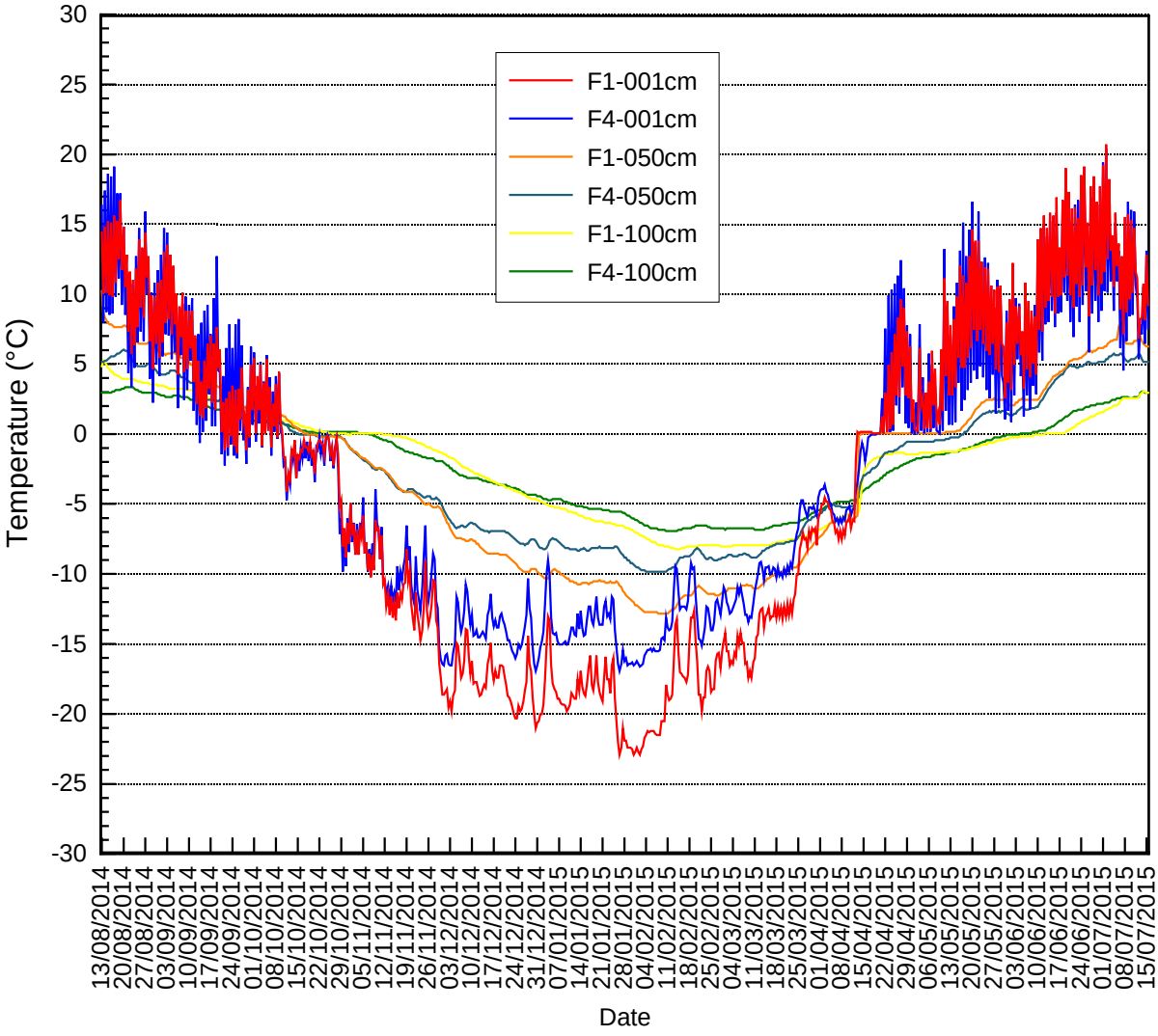

Fig. S3.2 Soil temperature at 1, 50, and 100 cm depth in *L. sibirica* forest stands of <0.1 km^2 (F1) and >5 km^2 (F4) size in the period from August 2014 to July 2015.

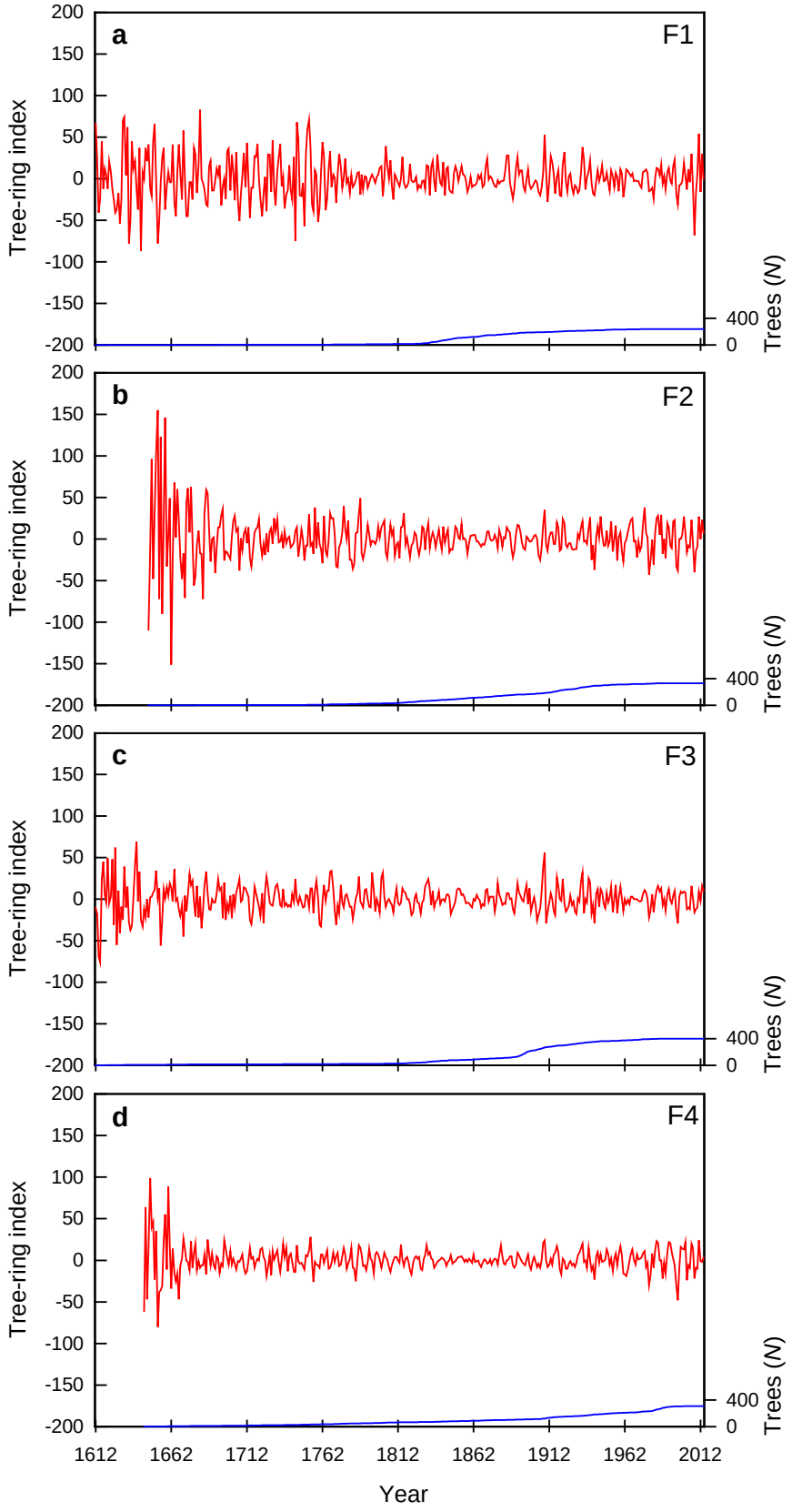

Fig. S3.3 Tree-ring index of *L. sibirica* trees from stands of different size (increasing from F1 to F4) in subregions with high forest-to-grassland ratio.

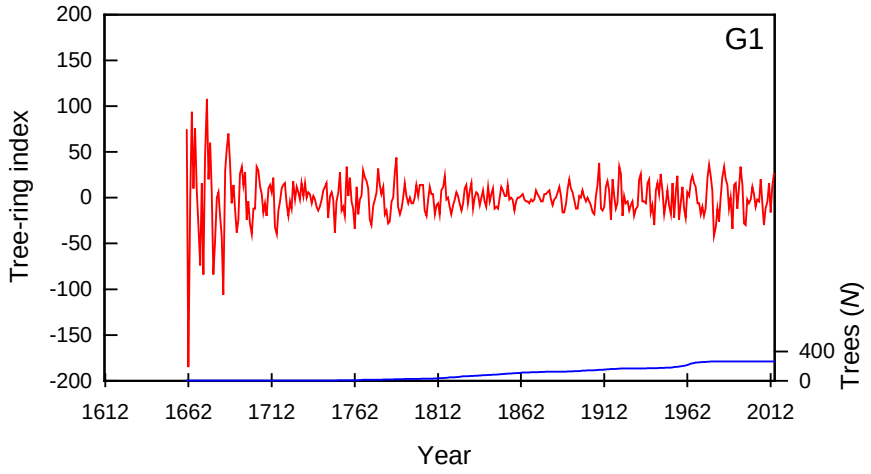

Fig. S3.4 Tree-ring index of *L. sibirica* trees from stands of in subregion with low forest-to-grassland ratio (G1).

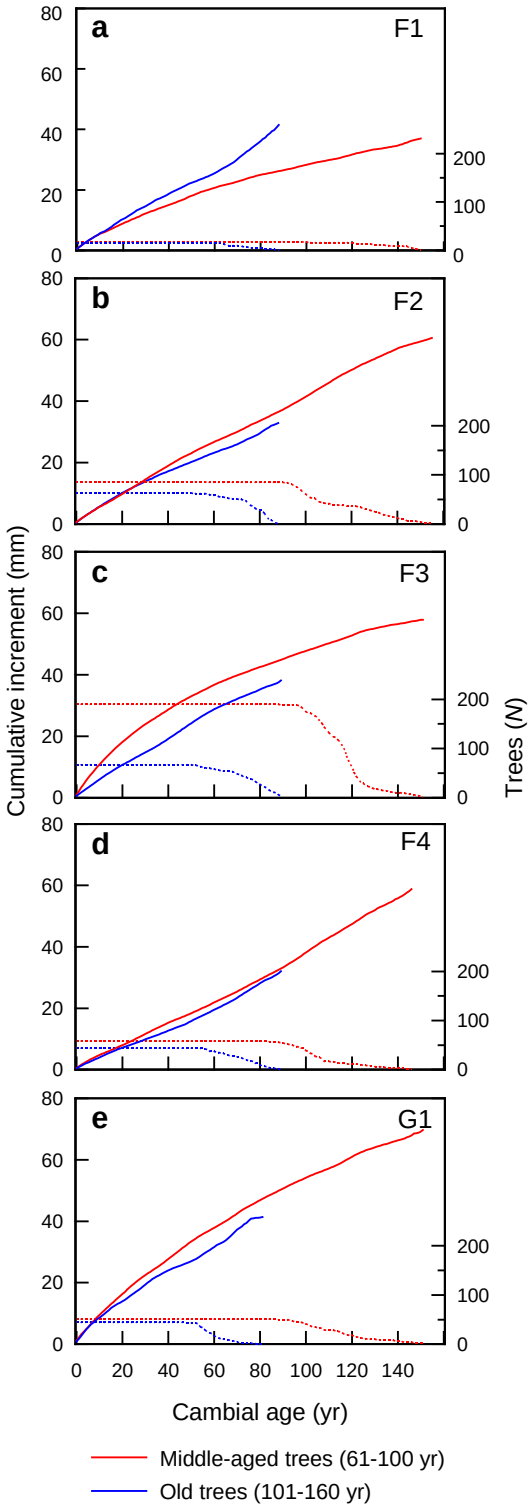

Fig. S3.5 Cumulative regional growth curves (RGC) for middle-aged (cambial age of 61−100 years) and old (101−160 years) *L. sibirica* trees in forest stands of (**a-d**) different size (increasing from F1/G1 to F4) in subregions with high (F1 to F4, south-eastern part of the study area) or (**e**) low (G1, north-western part) forest-to-grassland ratio.

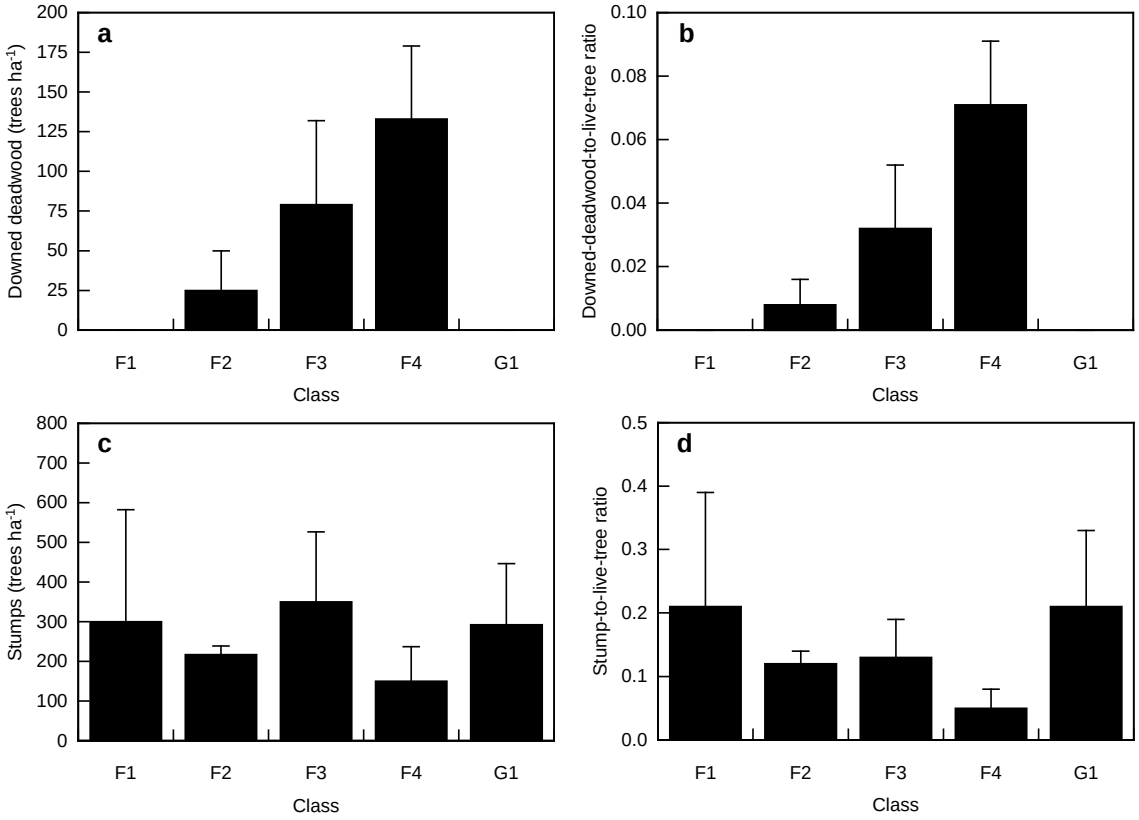

Fig. S3.6 Tree stumps (**a-b**) and downed deadwood (**c-d**) densities (**a, c**) and density ratio to live trees (**b, d**) of *L. sibirica* in forest stands of different size (increasing from F1/G1 to F4) in subregions with high (F1 to F4, south-eastern part of the study area) or low (G1, north-western part) forest-to-grassland ratio. None of the means differed significantly ($P \leq 0.05$, Duncan's multiple range test, $df_{model, error} = 4, 10$).

Chapter 4

Hydraulic traits and tree-ring width in *Larix sibirica* Ledeb. as affected by summer drought and forest fragmentation in the Mongolian forest steppe

Elmira Khansaritoreh, Bernhard Schuldt, Choimaa Dulamsuren

Accepted in **Annals of Forest Science**

4.1 Abstract

Key message **Wood-anatomical traits determining the hydraulic architecture of *Larix sibirica* in the drought-limited Mongolian forest-steppe at the southern fringe of the boreal forest respond to summer drought, but only weakly to variations in microclimate that depend on forest stand size.**

Context Siberian larch (*L. sibirica* Ledeb.) is limited by summer drought and shows increasing mortality rates in the Mongolian forest-steppe. The climate sensitivity of stemwood formation increases with decreasing forest stand size. The trees' hydraulic architecture is crucial for drought resistance and thus the capability to deal with climate warming.

Aims We studied whether hydraulic traits were influenced by temporal or forest size-dependent variations in water availability and were related to tree-ring width.

Methods Hydraulic traits (tracheid diameter, tracheid density, potential sapwood area-specific hydraulic conductivity) of earlywood were studied in stemwood series of 30 years (1985-2014) and were related to climate data. Tree-ring width was measured for the same period. Trees were selected in stands of four different size classes with increasing drought exposure with decreasing stand size.

Results Tracheid diameters and hydraulic conductivity decreased with decreasing late summer precipitation of the previous year and were positively correlated with tree-ring width. Forest stand size had only weak effects on hydraulic traits, despite known effects on stemwood increment.

Conclusion Decreasing tracheid diameters and thus hydraulic conductivity is a drought acclimation of *L. sibirica* in the Mongolian forest-steppe. These acclimations occur as a response to drought periods but are little site-dependent with respect to stand size.

Keywords

Wood anatomy, Tracheid diameters, Hydraulic conductivity, Tracheid density, Boreal forest, Forest fragmentation

4.2 Introduction

Stem wood formation is highly sensitive to variations in climate. In boreal forests, annual stem increment is usually limited by either low summer temperature or summer drought (Tei et al. 2017). Climate warming increasingly converts temperature-limited forests into drought-limited ones (Buermann et al. 2014). While the climatic limitation of stem increment is well studied and forms the basis for dendrochronology, effects on wood-anatomical features and trade-offs between tree-ring width and xylem anatomy are less well studied in boreal forests. Climate exerts effects not only on tree-ring width, but also on the occurrence of intra-annual wood-anatomical features (Yasue et al. 2000; Wang et al. 2002; De Grandpré et al. 2011); this includes traits of the xylem anatomy that are relevant for water transport (Eilmann et al. 2009; Fonti and Babushkina 2015).

Conduits for water transport should be wide to ensure high hydraulic conductivity, since the maximum flow rate depends on the conduit radius in the fourth power, according to Hagen-Poiseuille's law for the transport of fluids in cylindrical pipes (Tyree and Zimmermann 2002). Water transport is in turn the prerequisite for CO_2 assimilation. However, large conduit diameters increase the cavitation risk, which can result in hydraulic failure and ultimately tree mortality (Hacke et al. 2001; Cochard et al. 2004; Poyatos et al. 2013). The relationship between conduit diameter and embolism resistance is thought to be an indirect one that depends on pit structure (Sperry et al. 2006; Delzon et al. 2010). Trees show inter-annual and site-dependent plasticity in their hydraulic architecture to take up and transport water efficiently under moist conditions, but to reduce the risk of cavitation during drought (Poyatos et al. 2007; Bryukhanova and Fonti 2013). Relevant parameters that can be adapted to water supply include conduit diameters, conduit density, and the resulting hydraulic conductivity (Tyree and Zimmermann 2002; Tyree 2003; Pittermann et al. 2006). Dry conditions are usually associated with low hydraulic conductivity (Hacke and Sperry 2001; Sperry et al. 2006). Hydraulic conductivity results from the combination of conduit diameters and tracheid numbers in the sapwood.

The southernmost boreal forests in Inner Asia are mostly strongly drought-limited (Dulamsuren et al. 2010, 2013; Liu et al. 2013), although also temperature-limited forests occur especially at high elevations (Jacoby et al. 1996; D'Arrigo et al. 2000). The Mongolian

forest-steppe represents a widely drought-limited part of the boreal forest in this region, which is strongly dominated by Siberian larch (*Larix sibirica*). Here, Chenlemuge et al. (2015a, b) demonstrated increasing tracheid diameters and increasing hydraulic conductivity with increasing moisture availability.

Forests in the Mongolian forest-steppe are naturally fragmented, because they are largely limited to north-facing mountains slopes, which represent, aside from riverine habitats, the moistest sites in the landscape. Forest fragmentation is additionally promoted as the result of logging, livestock grazing, as well as drought- and fire-related forest declines (Khishigjargal et al. 2013; Lkhagvadorj et al. 2013; Dulamsuren et al. 2014). At present, Mongolia belongs to the countries with the highest decreases in forest cover loss (Hansen et al. 2013).
Studying the annual stem increment of *L. sibirica* in forest stands of different size, Khansaritoreh et al. (2017) found that the sensitivity of stemwood production to summer drought increased with decreasing stand size, because maximum air temperatures increased and relative humidity decreased with decreasing stand size. This means that anthropogenic forest fragmentation exacerbates the detrimental impact of global warming on tree growth in a region, which is exposed to temperature increases far above the global average (IPCC 2013) and where *L. sibirica* widely shows growth depressions, failure of regeneration, and increased mortality (Dulamsuren et al. 2010; Liu et al. 2013).

Since Chenlemuge et al. (2015a, b) established trade-offs between tree-ring width, tracheid diameter, tracheid density, and hydraulic conductivity in *L. sibirica*, we were interested in the question whether forest stand size also left an imprint in the tree's hydraulic architecture. Moreover, whereas several studies on the climate response of annual stem increment from the Inner Asian forest-steppes are published (D'Arrigo et al. 2000; De Grandpré et al. 2011; Dulamsuren et al. 2011, 2013), little is known on climate effect on hydraulic traits in *L. sibirica*. Therefore, we were also generally interested on the climate dependency of tracheid diameter, tracheid density, and hydraulic conductivity irrespective of stand size. The objective of our study was to test the hypotheses that (1) drought years cause signals in the trees' hydraulic architecture in addition to their effect on tree-ring width, (2) tracheid diameters that are crucial for shaping hydraulic conductivity are correlated with tree-ring width, (3) tracheid diameter, tracheid density, and hydraulic conductivity vary in dependence of stand size.

4.3 Materials and methods

4.3.1 Study area

The study was conducted in the Mongolian forest-steppe, which is the ecotone between the southernmost Siberian taiga and the Central Asian steppe grasslands. Field work was carried out in the Khangai Mountains in Zavkhan province (48°45' N, 98°16' E, 1700 m a.s.l.) near Tosontsengel, ca. 630 km W of Ulan Bator and 550 km SW of Lake Baikal, in August 2014. The Khangai Mountains represent a major mountain range of central and western Mongolia that constitutes much of Mongolia's forest-steppe area. The forest-steppe landscape consists of mosaics of Siberian larch forest islands occurring at variable size on north-facing slopes and grasslands covering south-facing slopes and dry valleys. Mongolia's boreal forests (ca. 73,800 km²; Dulamsuren et al. 2016) are strongly dominated by Siberian larch (*Larix sibirica* Ledeb.), which occupies 80% of the forest area (Tsogtbaatar 2004). Siliceous rock, including granite and metamorphic rock (e.g. schist), is the prevailing bedrock in our study region. The dominant forest soils are Cambisols and Leptosols.

4.3.2 Climate in Mongolia and our study area

The extreme continental climate of Mongolia is characterized by long cold winters, coined by the stable Siberian High Pressure Cell, and short warm summers with most rainfall in July. In most of the forest-steppe region, mean annual temperature is below or around zero. Mean annual precipitation is approximately 200-300 (-400) mm in most of the forest-steppe. Climatic data from our study area are available from 1964 (temperature) and 1968 (precipitation) according to records from Tosontsengel meteorological station. This study covers 30 years from 1985 to 2014 and in this period mean annual air temperature was -5.4 °C (July 15.3°C, January -31.2°C). Mean annual precipitation amounted to 232 mm, ranging from 148 to 430 mm. Mean growing season (May-September) air temperature has increased by 0.58°C decade^{-1} since 1985 (Fig. 4.1). In the growing seasons of this period, June and July showed the strongest increase in monthly temperature and a marked decrease in monthly precipitation (Fig. S4.1). August precipitation did not change over time, while August temperature has increased (like the mean growing season temperature) by c. 0.6 C decade^{-1}.

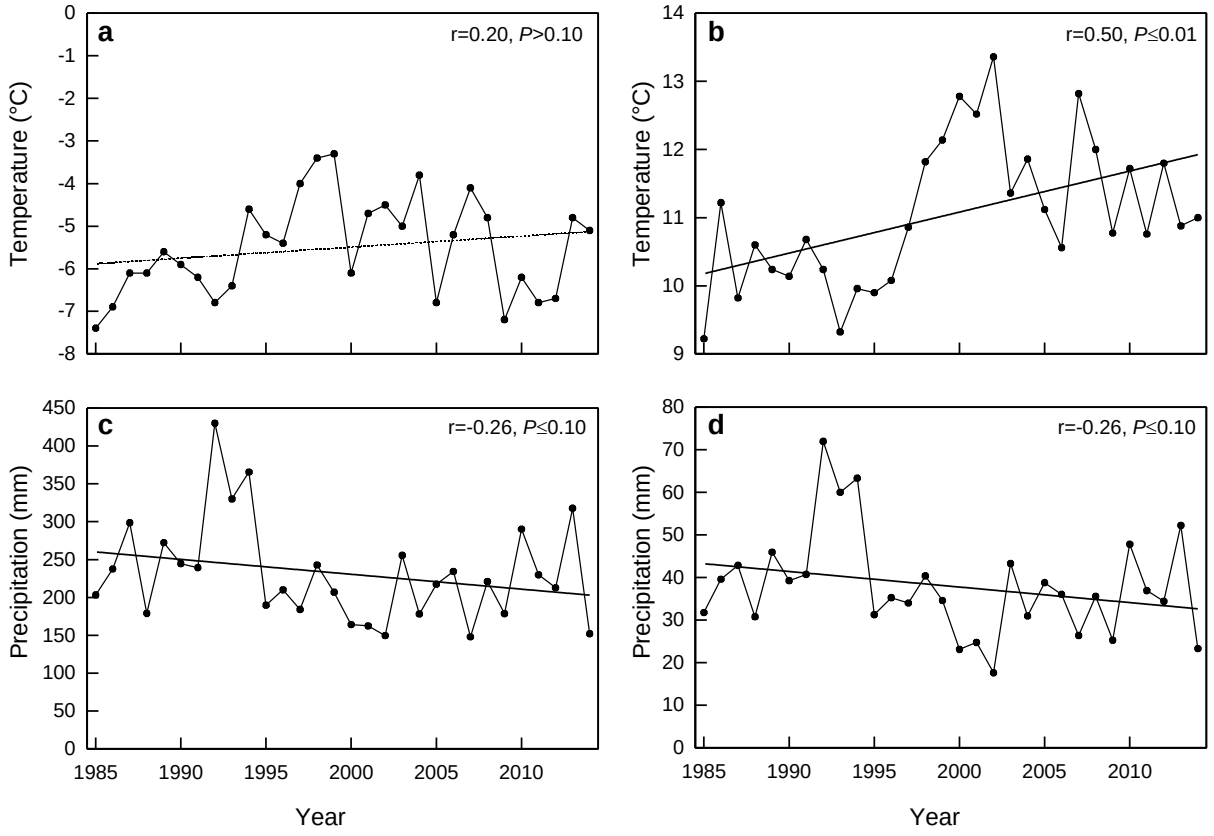

Fig. 4.1 Climate trends in Tosontsengel (48°45' N, 98°16' E, 1700 m a.s.l.), northwestern Mongolia, 1985-2014: **(a)** mean annual temperature, **(b)** mean growing season temperature, **(c)** annual precipitation, **(d)** growing season precipitation.

4.3.3 Study design and core sampling

We defined four different classes (F1 to F4) of forest stand size varying from <0.1 km^2 (F1) to >5.0 km^2 (F4) (Table 4.1) and selected two stands per size class (Fig. S4.2). Elevation of the selected stands varied between 1809 to 2135 m a.s.l. The distance of the sampled trees to the lower forest line was between 110 and 330 m. Forests of the different size classes were characterized by differences in microclimate and land use intensity (Khansaritoreh et al. 2017). Individual forest stands from different size classes were selected randomly based on remote-sensing analysis of forest distribution in the study region. Trees were selected in the interior of each forest stand and geographic positions of stands were determined by GPS.

Table 4.1 Main tree characteristics, mean sensitivity and autocorrelation of tree-ring width (arithmetic mean ± SE).

Size class	Forest size (km^2)	Height (m)	DBH (cm)	Ring width (mm)	Mean sensitivity (%)	Autocorrelation
F1	<0.1	20.2 ± 1.7 a	57.8 ± 4.3 a	0.29 ± 0.03 ab	39.6 ± 2.2 a	0.57 ± 0.06 a
F2	0.1-1.0	19.3 ± 0.8 a	36.9 ± 3.7 b	0.31 ± 0.10 a	37.8 ± 1.8 ac	0.67 ± 0.05 ab
F3	1.1-5.0	18.4 ± 1.0 a	30.4 ± 5.8 b	0.35 ± 0.08 a	35.7 ± 2.7 ac	0.68 ± 0.07 ab
F4	>5.0	19.5 ± 1.5 a	30.5 ± 2.0 b	0.25 ± 0.04 b	27.2 ± 1.1 b	0.82 ± 0.03 b

Number of samples: 5 trees per stand size class. Ring width data refers to the period 1985-2014. Stand size classes with same lower case letters are not statistically significant different (Tukey's test, $P \leq 0.05$, $df_{\text{model, error}} = 3, 15$). DBH: diameter at breast height.

We selected five trees per stand size (in total 20 individuals, Table 4.1) which were intact, stout, dominant, and of similar height to eliminate competition effects. Importance of height in relation with variation in conduit diameter and hydraulic properties has been earlier shown in several studies (Ryan and Yoder 1997; Woodruff et al. 2004; Koch et al. 2004; Pennisi 2005; Ryan et al. 2006; Domec et al. 2008; Anfodillo et al. 2013). While we kept height constant, variation in diameter at breast height (DBH) had to be accepted; F1 trees had significantly higher DBH than trees from the other stand sizes (Table 4.1). The suitability of this procedure was later reconfirmed by our data, since we found that variation in DBH did not influence anatomical traits. For example there was no significant correlation between DBH and tracheid diameters (P=0.24, r= 0.17). Non-metric multidimensional scaling (NMDS) ordination of tree-ring series results showed that our selected sample trees for anatomical studies from the individual stand size classes represented the entire stands of the same size class, because the sample trees are evenly distributed in the homogenous scatter plots (Fig. S4.3).

A total of 40 wood cores (i.e. two cores collected in close vicinity to each other from the same side of each tree) was collected at stem breast height (1.3 m height above the ground) using increment borer with an inner diameter of 5 mm. Samples were taken parallel to the contour lines of the mountain slopes to avoid compression wood.

4.3.4 Xylem anatomy analysis

All 20 cores were stored in 70 % ethanol prior to laboratory preparation. We applied two different procedures for dyeing samples based on their quality. In one procedure, the whole

cores were stained (before cutting) with safranin (1% in 50 % ethanol, Merck, Darmstadt, Germany) for 3 days followed by rinsing the samples with 70% ethanol three times while shaking for 12 h. Subsequently, the samples were soaked in distilled water for 3 days. In a second procedure, another subsample of wood cores was only soaked in distilled water to be softened and then microsections were dyed after cutting. The quality of the results of the staining procedures is slightly variable between individual samples; therefore, we selected the wood core subsample for analysis visually for every individual sample after staining. Wood cores (produced by both procedures) were cut with a sliding microtome (G.S.L. 1, WSL Birmensdorf, Switzerland) into semi-thin transverse sections (10-15 µm thick). To reduce distortions of the samples during cutting, a solution of corn starch, water and glycerol (Schneider and Gärtner 2013) was placed on the wood cores immediately before cutting. After cutting starch particles were removed by washing with water and ethanol. The unstained microsections were stained with a mixture of safranin and alcine blue for 1-2 minutes and subsequently rinsed with water. Dehydration of microsections was done firstly with 70 % ethanol and secondly with 99% ethanol. Afterwards microsections were fixed with Euparal adhesive and dried for 10 days at 50°C. Finally, the complete microsections were photographed at 100-150× magnification using a stereomicroscope equipped with an automatic stage (SteREOV20, Carl Zeiss MicroImaging GmbH, Jena, Germany; Software: AxioVision v4.8.2, Carl Zeiss MicroImaging GmbH).

Since water transport primarily takes place in the earlywood, whereas latewood has predominantly a mechanical function (Vaganov et al. 2006; Eilmann et al. 2006), we limited our analyses to earlywood formed between 1985 and 2014 (30 years). Image analysis was performed in Adobe Photoshop CS2 9.0 (Adobe Systems, San Jose, California, USA) and ImageJ software (Wayne Rasband, National Institute of Health, Bethesda, Maryland, USA) using the particle analysis function. We measured single and cumulative tracheid lumen areas (mm^2), tracheid density (TD, in N mm^{-2}) and idealized tracheid diameters (d, in µm) from both major (a) and minor (b) tracheid radii using the equation given by (White 1991) as $d = ((32(ab)^3)/(a^2+b^2))^{1/4}$. Hydraulic mean diameter (d_h, in µm), which puts more weight on large than small conducting vessels (Sperry et al. 1994), was calculated from d as $d_h = \sum d^5/\sum d^4$. According to the Hagen-Poiseuille equation, potential sapwood area-specific hydraulic conductivity (K_p, in kg m^{-1} MPa^{-1} s^{-1}) was calculated from the tracheid radii as $K_p = \pi (\sum r^4) \rho/(8 \eta A_{xylem})$, where η is the viscosity and ρ is the density of water at 20°C, while A_{xylem} is the

corresponding cross-sectional xylem area without pith and bark. In the stem wood, we analyzed a range of 63-1,033 tracheids per tree ring or 5,260-13,341 tracheids per complete cross section. The high variability is due to inter-annual variation in stem increment.

4.3.5 Tree ring analysis

One core per sample tree was prepared (mounted on wooden strips, cut lengthwise with a microtome and chalk added to enhance contrasts between the annual rings) for measurement of tree-ring width (TRW). TRW was measured and tree-ring data were evaluated with Time Series Analysis and Presentation (TSAP)-Win software (Rinntech, Heidelberg, Germany). We used a movable object table (Lintab 6, Rinntech) that electronically transmit shifts to a computer system equipped with TSAP-Win software to measure TRW (and the widths of earlywood and latewood separately) with a precision of 10 µm. All chronologies were cross-dated visually and checked for missing rings. Cross-dating accuracy was assessed by the calculation of coefficients of agreement ('Gleichläufigkeit' [GL]) and (standard) *t*-value (Eckstein and Bauch 1969). Only tree-ring series with GL>65% and t>3 were united to mean curves. The exact tree age could not be determined for all sample trees, since the center of most trees was rotten (14 out of 20 trees). However, we could make sure that all trees belonged to the same age class of >160 years. Information on mean tree age in the stand size classes F1 to F4 from our study area is available from Khansaritoreh et al. (2017, Table S4.1). Based on a much higher sample size of 1033 trees, that study showed a mean cambial age (±SE) of 157±9 years for F1 (N=176 trees), 146±12 years for F2 (N=146), 143±13 years for F3 (N=317), and 130±11 years for F4 (N=279); there was no significant difference in tree age between the stand sizes in that data set ($P \leq 0.05$, Duncan's multiple range test). Representativeness of our sample trees for the trees of the same age class from the studied forest stands was controlled by NMDS. For NMDS, we used a larger data set of all >160-year old trees from 400 m^2 plots in the studied forests that was available from Khansaritoreh et al. (2017). Any correlation of anatomical traits with TRW were made with complete TRW, which was closely correlated with earlywood width (r = 0.99, $P \leq 0.001$). The expressed population signal (EPS) was calculated using Arstan software (Cook and Holmes 1984) to quantify how well our tree-ring series represented the stem increment dynamics of the studied stands. We accepted a given tree-ring series as representative for the whole stand when EPS >0.85 (Wigley et al. 1984).

4.3.6 Climate-response analysis

Climate-response analysis was conducted separately for each tree using monthly means of temperature and monthly sums of precipitation from 1985 to 2014 to quantify the influence of current and prior year's climate on the tree-ring index and *d*. Since we knew about an intensive fire in the study area in 1996 that produced a strong growth anomaly in 1997, we removed that year from our analysis to focus on the effect of climate. This was done to exclude immediate effects of fire in the sampled stands; however, it should be noted that lagged effects and competition effects from any other disturbance influenced the analysis like in any other climate-response analysis. For the climate-response analysis, the individual tree-ring series were standardized in order to remove any age-related trends. Standardization was applied, although it has only a limited effect on the results in the short time span of only 30 years included in our analysis. We used a 32-year cubic spline function with a 50% frequency response (Cook and Kairiukstis 1990) for indexation of TRW data. We did not attempt any standardization for *d*, since we exclude the first years of growth with considerable tracheid dimension increase (Carrer et al. 2015).

Based on the monthly temperature and precipitation data and latitude of our study site, we calculated potential evapotranspiration (PET) after Thornthwaite (1948). PET was used to calculate the standardized precipitation-evapotranspiration index (SPEI) on a monthly resolution using version 1.6 of the R package "SPEI" (Vicente-Serrano et al. 2010). To find the shortest drought episodes, we selected SPEI1(resolution of only one month), because drought-sensitive tree species on shallow soils may be affected by short drought periods (Fonti and Babushkina 2015).Year-to-year variability of tree-ring width was expressed as mean sensitivity, which was calculated as the difference in TRW of two consecutive years divided by the mean TRW of these years. First-order autocorrelation analyzing the connecting between the increment in two consecutive years was calculated as a measure of the tree's physiological buffering capacity (Fritts 1976). Mean sensitivity and first-order autocorrelation were calculated from raw TRW data for the period from 1985-2014. Pointer years were calculated using the "PointRes" package in R (van der Maaten-Theunissen et al. 2015) to obtain information on climatically driven event years that might have influenced wood anatomy (Schweingruber et al. 1990). Since our data set of 20 trees was too small for calculating pointer years, we included data of 1280 *L. sibirica* trees within the same study area (Khansaritoreh et al. 2017).

4.3.7 Data processing and statistical analysis

Arithmetic means ± standard errors (SE) are given throughout the paper. Wood-anatomical and hydraulic data from each stem samples were first averaged for individual tree rings, then averaged (for each year) over the five trees of each stand size class. Data were tested for normality using the Shapiro-Wilk test. One-way analysis of variance (ANOVA) was combined with Tukey's post hoc test to find significant difference between stand size classes. To remove the age effect from time series, we used the R-package 'Dendrochronology Program Library in R' (dplR) 1.5.5 (Bunn 2008). Multiple regression analysis was used to quantify the response of the tree-ring index and *d* to climate. Kernel Density Estimation (KDE) was calculated for *d* of all samples grouped by the SPEI of the prior August, because precipitation of this month showed the most significant correlation with *d*. The NMDS was calculated using PAST 3.15 software (Ø. Hammer, Natural History Museum, University of Oslo, Norway). Correlation coefficients were calculated in linear and non-linear fits. If not mentioned otherwise, statistical analyses were carried out in R software (R Development Core Team).

4.4 Results

4.4.1 Hydraulic conductivity and anatomical traits

Mean diameters (d) and hydraulically weighted mean diameters (d_h) of tracheids as well as the theoretical sapwood area-specific hydraulic conductivity (K_p) were higher in the largest (F4) than in the smallest forest stands (F1; Table 4.2). Tracheid density was lower in the F4 than the F1 stands. Nevertheless, there was no consistent trend for constant changes of these parameters with increasing forest stand size from F1 to F4. There were many inter-annual fluctuations in time series of anatomical traits (d, d_h, TD, K_p) in all forest stand sizes (Fig. S4.4). Any linear temporal trends for d, d_h, TD, and K_p were absent, except for an increase of d (P<0.001), d_h (P=0.003), and K_p (P=0.001) and a decrease of TD (P<0.001) over time in F4.

Table 4.2. Anatomical parameters averaged over the period from 1985-2014 (arithmetic mean ± SE).

Stand size	d (µm)	d_h (µm)	TD (N mm^{-2})	K_p (kg m^{-1} MPa^{-1} s^{-1})
F1	29.4 ± 0.4 a	37.9 ± 0.4 a	610 ± 21 a	18.7 ± 0.4 a
F2	29.9 ± 0.9 a	38.1 ± 1.0 a	620 ± 42 a	19.6 ± 0.9 ac
F3	25.3 ± 1.7 b	32.8 ± 2.3 b	787 ± 115 b	13.1 ± 2.3 b
F4	31.2 ± 0.8 c	39.3 ± 1.2 c	548 ± 28 c	20.2 ± 1.6 c

Tracheid diameter (d), hydraulically weighted mean tracheid diameter (d_h), tracheid density (TD), potential sapwood area-specific hydraulic conductivity (K_p). Stand size classes with same lower case letters are not statistically significant different (Tukey's test results, $P \leq 0.05$, $df_{model,\ error} = 3, 596$).

4.4.2 Radial stem wood increment and stands size

Mean tree-ring width (TRW) for the period between 1985 and 2014 ranged from 0.25-0.35 mm and did not reveal any consistent trend for increase or decrease with the forest stand size (Fig. 4.2, Table 4.1). For the 20 sample trees, EPS reached 0.89 in 1895, which is long before our study interval from 1985-2014. Mean sensitivity decreased and first-order autocorrelation increased with forest stand size (Table 4.1). Tracheid diameter (d, d_h) and K_p increased with increasing TRW, whereas tracheid density (TD) decreased with TRW (Fig. 4.3).

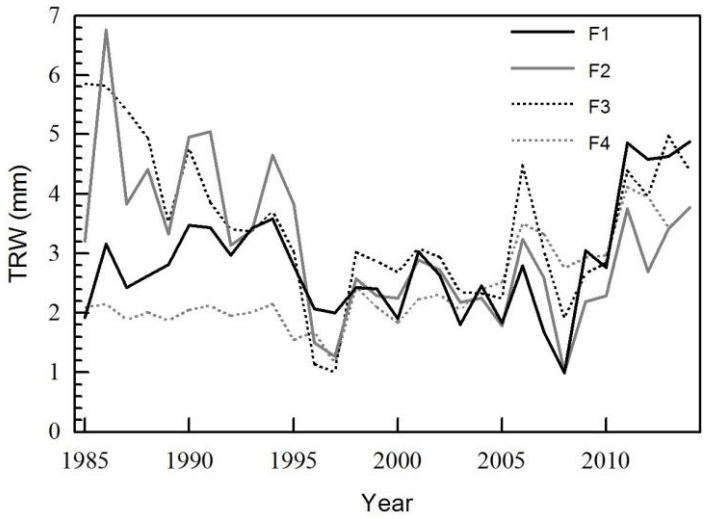

Fig. 4.2 Tree-ring chronologies of *L. sibirica* from the stand size classes F1 (<0.1 km^2), F2 (0.1−1 km^2), F3 (1.1−5 km^2), and F4 (>5 km^2) for the period of 1985-2014.

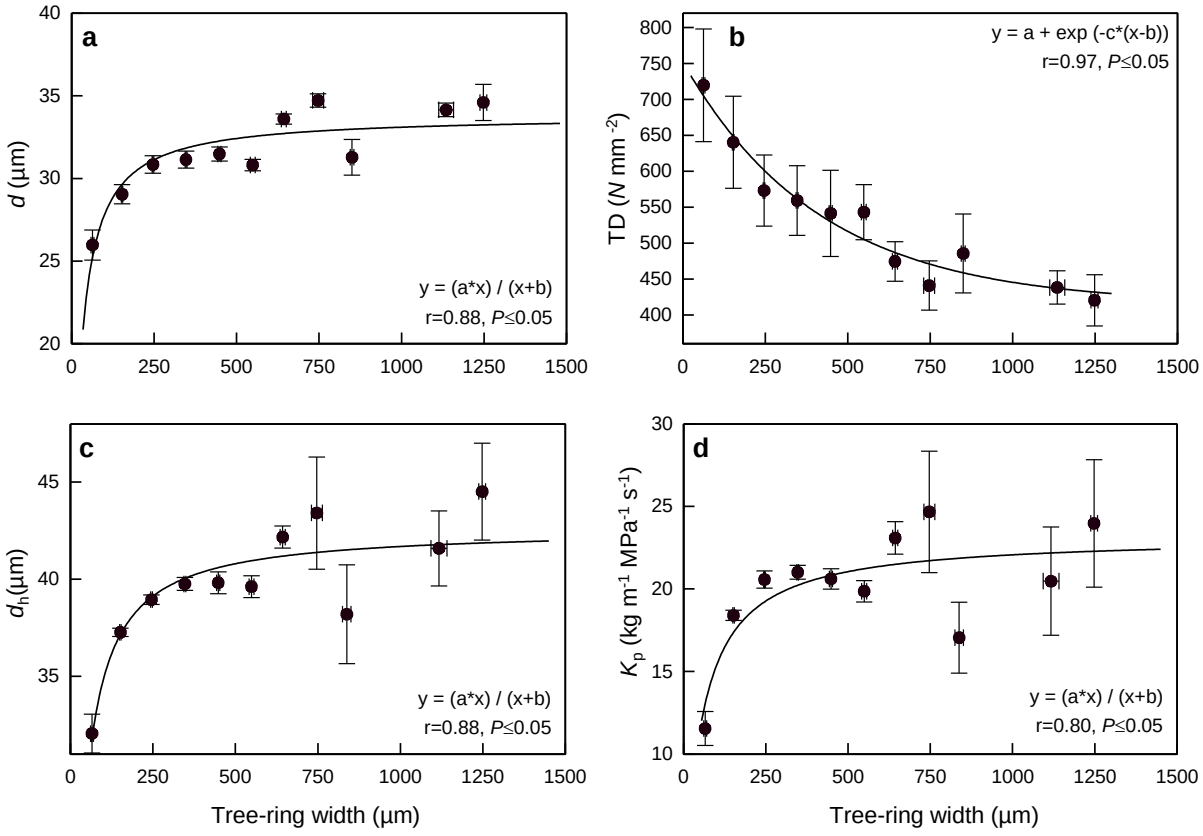

Fig. 4.3 (a) Tracheid diameter (*d*), **(b)** tracheid density (TD), **(c)** hydraulically weighted mean tracheid diameter (d_h), and **(d)** potential sapwood area-specific hydraulic conductivity (K_p) versus tree-ring width (TRW, pooled in classes of 100 µm). Bars indicate SE.

4.4.3 Climate response and tracheid size variation with summer drought

Climate-response analysis revealed correlations of the tree-ring index and the hydraulic traits with the precipitation of the previous year (Table 4.3). The August precipitation of the previous year was nearly consistently correlated with the tree-ring index, d, and d_h (positive correlations) as well as with TD (negative correlations). K_p as a value derived from d was only significant at $P \leq 0.05$ in the smallest forests of the size classes F1 and F2. June precipitation of the previous year was positively correlated with the tree-ring index in all except the largest forests (F1 to F3), but was only sporadically correlated with the hydraulic parameters. The frequency distributions of d in dependence of previous year's August SPEI also highlights the influence of water availability in late summer (Fig. 4.5). Tracheid diameters were smaller under dry conditions (SPEI -1) than at better water supply (SPEI ≥0). Except for K_p, which only increased with the previous years' August precipitation in small stands (F1, F2), stand size had no control of the occurrence of correlations between hydraulic traits and climate parameters.

Table 4.3 Response of the tree-ring index, tracheid diameter (*d*), hydraulically weighted mean tracheid diameter (d_h), tracheid density (TD), and potential sapwood area-specific hydraulic conductivity (K_p) of *Larix sibirica* trees from different stand size classes to monthly temperature and precipitation of the year of and the year prior to tree ring formation.

	Temperature							Precipitation											
	Prior year						Current year	Prior year									Current year		
	3	4	5	6	7	8	4	3	4	5	6	7	8	10	11	12	2	3	5	6
Tree-ring index:																				
F1								□			●		●		●					
F2											●		●		○					○
F3								□			●	○	●		●					
F4													●							
Tracheid diameter (*d*):																				
F1													●		○	●				
F2										○	●		●							
F3															○					
F4						□	○	■	●				●							
Hydraulically weighted tracheid mean diameter (d_h):																				
F1													○							
F2											●		●		○					
F3													●	■		●	□		●	●
F4		○			●	■		■	●				●							
Tracheid density (TD):																				
F1				□									■							
F2										□	■		■	□	■					
F3													■	○	□					
F4	□		●		■	●					○		■			○		○		
Potential sapwood area-specific hydraulic conductivity (K_p):																				
F1													●							
F2										●	●		●		●					
F3										○				□	●					
F4						□		■	●				○							

Correlation significant ($P \leq 0.05$): ● positive, ■ negative correlation; marginally significant ($P \leq 0.10$): ○ positive, □ negative correlation. Months are identified with numbers 1 to 12; months without correlation are not listed.

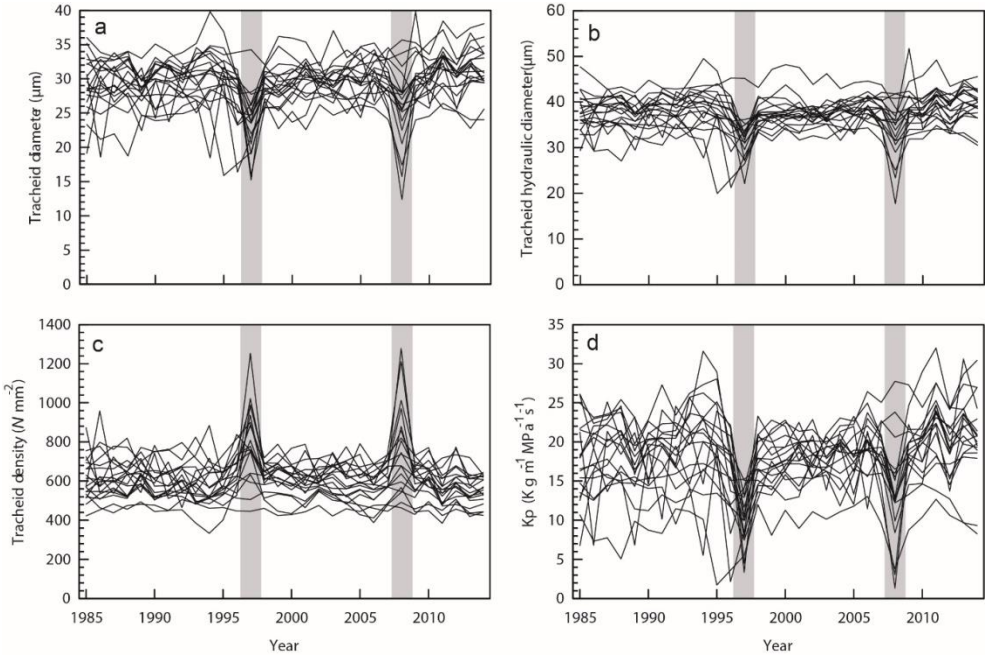

Fig. 4.4 Time-series of (a) *d*, (b) $d_{h,}$ (c) TD, (d) K_p, over the period 1985-2014. Pointer years 1997 and 2008 are shaded in grey.

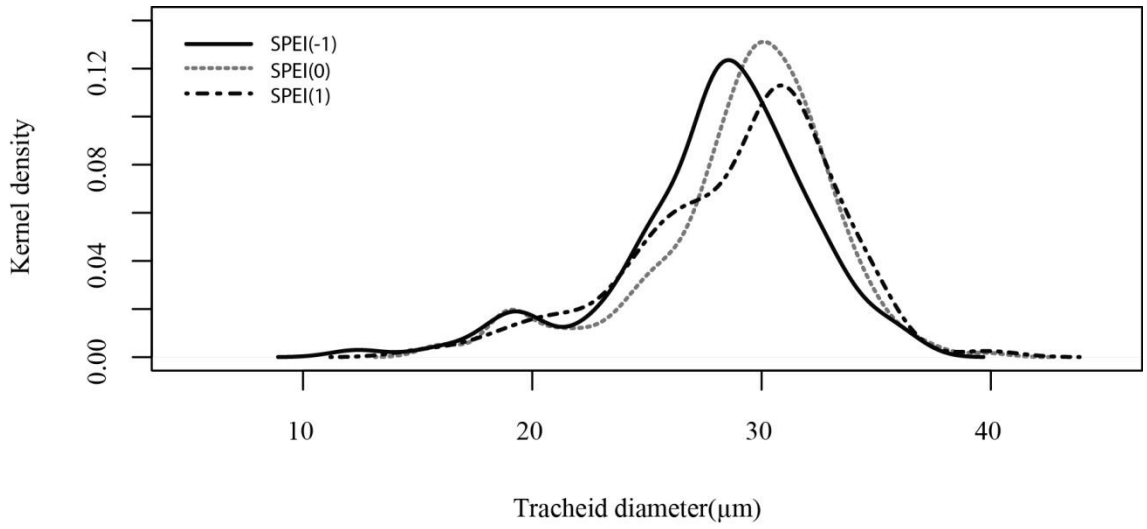

Fig. 4.5 Density distributions of all tracheid diameters grouped per standardized precipitation-evapotranspiration index (SPEI) of prior year August. Negative and positive SPEI indicate dryness and wetness respectively. The density distributions were calculated with a Gaussian smoothing and the "nrd0" bandwidth using the "density" function of R (R Development Core Team, 2013). Tracheid data from 6, 13, 6 years were included in the classes of SPEI −1, 0, and 1 respectively. Lines for the SPEI -2 and 2 are not shown since only found in 2 and 3 years.

4.4.4 Pointer years

From 1985-2014, we found negative pointer years in 1997 and 2008 and positive pointer year in 2006 (Fig. S4.5). The negative pointer years were associated with low values of d, d_h, and K_p, but high TD (Fig. 4.4). The pointer year in 1997 followed an intense forest fire in 1996, whereas the pointer year in 2008 followed 2 years with below-average precipitation in August (to, respectively, 35 and 75 % of the mean August precipitation in the period 1985-2014), which was identified as significant for stemwood production in the climate-response analysis (Table 4.3).

4.5 Discussion

Our analyses provide multiple evidence that summer drought in the previous year affects not only tree-ring width, but also the hydraulic architecture of *L. sibirica*. Tracheid diameters (d, d_h) and the potential sapwood area-specific hydraulic conductivity (K_p) were strongly reduced due to drought. Climate-response analysis showed that the amount of precipitation in late summer (August) of the previous year was most influential for determining tracheid diameters and hydraulic conductivity in the consecutive growing season. This relationship coincides with reductions of tree-ring width by drought in the previous growing season that was repeatedly found in water-limited *L. sibirica* forests (Dulamsuren et al. 2011, 2013; Tei et al. 2017). The influence of the climate in the prior year is often thought (but not proven) to be mediated by the climatic limitation of the tree's capability to build up stocks of non-structural carbohydrates. Carbohydrate reserves from the previous year need to be used, since most wood is formed in the early growing season (Begum et al. 2010). However, the relationships between non-structural carbohydrate pools, climate, and wood formation are complex and far from being completely understood (Oberhuber et al. 2011; Simard et al. 2013; Palacio et al. 2014).

Whether low tracheid diameters are just the consequence of low annual stem increment or can vary independently of each other is not completely clear. There are several examples of reduced conduit diameters at low tree-ring width (Vaganov et al. 2006; Martin-Benito et al. 2013; Ziaco et al. 2014) in agreement with our findings. However, while Khansaritoreh et al. (2017) demonstrated an increasing drought sensitivity of stemwood formation with decreasing forest stand size, we found only loose relations between stand size and hydraulic

traits. Although d, d_h, and K_p were higher and tracheid density (TD) was lower in the largest forests than in the smallest stands, there was no consistent trend between these parameters and stand size. Moreover, for most parameters, we did not find a consistent change of the relationship of these parameters to climate variables along with forest stand size, in contrast to the observations of Khansaritoreh et al. (2017) for annual stem increment. The only exception was the correlation between K_p and the previous year's August precipitation in the small stands of the size classes F1 and F2, but not in the larger stands (F3, F4). Probably, the more extreme microclimate of the small stands with high maximum temperatures and low humidity increased to responsiveness of K_p to late summer precipitation. We can only speculate why this relationship of stand size with tree-ring width was not more widespread for the wood-anatomical and hydraulic parameters. A possible explanation could be the existence of different climatic controls for cell division and cell differentiation. Moreover, it could play a role that we kept tree height constant in the present study, since tracheid diameter is known to be related to tree height, while tree height and diameter are not closely correlated (Anfodillo et al. 2012; Carrer et al. 2015).

The observed reduction of tracheid diameters as the result of summer drought is beneficial for the trees to prevent hydraulic failure and potentially mortality (Sperry et al. 2006; McDowell 2011; Sevanto et al. 2014). Combined with low tracheid density, the formation of low-diameter tracheid reduces hydraulic conductivity. *L. sibirica* is also known for low fine-root mass during drought (Chenlemuge et al. 2013), providing evidence of low capacity for water transport right from the beginning of the plant's hydraulic pathway as the consequence of preceding drought events. Unfortunately, we have no reliable data of defoliation events and thus Huber values available for *L. sibirica* to quantify the sapwood-to-leaf area ratio (Carter and White 2009), which would be helpful for a complete understanding of the drought response in this species. A reduction of transpiration by needle abscission and the closure of stomata would be a likely strategy to form drought resistance in addition to acclimations of the root system (Chenlemuge et al. 2013) and the stem xylem (this study). Studying sites of different macroclimate or competition, Chenlemuge et al. (2015a, b) found increasing tracheid diameter and hydraulic conductivity with increasing water availability in root, stem, and branch xylem of *L. sibirica*. Stomatal regulation is generally sensitive in conifers, but less sensitive in *L. sibirica* than in *Pinus sylvestris*, which is another drought-tolerant tree species at the southern edge of the boreal forest (Dulamsuren et al. 2009a, b).

4.6 Conclusion

Tracheid diameters (d, d_h), potential sapwood area-specific hydraulic conductivity (K_p), and tracheid density (TD) were shown to vary in *L. sibirica* from the Mongolian forest-steppe ecotone with temporal variations in climate. In agreement with our first hypothesis, drought in the previous years' late summer reduced tracheid diameters and hydraulic conductivity, but increased tracheid density in the following growing season. Tree-ring width that was shown earlier also to be reduced by summer drought in the preceding year was correlated with tracheid diameter in support of our second hypotheses. Forest fragmentation and the resulting variation in stand climate is apparently only a weak determinant of the hydraulic architecture in *L. sibirica*, which largely falsifies our third hypothesis. Our findings on the influence of dry late summers on the hydraulic traits in *L. sibirica* clearly suggest that the trend for increasing summer drought that is observed at the southern fringe of the boreal forest in Inner Asia not only leads to reduced stemwood formation, but also to acclimations of the hydraulic architecture of *L. sibirica*. These acclimations might ensure some protection against hydraulic failure and tree mortality, but reported cases of *L. sibirica* mortality in this region (Liu et al. 2013; Dulamsuren et al. unpublished) demonstrate that this acclimation of the hydraulic system is not capable of keeping pace with the rapid increase in aridity in Inner Asia.

Acknowledgments

The study was supported by a grant of the Volkswagen Foundation to M. Hauck, Ch. Dulamsuren and Ch. Leuschner for the project "Forest regeneration and biodiversity at the forest-steppe border of the Altai and Khangai Mountains under contrasting developments of livestock numbers in Kazakhstan and Mongolia". E. Khansitoreh received an Erasmus Mundus Scholarship in the Salam 2 program. We are thankful to the director of the Tarvagatai Nuruu National Park, Ms. D. Tuya, for her support during field work.

References

Anfodillo T, Deslauriers A, Menardi R, Tedoldi L, Petit G, Rossi S (2012) Widening of xylem conduits in a conifer tree depends on the longer time of cell expansion downwards along the stem. J Exp Bot 63:837-845

Anfodillo T, Petit G, Crivellaro A (2013) Axial conduit widening in woody species: A still neglected anatomical pattern. IAWA J 34:352-364

Begum S, Nakaba S, Oribe Y, Kubo T, Funada R (2010) Changes in the localization and levels of starch and lipids in cambium and phloem during cambial reactivation by artificial heating of main stems of *Cryptomeria japonica* trees. Ann Bot 106:885-895

Bryukhanova M, Fonti P (2013) Xylem plasticity allows rapid hydraulic adjustment to annual climatic variability. Trees 27:485-496

Buermann W, Parida B, Jung M, MacDonald GM, Tucker CJ, Reichstein M (2014) Recent shift in Eurasian boreal forest greening response may be associated with warmer and drier summers. Geophys Res Lett 41:1995-2002

Bunn AG (2008) A dendrochronology program library in R (dplR). Dendrochronologia 26:115-124

Carrer M, Von Arx G, Castagneri D, Petit G (2015) Distilling allometric and environmental information from time series of conduit size: The standardization issue and its relationship to tree hydraulic architecture. Tree Physiol 35:27-33

Carter JL, White DA (2009) Plasticity in the Huber value contributes to homeostasis in leaf water relations of a mallee Eucalypt with variation to groundwater depth. Tree Physiol 29:1407-1418

Chenlemuge Ts, Dulamsuren Ch, Hertel D, Schuldt B, Leuschner C, Hauck M (2015a) Hydraulic properties and fine root mass of *Larix sibirica* along forest edge-interior gradients. Acta Oecologica 63:28-35

Chenlemuge Ts, Hertel D, Dulamsuren Ch, Khishigjargal M, Leuschner C, Hauck M (2013) Extremely low fine root biomass in *Larix sibirica* forests at the southern drought limit of the boreal forest. Flora 208:488-496

Chenlemuge Ts, Schuldt B, Dulamsuren Ch, Hertel D, Leuschner C, Hauck M (2015b) Stem increment and hydraulic architecture of a boreal conifer (*Larix sibirica*) under contrasting macroclimates. Trees 29:623-636

Cochard H, Froux F, Mayr S, Coutand C (2004) Xylem wall collapse in water-stressed pine

needles. Plant Physiol 134:401-408

Cook E, Holmes R (1984) Program ARSTAN user manual. Laboratory of Tree-Ring Research, University of Arizona, Tucson, Arizona

Cook E, Kairiukstis L (1990) Methods of dendrochronology. Springer, Dordrecht

D'Arrigo R, Jacoby G, Pederson N, Frank D, Buckley B, Nachin B, Mijiddorj R, Dugarjav C (2000) Monogolian tree-rings, temperature sensitivity and reconstructions of Northern Hemisphere temperature. Holocene 10:669-672

De Grandpré L, Tardif JC, Hessl A, Pederson N, Conciatori F, Green TR, Oyunsanaa B, Baatarbileg N (2011) Seasonal shift in the climate responses of *Pinus sibirica*, *Pinus sylvestris*, and *Larix sibirica* trees from semi-arid, north-central Mongolia. Can J For Res 41:1242-1255

Delzon S, Douthe C, Sala A, Cohard H (2010) Mechanism of water-stress induced cavitation in conifers: bordered pit structure and function support the hypothesis of seal capillary-seeding. Plant Cell Environ 33:2101-2111

Domec J-C, Lachenbruch B, Meinzer FC, Woodruff DR, Warren JM, McCulloh KA (2008) Maximum height in a conifer is associated with conflicting requirements for xylem design. Proc Natl Acad Sci USA 105:12069-12074

Dulamsuren Ch, Hauck M, Bader M, Osokhjargal D, Oyungerel Sh, Nyambayar S, Runge M, Leuschner C (2009a) Water relations and photosynthetic performance in *Larix sibirica* growing in the forest-steppe ecotone of northern Mongolia. Tree Physiol 29:99-110

Dulamsuren Ch, Hauck M, Bader M, Oyungerel Sh, Osokhjargal D, Nyambayar S, Leuschner C (2009b) The different strategies of *Pinus sylvestris* and *Larix sibirica* to deal with summer drought in a northern Mongolian forest-steppe ecotone suggest a future superiority of pine in a warming climate. Can J For Res 39:2520-2528

Dulamsuren Ch, Hauck M, Khishigjargal M, Leuschner HH, Leuschner C (2010) Diverging climate trends in Mongolian taiga forests influence growth and regeneration of *Larix sibirica*. Oecologia 163:1091-1102

Dulamsuren Ch, Hauck M, Leuschner HH, Leuschner C (2011) Climate response of tree-ring width in *Larix sibirica* growing in the drought-stressed forest-steppe ecotone of northern Mongolia. Ann For Sci 68:275-282

Dulamsuren Ch, Khishigjargal M, Leuschner C, Hauck M (2014) Response of tree-ring width to climate warming and selective logging in larch forests of the Mongolian Altai. J Plant Ecol 7:24-38

Dulamsuren Ch, Klinge M, Degener J, Khishigjargal M, Chenlemuge Ts, Bat-Enerel B, Yeruult Yo, Saindovdon D, Ganbaatar Kh, Tsogtbaatar J, Leuschner C, Hauck M (2016) Carbon pool densities and a first estimate of the total carbon pool in the Mongolian forest-steppe. Glob Chang Biol 22:830-844

Dulamsuren Ch, Wommelsdorf T, Zhao F, Xue Y, Zhumadilov BZ, Leuschner C, Hauck M (2013) Increased summer temperatures reduce the growth and regeneration of *Larix sibirica* in southern boreal forests of eastern Kazakhstan. Ecosystems 16:1536-1549

Eckstein D, Bauch J (1969) Beitrag zur Rationalisierung eines dendrochronologischen Verfahrens und zur Analyse seiner Aussagesicherheit. Forstwiss Centralbatt 88:230-250

Eilmann B, Weber P, Rigling A, Eckstein D (2006) Growth reactions of *Pinus sylvestris* L. and *Quercus pubescens* Willd. to drought years at a xeric site in Valais, Switzerland. Dendrochronologia 23:121-132

Eilmann B, Zweifel R, Buchmann N, Fonti P, Rigling A (2009) Drought-induced adaptation of the xylem in Scots pine and pubescent oak. Tree Physiol 29:1011-1020

Fonti P, Babushkina EA (2015) Tracheid anatomical responses to climate in a forest-steppe in Southern Siberia. Dendrochronologia 39:32-41

Fritts HC (1976) Tree rings and climate. Academic Press, London

Hacke UG, Sperry JS (2001) Functional and ecologycal xylem anatomy. Perspect Plant Ecol Evol Syst 4:97-115

Hacke UG, Sperry JS, Pockman WT, Davis SD, McCulloh KA (2001) Trends in wood density and structure are linked to prevention of xylem implosion by negative pressure. Oecologia 126:457-461

Hansen MC, Potapov PV, Moore R, Hancher M, Turubanova SA, Tyukavina A, Thau D, Stehman SV, Goetz SJ, Loveland TR, Kommareddy A, Egorov A, Chini L, Justice CO, Townshend JRG (2013) High-resolution global maps of 21st-century forest cover change. Science 342:850-853

IPCC (2013) Climate change 2013: the physical science basis. Contribution of working group I to the fifth assessment report of the Intergovernmental Panel on Climate Change. Cambridge University Press, Cambridge

Jacoby GC, D'Arrigo RD, Davaajamts T (1996) Mongolian tree-rings and 20th-century warming. Science 273:771-773

Khansaritoreh E, Dulamsuren Ch, Klinge M, Ariunbaatar T, Bat-Enerel B, Batsaikhan G, Ganbaatar Kh, Saindovdon D, Yeruult Yo, Tsogtbaatar J, Tuya D, Leuschner C, Hauck M

(2017) Higher climate warming sensitivity of Siberian larch in small than large forest islands in the fragmented Mongolian forest steppe. Glob Chang Biol 23:3675-3689

Khishigjargal M, Dulamsuren Ch, Lkhagvadorj D, Leuschner C, Hauck M (2013) Contrasting responses of seedling and sapling densities to livestock density in the Mongolian forest-steppe. Plant Ecol 214:1391-1403

Koch GW, Sillett SC, Jennings GM, Davis SD (2004) The limits to tree height. Nature 428:851-854

Liu H, Park Williams A, Allen CD, Guo D, Wu X, Anenkhonov OA, Liang E, Sandanov DV, Yin Y, Qi Z, Badmaeva NK (2013) Rapid warming accelerates tree growth decline in semi-arid forests of Inner Asia. Glob Chang Biol 19:2500-2510

Lkhagvadorj D, Hauck M, Dulamsuren Ch, Tsogtbaatar J (2013) Pastoral nomadism in the forest-steppe of the Mongolian Altai under a changing economy and a warming climate. J Arid Environ 88:82-89

Martin-Benito D, Beeckman H, Cañellas I (2013) Influence of drought on tree rings and tracheid features of *Pinus nigra* and *Pinus sylvestris* in a mesic Mediterranean forest. Eur J For Res 132:33-45

McDowell NG (2011) Mechanisms linking drought, hydraulics, carbon metabolism, and vegetation mortality. Plant Physiol 155:1051-1059

Oberhuber W, Swidrak I, Pirkebner D, Gruber A (2011) Temporal dynamics of nonstructural carbohydrates and xylem growth in *Pinus sylvestris* exposed to drought. Can J For Res 41:1590-1597

Palacio S, Hoch G, Sala A, Körner C, Millard P (2014) Does carbon storage limit tree growth? New Phytol 201:1096-1100

Pennisi E (2005) Tree growth: The sky is not the limit. Science 310:1896-1897

Pittermann J, Sperry JS, Wheeler JK, Hacke UG, Sikkema EH (2006) Mechanical reinforcement of tracheids compromises the hydraulic efficiency of conifer xylem. Plant Cell Environ 29:1618-1628

Poyatos R, Aguadé D, Galiano L, Mencuccini M, Martínez-Vilalta J (2013) Drought-induced defoliation and long periods of near-zero gas exchange play a key role in accentuating metabolic decline of Scots pine. New Phytol 200:388-401

Poyatos R, Martínez-Vilalta J, Čermák J, Ceulemans R, Granier A, Irvine J, Köstner B, Lagergren F, Meiresonne L, Nadezhdina N, Zimmermann R, Llorens P, Mencuccini M (2007) Plasticity in hydraulic architecture of Scots pine across Eurasia. Oecologia

153:245-259

Ryan MG, Phillips N, Bond BJ (2006) The hydraulic limitation hypothesis revisited. Plant Cell Environ 29:367-381

Ryan MG, Yoder BJ (1997) Hydraulic limits to tree height and tree growth: what keeps trees from growing beyond a certain height? Bioscience 47:235-242

Schneider L, Gärtner H (2013) The advantage of using a starch based non-Newtonian fluid to prepare micro sections. Dendrochronologia 31:175-178

Schweingruber FH, Eckstein D, Serre-Bachet F, Bräker OU (1990) Identification, presentation and interpretation of event years and pointer years in dendrochronology. Dendrochronologia 8:9-38

Sevanto S, Mcdowell NG, Dickman LT, Pangle R, Pockman WT (2014) How do trees die? A test of the hydraulic failure and carbon starvation hypotheses. Plant Cell Environ 37:153-161

Simard S, Giovannelli A, Treydte K, Traversi ML, King GM, Frank D, Fonti P (2013) Intra-annual dynamics of non-structural carbohydrates in the cambium of mature conifer trees reflects radial growth demands. Tree Physiol 33:913-923

Sperry J, Nichols K, Sullivan J, Eastlack S (1994) Xylem embolism in ring-porous, diffuse-porous, and coniferous trees of northern Utah and interior Alaska. Ecology 75:1736-1752

Sperry JS, Hacke UG, Pittermann J (2006) Size and function in conifer tracheids and angiosperm vessels. Am J Bot 93:1490-1500

Tei S, Sugimoto A, Yonenobu H, Matsuura Y, Osawa A, Sato H, Fujinuma J, Maximov T (2017) Tree-ring analysis and modeling approaches yield contrary response of circumboreal forest productivity to climate change. Glob Chang Biol. doi: 10.1111/gcb.13780

Thornthwaite CW (1948) An approach toward a rational classification of climate. Geogr Rev 38:55-94

Tsogtbaatar J (2004) Deforestation and reforestation needs in Mongolia. For Ecol Manage 201:57-63

Tyree MT (2003) Hydraulic limits on tree performance: transpiration, carbon gain and growth of trees. Trees 17:95-100

Tyree MT, Zimmermann MH (2002) Xylem structure and the ascent of sap. Springer, Berlin

Vaganov E, Hughes M, Shashkin A (2006) Growth dynamics of conifer tree rings. Springer, Berlin

van der Maaten-Theunissen M, van der Maaten E, Bouriaud O (2015) PointRes: An R package to analyze pointer years and components of resilience. Dendrochronologia 35:34-38

Vicente-Serrano S, Beguería S, López-Moreno J (2010) A multiscalar drought index sensitive to global warming: the standardized precipitation evapotranspiration index. J Clim 23:1696-1718

Wang L, Payette S, Bégin Y (2002) Relationships between anatomical and densitometric characteristics of black spruce and summer temperature at tree line in northern Quebec. Can J For Res 32:477-486

White F (1991) Viscous fluid flow. MacGraw, New York

Wigley TML, Briffa KR, Jones PD, Wigley TML, Briffa KR, Jones PD (1984) On the average value of correlated time series, with applications in dendroclimatology and hydrometeorology. J Clim Appl Meteorol 23:201-213

Woodruff DR, Bond BJ, Meinzer FC (2004) Does turgor limit growth in tall trees? Plant Cell Environ 27:229-236

Yasue K, Funada R, Kobayashi O, Ohtani J (2000) The effects of tracheid dimensions on variations in maximum density of *Picea glehnii* and relationships to climatic factors. Trees 14:223-229

Ziaco E, Biondi F, Rossi S, Deslauriers A (2014) Climatic influences on wood anatomy and tree-ring features of Great Basin conifers at a new mountain observatory. Appl Plant Sci. doi: 10.3732/apps.1400054

Supporting information

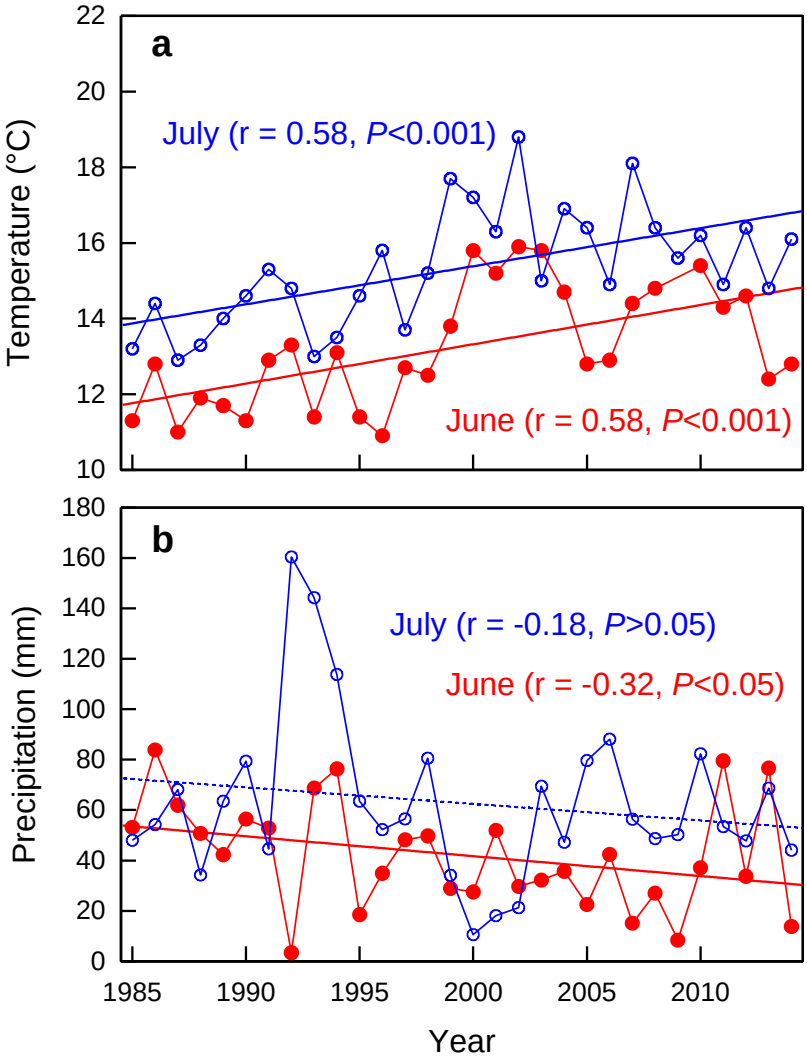

Fig. S4.1 Trends for June and July **(a)** temperature and **(b)** precipitation in Tosontsengel, Mongolia from 1985-2014.

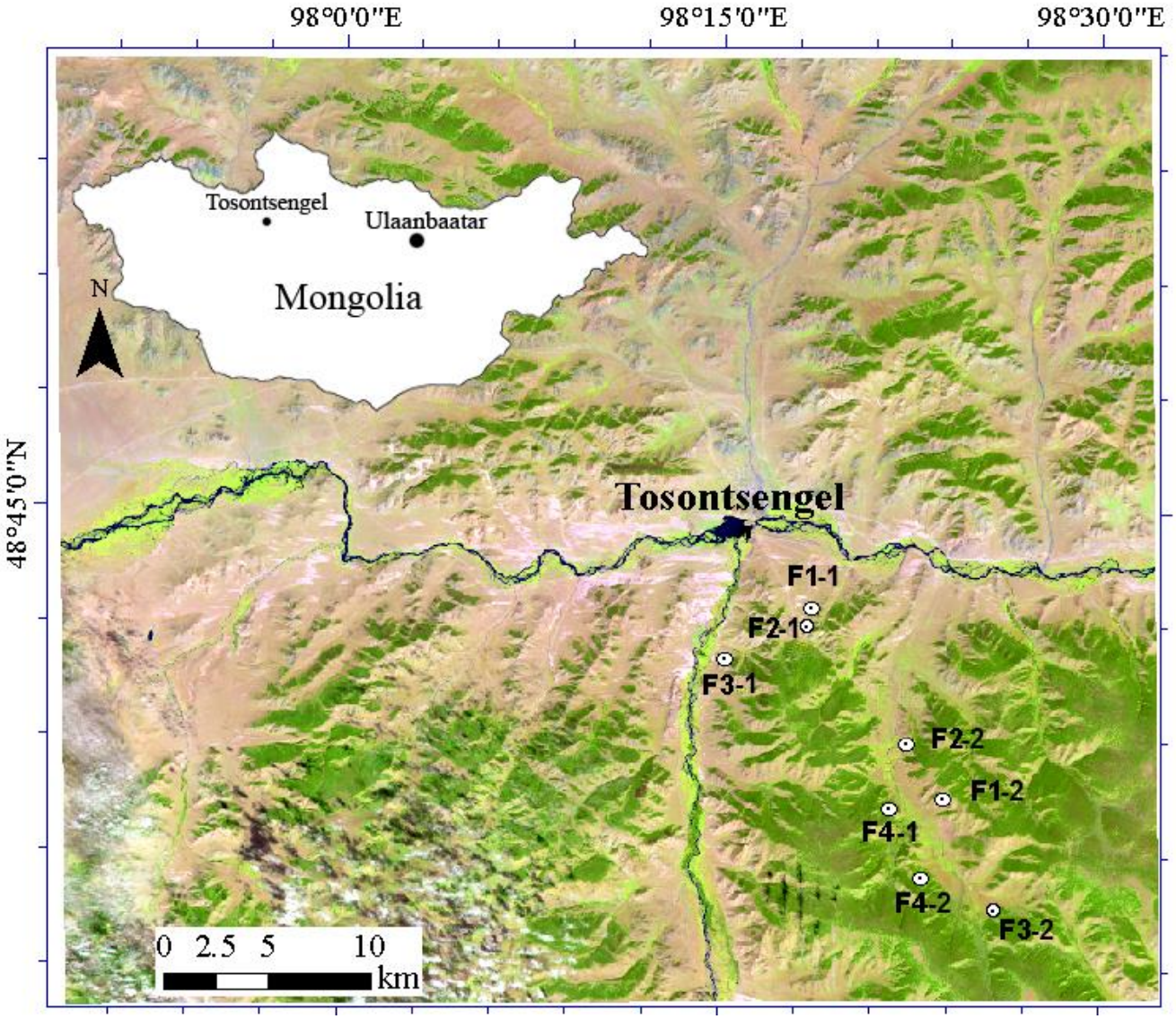

Fig. S4.2 Location of the study area near Tosontsengel, north-western Mongolia. Samples were taken from *L. sibirica* forest stands of different size (F1: <0.1 km^2, F2: 0.1−1 km^2, F3: 1.1−5 km^2, F4: >5 km^2).

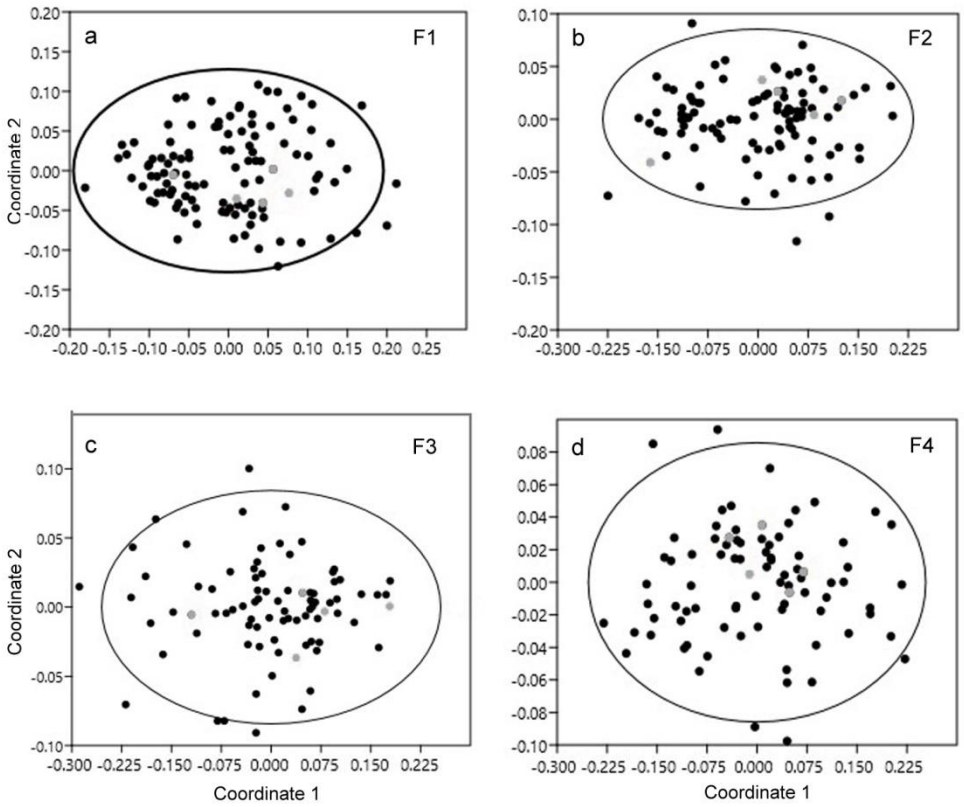

Fig. S4.3 NMDS ordination of tree-ring series from stands of different size (a) F1 (<0.1 km^2), (b) F2 (0.1−1 km^2), (c) F3 (1.1−5 km^2), (d) F4 (>5 km^2). Grey circles represent sample trees for wood-anatomical analysis (five trees per size class). Black trees represent the complete tree population of the same age class (>160 years; data from Khansaritoreh et al., 2017). Ellipses mark the area where 95% of all samples are present.

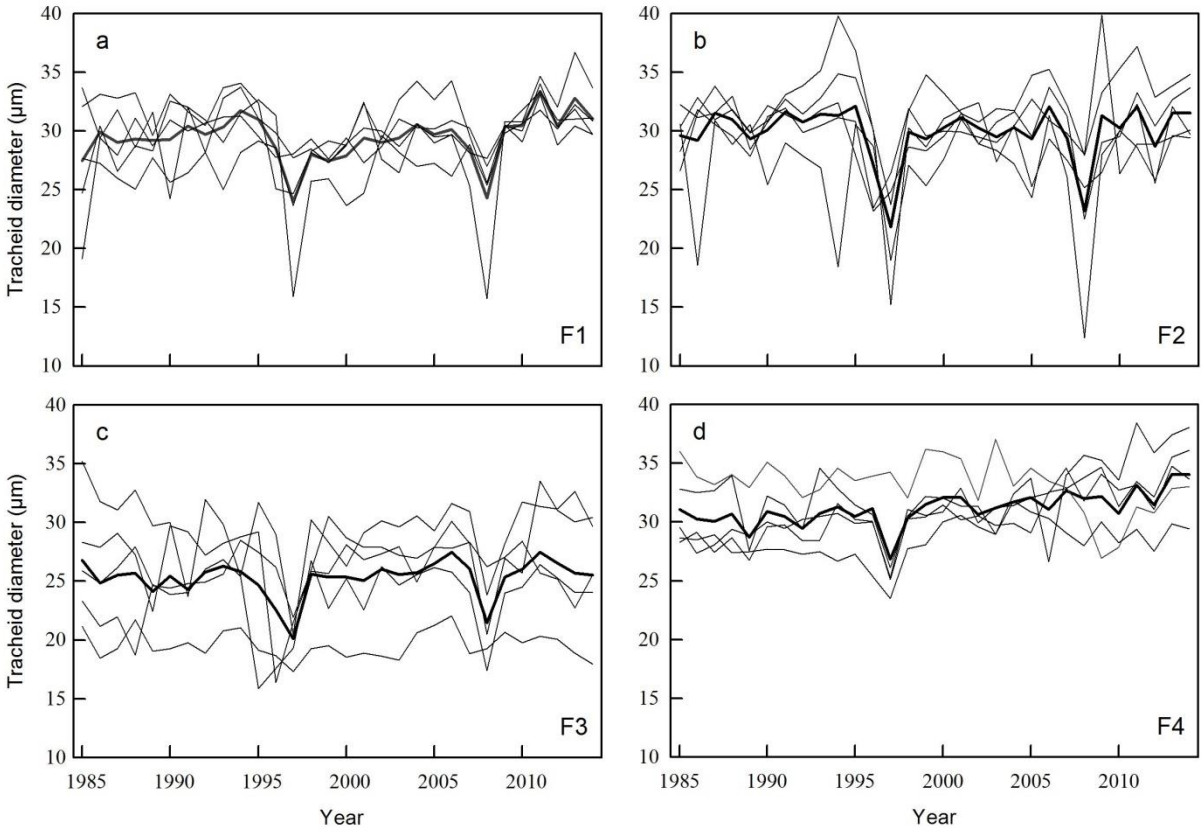

Fig. S4.4 Time-series of tracheid diameters (*d*) from stands of different size (a) F1 (<0.1 km^2), (b) F2 (0.1−1 km^2), (c) F3 (1.1−5 km^2), (d) F4: (>5 km^2) for the period of 1985-2014. Bold lines are mean curves.

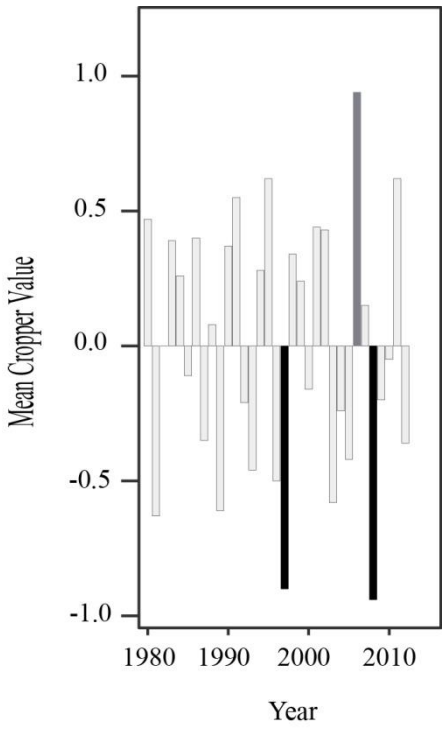

Fig. S4.5 Pointer years based on TRW of 1280 sample. Grey: positive, black: negative pointer years (Cropper threshold = 0.5).

Chapter 5

Synthesis

Synthesis

Long-lasting pastoral land use along with changing semiarid and continental climate in Mongolia strongly affect the forest-steppe ecotone in the northern part of the country where landscapes have naturally been formed by larch forest islands embedded in grasslands.

As described in the previous chapters, in addition to climate warming, the spatial heterogeneity in terms of forest structure and land use intensity persuaded us to design a case study (chapter 2) to investigate how these factors affect age structure and stem increment in two neighboring forest regions (20 km apart from each other) differing in logging and grazing intensity. Besides, the fragmented forests with varying sizes and microclimates provided remarkable opportunity to examine substantial variations in many forest characteristics between different patch sizes (chapter 3). Furthermore, a study on radial wood anatomy variation in larch trees from different patch sizes in response to climate change has been conducted in chapter 4.

The following chapter sections address concluding remarks of each study briefly and present principal information resulting from our studies which are essential for forest management in the local and regional scale.

5.1 Impact of land use on stem increment, age and stand structure

We found striking differences in age structure of site A (heavy logging during the twentieth century) in comparison to site B (sporadic timber harvest), whereas stand structure including stand density and basal area did not differ significantly between both sites (chapter 2). Influence of heavy logging in site A was reflected in decline of old (cambial age of 101−160 years) and very old (>160 years) *L. sibirica* trees; consequently there is a considerable presence of middle-aged trees (61−100 years) which could benefit from space resulting from logging of older trees. Altering age structure of forests due to the reducing number of old trees after extreme logging is worldwide (Lindenmayer et al. 2012) and considerable presence of middle-aged trees in site A can be attributed to less attraction of these trees for logger until 1990 when they were too young and small. Moreover, complete absence of young trees (<60 years) is another point which should be taken into account as a negative effect of increasing soil temperature and reducing soil moisture after clear-cutting inhibiting the germination success and seedling survival (Dulamsuren et al. 2008).

Several studies have been conducted in northern parts of Mongolia and Kazakhstan to examine the effects of climate factors (temperature and precipitation) on tree-ring width of larch trees which mostly confirm the positive correlation between tree ring formation and summer (current and prior year) precipitation (Dulamsuren et al. 2010a, b, 2011, 2013; De Grandpré et al. 2011). However, the effect of temperature could not be generalized and, depending on the regional climate regime, can reinforce tree ring growth if appropriate precipitation is available (D'Arrigo et al. 2000; Dulamsuren et al. 2010a, 2014). In our study, also both sites showed a high sensitivity of the tree-ring index to summer drought, but this sensitivity was more pronounced in the formerly heavily logged site A in comparison with site B. Deviations in the climate response of the tree-ring index between sites with largely identical topography, elevation, climate, and edaphic characteristics, probably results from different land use histories which led to different age structures. Middle-aged trees which constituted the main part of the tree population in site A were more sensitive to high summer temperatures than site B trees and they showed a negative correlation in particular with June temperature. Dominancy of middle-aged trees which are normally more productive than older trees (Schulze et al. 1999; Bond-Lamberty et al. 2004; Girardin et al. 2011), results in increasing water need (Jassal et al. 2009; Bond-Lamberty et al. 2009). Therefore it is possible that in middle-aged trees of site A, stomatal conductance and carbon assimilation decrease due to the rising saturation deficits under the increasing summer temperatures associated with semi-arid climate of the Inner Asian forest-steppes (Li et al. 2006; Dulamsuren et al. 2009).

Sharp increases in missing ring frequency and tree mortality as indicators of summer drought susceptibility in both sites since the late twentieth century, have been found in other parts of the Mongolian forest-steppe as well (Liu et al. 2013; Khishigjargal et al. 2014).

In agreement with many studies which addressed differences between tree growth and anatomical traits in forest edges and interiors in the forest-steppe of Mongolia (Dulamsuren et al. 2009, 2010b, 2011, 2014; Khishigjargal et al. 2013; Chenlemuge et al. 2015a), trees at both sites showed higher radial stem increment at forest edges than in the forest interior in the mid-twentieth century apparently due to the lower stand density and thus lower intraspecific competition for resources in the cooler mid-twentieth century. However, accelerating climate warming at the global level (IPCC 2013) changed these trends and similar growth rates have been observed since the late twentieth century.

In summary, our findings of chapter 2 suggest that the unfavorable influence of climate warming on forests in the drought-sensitive forest-steppes of Inner Asia might be aggravated by heavy logging.

5.2 Effect of forest fragmentation and isolation on climate warming sensitivity and changing microclimate

Although several studies have been conducted on *Larix sibirica* in many forest-steppe regions of Mongolia in context of tree ring researches, comprehensive investigations which focus on the direct influence of forest fragmentation on tree growth and stand characters were studied for the first time. Our finding in chapter 3 clearly revealed that the small forest stands in the forest-dominated subregion (F1, F2), and the smallest stands (F1) in particular, had a more extreme microclimate (lower minimum and higher maximum air temperatures and lower relative air humidity) with higher annual amplitudes than the large forests (F3, F4). Moreover, mean sensitivity of TRW increased with decreasing stand size, whereas first-order autocorrelation decreased. Therefore trees in smaller forest stands suffer more from climate warming since they cannot withstand harsh climatic conditions and thus fail to keep the appropriate photosynthetic activity of the canopy which leads to negative consequences for stemwood production.

Results of the climate response analysis showed that the tree-ring index in the trees of size classes F1 to F3 (<5 km^2 size, with warmer and drier microclimate in summer), but not in large forest stands of >5 km^2, was mostly positively correlated with previous year's June and August precipitation. Correlation with precipitation of the prior summer has been reported in literatures e.g. (Bräuning 1999; Pederson et al. 2001; Kharuk et al. 2015), but the interesting results of our study gives evidence that more intense drought exposure is indeed the cause of the higher climate sensitivity of stemwood production in small forests.

The result of missing ring frequency analyses was consistent with chapter 2 and observations in many other parts of Mongolia, which declared that missing ring frequency has strongly increased after 1970. This ascending trend was pronounced in small forests, in particular in the grassland-dominated areas (G1) with more tense water relations due to the growing season drought (Lorimer et al. 1999; Khishigjargal et al. 2014; Liang et al. 2016). Stronger correlation of G1 (forests isolated in grasslands) tree-ring index, even more than F1s, with prior summer precipitation was in line with missing ring results.

Based on the chronologies, a switch in growth of trees between the large stands (F4) and smaller forests (F1-F3) has occurred since 200 years ago. Recent faster growth of F4 trees (unlike in the past) could be attributed to intensified (deep) permafrost melt in large forests during summer time by higher temperature in the active layer of soil. Melted permafrost can provide water supply for vegetation which is known as a critical factor for tree growth (Sugimoto et al. 2003; Lopez et al. 2010; Sharkhuu and Sharkhuu 2012).

In addition to negative effects of forest fragmentation on tree growth and productivity in the current stage, the future of these disturbed forests will be in danger due to a reduction in forest regeneration. Descending trends in regeneration along with decreasing stand sizes are supported by combined effects of lower moisture availability and much higher grazing pressure in the small stands. Tripled increase in goat numbers since the early 1990s which graze more in the forest edges and small forests than in the interior of large forests, together with climate warming hamper the larch sapling survival (Lkhagvadorj et al. 2013).

Based on findings of Dulamsuren et al. (2014), selective logging is usually more extreme in small forests than in the interior of large forests in the Mongolian forest-steppe leading to reduced stand density and competition, which consequently improves water supply and growth of remaining trees (Dulamsuren et al. 2010b; Chenlemuge et al. 2015a). These findings are in agreement with results of Gradel et al. (2017) which emphasize on the significant positive effect of reduced competition after thinning on growth increase in birch and larch trees. Therefore we assumed that the tolerance of trees to drought periods in small stands must be increased, however our finding of a higher climate warming sensitivity contradicts this fact. This likely reveals that logging did not have a decisive impact on the detected differences in climate-warming sensitivity in our study.

A presented model by (Ishii and Fujita 2013) is in line with our findings and suggests that, where precipitation decreases and/or livestock increases, vegetation degradation will happen extremely. In summary, our results conclude that the larch trees in small and isolated forest patches resulted from combined effects of logging, fire, and forest grazing, are more vulnerable to climate warming than larch in continuous forests. Consequently it is predictable that in areas as the Mongolian forest-steppes where climate change is associated with anthropogenic disturbance, drought-limited forests will be seriously threatened by fragmentation in the future.

5.3 Effect of drought on hydraulic traits and relations to tree-ring width in *Larix sibirica*

Quantitative wood anatomy as a very powerful tool gives us a valuable insight into the relationships between tree growth and environmental parameters in decadal to centennial scale (von Arx et al. 2016). In Mongolian forest-steppes some studies have been conducted in case of larch tree anatomy, (e.g. Khishigjargal et al. 2014; Chenlemuge et al. 2015a, b) but our study (chapter 4) is the first one addressing the question whether hydraulic traits were influenced by temporal or forest size-dependent variations in water availability and were related to tree-ring width in *L. sibirica* in the north-western of Mongolia (near Tosontsengel).

Generally trees react to increasing drought stress by producing smaller tracheids which lead to lower hydraulic conductivity. This down-regulation of tracheid size with increasing aridity limit tree growth, prevent hydraulic failure and potentially mortality (Sperry et al. 2006; McDowell 2011; Sevanto et al. 2014). Indeed, it is a trade-off to decrease hydraulic efficiency and improve hydraulic safety in drought conditions. In contrast, higher hydraulic conductivity in stem, branch and root influences productivity and elevates stem increment (Hacke and Sperry 2001; Tyree and Zimmermann 2002; Cochard et al. 2004; Chenlemuge et al. 2015b; Fonti and Babushkina 2015).

In our study, we found that variations in climate affect tracheid diameters (d, d_h), potential sapwood area-specific hydraulic conductivity (K_p), and tracheid diameter (TD) in *L. sibirica*. Drought in the previous years' late summer reduced tracheid diameters and hydraulic conductivity, but increased tracheid density in the preceding growing season. This correlation coincides with a negative effect of the prior years' drought on tree-ring width in water-limited *L. sibirica* forests (Dulamsuren et al. 2011, 2013; Tei et al. 2017). Same responses of tree-ring width and tracheid diameter to climate confirm our hypothesis of a close correlation of TRW and d as well. The probable (but not proven) cause of the previous years' climate influence on tree growth is the restriction of the trees' potential to produce and reserve non-structural carbohydrates which are necessary for wood formation in the early following growing season (Begum et al. 2010). Despite the decisive effect of forest fragmentation and the resulting variation in stand climate on the increased climate sensitivity of stemwood formation in *L. sibirica* (chapter 3), we found that hydraulic architecture is poorly influenced. In addition, we did not find any constant trend between a decrease of stand size and

anatomical traits; though d, d_h, and K_p were higher and tracheid density (TD) was lower in the largest forests than in the smallest stands.

In total, reduction of tracheid size, decreased fine-root mass, lessening of transpiration by needle abscission and the closure of stomata, are presumably *L. sibirica*'s strategies to be compatible and resistant against drought (Hacke et al. 2001; Pittermann et al. 2006; Chenlemuge et al. 2013).

5.4 Conclusion

Effects of land use intensity, forest fragmentation and climate warming on stem increment and hydraulic architecture of *Larix sibirica* growing at the southern fringe of the Eurosiberian boreal forest in the Mongolian forest-steppe were studied. Apparent climate-sensitivity of the trees in the heavily logged forests and small forest stands reveal that anthropogenic disturbance and forest fragmentation exacerbates the detrimental impact of climate warming on forests which are exposed to temperature increases far above the global average in Inner Asia (IPCC 2013). Although forest fragmentation resulted from logging, fire, and forest grazing, clearly affects annual stem increment, forest regeneration and microclimate, its effect on hydraulic architecture did not show a linear correlation with decreasing forest stand size. However, anatomic parameters (e.g. tracheid diameter, tracheid density and …) like tree-ring width, significantly correlated with climate, in particular with late summer precipitation of the prior year. Therefore, albeit summer drought has a negative effect on stemwood formation and tree growth, reduction of tracheid diameter size can protect *L. sibirica* trees against hydraulic failure and mortality. Vulnerability of larch tree growth and regeneration, even though adaptation mechanisms, increases necessity of conservation of moisture-limited Inner Asian forest against anthropogenic factors to minimize the unavoidable influence of harsh climatic condition.

Further studies with more replications on the stand level in land use and fragmentation studies are suggested because of high spatial heterogeneity in small scales at the Mongolian forest-steppes. Moreover, studying more anatomical traits (e.g. cell wall thickness, amount of radial rays, cell grouping, pit characteristics) in longer periods with larger sample size are highly recommended to generalize the dendrochronological and anatomical results.

References

Begum S, Nakaba S, Oribe Y, et al (2010) Changes in the localization and levels of starch and lipids in cambium and phloem during cambial reactivation by artificial heating of main stems of Cryptomeria japonica trees. Ann Bot 106:885–895. doi: 10.1093/aob/mcq185

Bond-Lamberty B, Peckham S, Gower ST, Ewers BE (2009) Effects of fire on regional evapotranspiration in the central Canadian boreal forest. Glob Chang Biol 15:1242–1254. doi: 10.1111/j.1365-2486.2008.01776.x

Bond-Lamberty B, Wang C, Gower ST (2004) Net primary production and net ecosystem production of a boreal black spruce wildfire chronosequence. Glob Chang Biol 10:473–487. doi: 10.1111/j.1529-8817.2003.0742.x

Bräuning A (1999) Dendroclimatological Potential of Drought-Sensitive tree Stands in Southern Tibet for the Reconstruction of Monsoonal Activity. IAWA J 20:325–338. doi: 10.1163/22941932-90000695

Chenlemuge T, Dulamsuren C, Hertel D, et al (2015a) Hydraulic properties and fine root mass of Larix sibirica along forest edge-interior gradients. Acta Oecologica 63:28–35. doi: 10.1016/j.actao.2014.11.008

Chenlemuge T, Hertel D, Dulamsuren C, et al (2013) Extremely low fine root biomass in Larix sibirica forests at the southern drought limit of the boreal forest. Flora Morphol Distrib Funct Ecol Plants 208:488–496. doi: 10.1016/j.flora.2013.08.002

Chenlemuge T, Schuldt B, Dulamsuren C, et al (2015b) Stem increment and hydraulic architecture of a boreal conifer (Larix sibirica) under contrasting macroclimates. Trees - Struct Funct 29:623–636. doi: 10.1007/s00468-014-1131-x

Cochard H, Froux F, Mayr S, Coutand C (2004) Xylem wall collapse in water-stressed pine needles. Plant Physiol 134:401–8. doi: 10.1104/pp.103.028357

D'Arrigo R, Jacoby G, Pederson N, et al (2000) Monogolian tree-rings, temperature sensitivity and reconstructions of Northern Hemisphere temperature. The Holocene 10:669–672. doi: 10.1191/09596830094926

De Grandpré L, Tardif JC, Hessl A, et al (2011) Seasonal shift in the climate responses of Pinus sibirica , Pinus sylvestris , and Larix sibirica trees from semi-arid, north-central Mongolia. Can J For Res 41:1242–1255. doi: 10.1139/x11-051

Dulamsuren C, Hauck M, Bader M, et al (2009) Water relations and photosynthetic performance in Larix sibirica growing in the forest-steppe ecotone of northern Mongolia. Tree Physiol 29:99–110. doi: 10.1093/treephys/tpn008

Dulamsuren C, Hauck M, Khishigjargal M, et al (2010a) Diverging climate trends in Mongolian taiga forests influence growth and regeneration of Larix sibirica. Oecologia 163:1091–1102. doi: 10.1007/s00442-010-1689-y

Dulamsuren C, Hauck M, Leuschner C (2010b) Recent drought stress leads to growth reductions in Larix sibirica in the western Khentey, Mongolia. Glob Chang Biol 16:3024–3035. doi: 10.1111/j.1365-2486.2009.02147.x

Dulamsuren C, Hauck M, Leuschner HH, Leuschner C (2011) Climate response of tree-ring width in Larix sibirica growing in the drought-stressed forest-steppe ecotone of northern Mongolia. Ann For Sci 68:275–282. doi: 10.1007/s13595-011-0043-9

Dulamsuren C, Hauck M, Mühlenberg M (2008) Insect and small mammal herbivores limit tree establishment in northern Mongolian steppe. Plant Ecol 195:143–156. doi: 10.1007/s11258-007-9311-z

Dulamsuren C, Khishigjargal M, Leuschner C, Hauck M (2014) Response of tree-ring width to climate warming and selective logging in larch forests of the Mongolian Altai. J Plant Ecol 7:24–38. doi: 10.1093/jpe/rtt019

Dulamsuren C, Wommelsdorf T, Zhao F, et al (2013) Increased Summer Temperatures Reduce the Growth and Regeneration of Larix sibirica in Southern Boreal Forests of Eastern Kazakhstan. Ecosystems 16:1536–1549. doi: 10.1007/s10021-013-9700-1

Fonti P, Babushkina EA (2015) Tracheid anatomical responses to climate in a forest-steppe in Southern Siberia. Dendrochronologia 39:32–41. doi: 10.1016/j.dendro.2015.09.002

Girardin MP, Bernier PY, Gauthier S (2011) Increasing potential NEP of eastern boreal North American forests constrained by decreasing wildfire activity. Ecosphere 2:art25. doi: 10.1890/ES10-00159.1

Gradel A, Ammer C, Ganbaatar B, et al (2017) On the Effect of Thinning on Tree Growth and Stand Structure of White Birch (Betula platyphylla Sukaczev) and Siberian Larch (Larix sibirica Ledeb.) in Mongolia. Forests 8:105. doi: 10.3390/f8040105

Hacke UG, Sperry JS (2001) Functional and ecologycal xylem anatomy. Perspect Plant Ecol Evol Syst 4:97–115. doi: 10.1007/978-3-319-15783-2

Hacke UG, Sperry JS, Pockman WT, et al (2001) Trends in wood density and structure are linked to prevention of xylem implosion by negative pressure. Oecologia 126:457–461. doi: 10.1007/s004420100628

IPCC (2013) Climate Change 2013: The Physical Science Basis. Contribution of Working Group I to the Fifth Assessment Report of the Intergovernmental Panel on Climate Change. Intergov Panel Clim Chang Work Gr I Contrib to IPCC Fifth Assess Rep (AR5)(Cambridge Univ Press New York) 1535. doi: 10.1029/2000JD000115

Ishii R, Fujita N (2013) A Possible Future Picture of Mongolian Forest-Steppe Vegetation Under Climate Change and Increasing Livestock: Results from a New Vegetation Transition Model at the Topographic Scale. In: The Mongolian Ecosystem Network. pp 65–82

Jassal RS, Black TA, Spittlehouse DL, et al (2009) Evapotranspiration and water use efficiency in different-aged Pacific Northwest Douglas-fir stands. Agric For Meteorol 149:1168–1178. doi: 10.1016/j.agrformet.2009.02.004

Kharuk VI, Ranson KJ, Im ST, Petrov IA (2015) Climate-induced larch growth response within the central Siberian permafrost zone. Environ Res Lett 10:125009. doi: 10.1088/1748-9326/10/12/125009

Khishigjargal M, Dulamsuren C, Leuschner HH, et al (2014) Climate effects on inter- and intra-annual larch stemwood anomalies in the Mongolian forest-steppe. Acta Oecologica

55:113–121. doi: 10.1016/j.actao.2013.12.003

Khishigjargal M, Dulamsuren C, Lkhagvadorj D, et al (2013) Contrasting responses of seedling and sapling densities to livestock density in the Mongolian forest-steppe. Plant Ecol 214:1391–1403. doi: 10.1007/s11258-013-0259-x

Li S-G, Tsujimura M, Sugimoto A, et al (2006) Seasonal variation in oxygen isotope composition of waters for a montane larch forest in Mongolia. Trees 20:122–130. doi: 10.1007/s00468-005-0019-1

Liang E, Leuschner C, Dulamsuren C, et al (2016) Global warming-related tree growth decline and mortality on the north-eastern Tibetan plateau. Clim Change 134:163–176. doi: 10.1007/s10584-015-1531-y

Lindenmayer DB, Laurance WF, Franklin JF (2012) Global Decline in Large Old Trees.

Liu H, Park Williams A, Allen CD, et al (2013) Rapid warming accelerates tree growth decline in semi-arid forests of Inner Asia. Glob Chang Biol 19:2500–2510. doi: 10.1111/gcb.12217

Lkhagvadorj D, Hauck M, Dulamsuren C, Tsogtbaatar J (2013) Twenty Years After Decollectivization: Mobile Livestock Husbandry and Its Ecological Impact in the Mongolian Forest-Steppe. Hum Ecol 41:725–735. doi: 10.1007/s10745-013-9599-3

Lopez ML, Shirota T, Iwahana G, et al (2010) Effect of increased rainfall on water dynamics of larch (Larix cajanderi) forest in permafrost regions, Russia: an irrigation experiment. J For Res 15:365–373. doi: 10.1007/s10310-010-0196-7

Lorimer CG, Dahir SE, Singer MT (1999) Frequency of partial and missing rings in Acer saccharum in relation to canopy position and growth rate. Plant Ecol 143:189–202. doi: 10.1023/A:1009847819158

McDowell NG (2011) Mechanisms linking drought, hydraulics, carbon metabolism, and vegetation mortality. Plant Physiol 155:1051–9. doi: 10.1104/pp.110.170704

Pederson N, Jacoby GC, D'Arrigo RD, et al (2001) Hydrometeorological Reconstruction for Northeastern Mongolia Derived from Tree Rings: 1651--1995. J Clim 14:872–881. doi: 10.1175/1520-0442(2001)014<0872:HRFNMD>2.0.CO;2

Pittermann J, Sperry JS, Hacke UG, et al (2006) Inter-tracheid pitting and the hydraulic efficiency of conifer wood: the role of tracheid allometry and cavitation protection. Am J Bot 93:1265–73. doi: 10.3732/ajb.93.9.1265

Schulze E-D, Lloyd J, Kelliher FM, et al (1999) Productivity of forests in the Eurosiberian boreal region and their potential to act as a carbon sink -- a synthesis. Glob Chang Biol 5:703–722. doi: 10.1046/j.1365-2486.1999.00266.x

Sevanto S, Mcdowell NG, Dickman LT, et al (2014) How do trees die? A test of the hydraulic failure and carbon starvation hypotheses. Plant, Cell Environ 37:153–161. doi: 10.1111/pce.12141

Sharkhuu N, Sharkhuu A (2012) Effects of Climate Warming and Vegetation Cover on Permafrost of Mongolia. Springer Netherlands, pp 445–472

Sperry JS, Hacke UG, Pittermann J (2006) Size and function in conifer tracheids and angiosperm vessels. Am J Bot 93:1490–1500. doi: 10.3732/ajb.93.10.1490

Sugimoto A, Naito D, Yanagisawa N, et al (2003) Characteristics of soil moisture in permafrost observed in East Siberian taiga with stable isotopes of water. Hydrol Process 17:1073–1092. doi: 10.1002/hyp.1180

Tei S, Sugimoto A, Yonenobu H, et al (2017) Tree-ring analysis and modeling approaches yield contrary response of circumboreal forest productivity to climate change. Glob Chang Biol. doi: 10.1111/gcb.13780

Tyree MT, Zimmermann MH (2002) Xylem Structure and the Ascent of Sap. Springer Berlin Heidelberg, Berlin, Heidelberg

von Arx G, Crivellaro A, Prendin AL, et al (2016) Quantitative Wood Anatomy—Practical Guidelines. Front Plant Sci. doi: 10.3389/fpls.2016.00781

Acknowledgments

First of all, I would like to thank my dear supervisor, Dr. Choimaa Dulamsuren not only for introducing me into the dendrochronology world, but also for the constant support with her nice personality and hearty laughs. I am grateful to my supervisors, Prof. Dr. Markus Hauck and Prof. Dr. Christoph Leuschner for providing me the opportunity to study in the international atmosphere, and to compile my thesis and papers.

I want to thank Dr. Bernhard Schuldt for supporting my research in the third part and helping me to overcome many challenges in the wood anatomical studies.
I gratefully acknowledge the support of the Erasmus Mundus Scholarship 'Salam 2 program' for funding my PhD which opened the new window in my life to a different world.
Special thanks go to my Mongolian friends and colleagues who assisted me a lot in the field work, they were wonderful hosts.
Thank to Dr. Heinz Coners and Mrs. Astrid Röben for their endless help, whenever I needed them.
I would like to thank all of my nice colleagues and gardeners in the Plant Ecology department and new botanical garden.
Sincere thanks go to my close friends Julia, Regine and Natalia who spent happy times with me and supported me a lot during these years. I will never forget our memories together. Special thanks to Regine for proof reading my thesis.
I am grateful to all my Iranian friends in Göttingen, we spent much time together and built a small Iran in the heart of Germany.
The last but not the least, I am grateful to my family, especially my lovely mother who never stopped encouraging me to proceed in my life. She gave me strength with her promising messages everyday.

Finally I would like to thank my perfect husband who eagerly enabled my education through his unlimited love and help over the last 10 years. If he had not accompanied me, this journey would not have been completed.

Declaration of originality and certificate of ownership

I, Elmira Khansaritoreh, hereby declare that I am the sole author of this dissertation entitled 'Effects of Land Use, Habitat Fragmentation and Climate Warming on Stem Increment, Regeneration, and Hydraulic Architecture of *Larix sibirica* in the Mongolian Forest-Steppe'. All references and data sources that were used in the dissertation have been appropriately acknowledged. I furthermore declare that this work has not been submitted elsewhere in any form as part of another dissertation procedure.

Göttingen, August 31, 2017

_____
(Elmira Khansaritoreh)